SISSA

International School for Advanced Studies

PhD course in statistical physics

Out of equilibrium many-body systems: adiabaticity, statistics of observables and dynamical phase transitions

Thesis submitted for the degree of
Doctor Philosophiae

Supervisor:
Dr. Alessandro Silva

Candidate:
Pietro Smacchia

academic year 2013/2014

Contents

Summary

This thesis reports the results obtained during my PhD research in the field of out of equilibrium quantum many-body systems. Chapter 1 consists in a brief introduction of the field and the introduction of concept that are useful for the following chapters.

In Chapter 2 the statistics of the work as a tool for characterizing the dynamics of many-body quantum systems is introduced its general features discussed. Then, such a statistics is computed for generic time-dependent protocols (both global and local) in the quantum Ising chain and in the Gaussian field theory, showing, in particular, that in its low-energy part there are features that are independent of the details of the specific chosen protocol.

Chapter 3 is devoted to the study of the dynamical phase transition in the $O(N)$ quantum vector model in the $N \to \infty$ limit, whose critical properties in generic dimensions are characterized. Moreover, a strong connection between such a transition and the statistics of excitations produced in a double quench as a function of the waiting time is showed. The chapter ends by studying the fate of the dynamical transition and the its critical properties when a ramp of finite duration τ is applied to the system instead of a sudden quench. In particular, we will show that when $\tau \to \infty$ the critical point tends to the equilibrium critical point (at zero temperature) in a power-law fashion and that for every finite τ the critical properties are always the same (and different from the equilibrium critical properties).

Finally in Chapter 4 we will discuss the emergence of a non adiabatic behavior in the dynamics of the order parameter for a low dimensional quantum system

driven within a gapped phase by considering in detail the case of a quantum Ising chain subject to a linear variation in time of the transverse field, showing that, no matter how slowly the ramp is performed, such a change leads eventually to the disruption of the order.
The results of Chapter 2 are contained in two publications:

- P. Smacchia and A. Silva, Phys. Rev. Lett. **109**, 037202 (2012)
- P. Smacchia and A. Silva, Phys. Rev. E **88**, 042109 (2013)

The results presented in Chapter 3 will appear in two manuscript still in preparation, while the results of Chapter 4 are contained in

- A. Maraga, P. Smacchia, M. Fabrizio and A. Silva, arXiv:1402.2789, submitted to Phys. Rev. B

Chapter 1

Dynamics of Isolated Quantum Systems

1.1 Experimental Motivations

The study of the out of equilibrium dynamics of isolated quantum many-body systems is nowadays a very active and fascinating area of condensed matter and statistical physics. Even tough the first studies in this context have been made right after the birth of quantum mechanics [128], this topic has been overlooked for a long time, with the exception of some works in the 1970s [5–7, 92]. At the same time unitary coherent dynamics nearly impossible to observe experimentally, due to the fact that dissipative effects in ordinary condensed matter systems take place on very short time scales (order of a picosecond).

The situation has been drastically changed by a series of experimental breakthroughs, especially in the context of the physics of cold atoms (for an extensive review see [13]), which allow the realization of highly tunable artificial systems in which decoherence and dissipative effects are strongly suppressed. The first important step in this direction was the experimental observation of Bose-Einstein condensation in 1995 [2, 14, 32], made possible by the development of laser and evaporative cooling techniques, which enable the reaching of temperatures of the order of nano kelvin. This was later followed by the realization of a Fermi

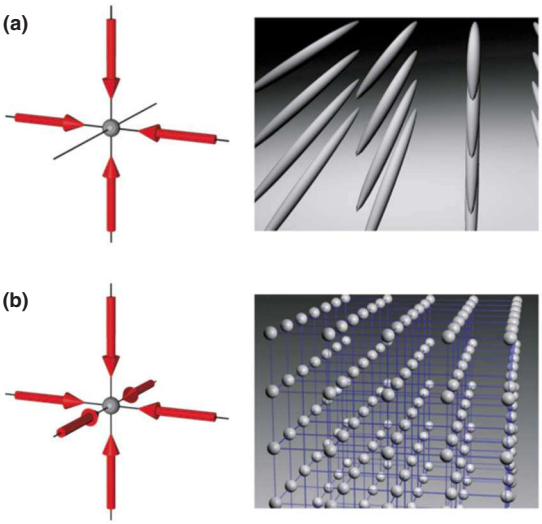

Figure 1.1: *Schematic representation of (a) two- and (b) three- dimensional optical lattice. In (a) the atoms are confined in a array of one-dimensional tubes. Taken from [13]*

degenerate gas [35]. However, two crucial steps that have considerably enlarged the range of experiments realizable with these systems: the development of Feshbach resonance techniques [31, 62] and of optical potentials [56]. Indeed, the former allow to control and tune the inter-particle interaction by changing the external magnetic field, while the latter, which exploit the dipolar interaction between the atoms and laser light depending on the intensity of the laser beam, can be made spatial dependent and, in particular, periodic, creating the so-called optical lattices [54] by overlapping two counterpropagating beams. This made also possible to control the dimensionality of the system, creating low-dimensional configurations, as schematically shown in Fig. 1.1 for the case of one dimensional system.

The great tunability of such systems has made it possible to construct experimentally controllable systems that can accurately be described by simple models, which in the past were mainly used to describe the low energy physics of complex systems. However, from the point of view of non equilibrium physics, the possibility of changing the interaction and the external in time is a crucial feature, which together with their weak coupling with the environment allows

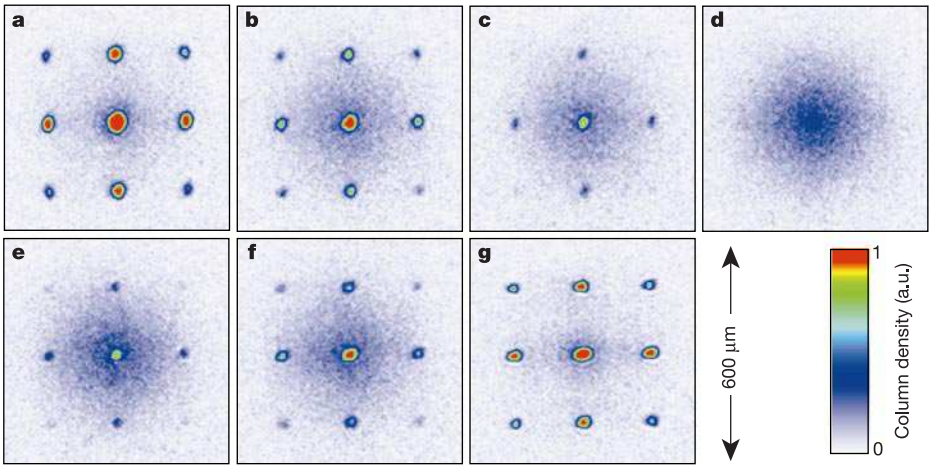

Figure 1.2: *Time of flight measured interference pattern [55] for times t equal to (a) 0 μs, (b) 100μs, (c) 150μs, (d) 250μs, (e) 350μs, (f) 400μs and (g) 500μs.*

the observation of the coherent dynamics of many-body quantum systems on quite long time scales compared to traditional condensed matter systems. This was clearly shown by a seminal experiment performed by Prof. Bloch's group in Munich in 2002 [55]. Here, they loaded ultracold bosonic atoms in a three dimensional optical lattice, where they are known to undergo a superfluid-Mott insulator transition as a function of the lattice depth [54], preparing the system in a superfluid phase. Then, the depth of the optical lattice was rapidly increased (in such a way lowering the hopping amplitude) up to a value that at equilibrium would have corresponded to a Mott insulating state. Finally, the system was let evolve for a variable time t after which the momentum distribution was measured by time of flights measurements. As we can seen from Fig. 1.2 the initial state shows a distinct interference pattern, which clearly proves the coherence of the the superfluid phase, then after a certain time ($\sim 250\mu s$) such a pattern is completely destroyed, just to be restored some time later ($\sim 500\mu s$). Such a collapse and revival of the wave function is a clear proof of the the fact that the system retains its coherence during the evolution.

1.2 Different protocols and "time universality"

Non equilibrium dynamics is potentially a vast field: there are many different ways in which a system can be taken out of equilibrium and, in general, the outcome is expected to be sensible to the particular choice made. For an isolated system the most natural procedure is to vary in time (in a local or global way) one or more parameters λ of its Hamiltonian $H[\boldsymbol{\lambda}]$. In this setting there is still a large amount of freedom in the choice of the way such parameters are changed in time from their initial $\boldsymbol{\lambda}_i$ to their final values $\boldsymbol{\lambda}_f$. For example one may still choose the amount of time τ in which the variation is performed, and the precise functions $\boldsymbol{\lambda}(t)$, whose extreme values are fixed, i.e. $\boldsymbol{\lambda}(0) = \boldsymbol{\lambda}_i$ and $\boldsymbol{\lambda}(\boldsymbol{\tau}) = \vec{\lambda}_f$. We will refer to different choices as different protocols.

The two extreme cases, already very rich, of a sudden change, the so-called *quantum quench* [18], and a very slow, nearly adiabatic one (known under the oxymoron "slow quench"), are the two most studied cases in the literature, while more generic protocols are hardly addressed. There are, however, various motivations for their study. Indeed, they can be important in the context of quantum information and quantum optimization problems [21], in which one usually looks for the best protocol to achieve a certain goal, usually described as the minimization of a certain figure of merit (for example the fidelity for a protocol crossing a quantum critical point [20]), or to deal with experimental situations where a sudden or adiabatic variation can be difficult to implement [37].

There are, also, more fundamental motivations. Indeed, for a systematic characterization of nonequilibrium phenomena it is important to understand what dynamical features (time dependence of observables, their fluctuations, etc...) are robust (or partially robust) with respect to changes of the protocol. A typical example can be the independence on the duration of the protocol τ. This feature would thus be independent on the exact detail of the protocol chosen, depending only on some of its gross features, a situation that resembles the usual concept of universality in equilibrium statistical physics, which denotes

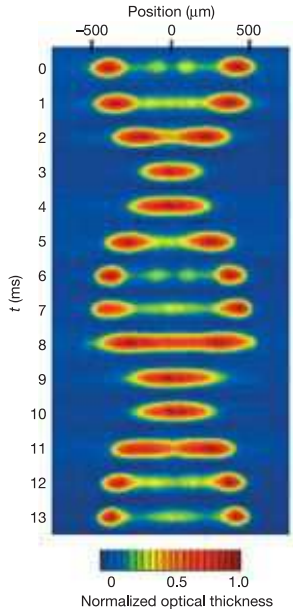

Figure 1.3: *Absorption images in the first oscillation cycle clearly showing the lack of thermalization. Taken from [67]*

independence of physical properties on the microscopic details of the systems, allowing, for example, to describe phase transitions of real systems using simple models with the same gross features, such as dimensionality and symmetry.
With this analogy in mind, we will refer to the independence on the detail of the out of equilibrium protocol as "time universality".

1.3 Stationary States

Among all the different fascinating questions that can be asked regarding the evolution following a generic out of equilibrium protocol, an important issue is the one of the stationary state attained after a very long time.
First of all one should ask *if* such a state exist, a question that has a definitely negative answer in a finite system, due to quantum recurrence. However, in the thermodynamic limit our intuition suggests that if one focuses the attention to a small portion of the system, the rest will act as a bath and a stationary

state will be reached. Consequently one should investigate the nature of such a state: can it be described by a thermal ensemble? Or in other words, does the system *thermalize* at long time scales? Such an interesting study about the thermalization, or lack of it, for quantum isolated systems has been boosted by a ground-breaking experiment in a 1D Bose gas performed by Kinoshita et al. in 2006 [67], also known as "the quantum Newton cradle". There, an array of tightly confined tubes of ultracold ^{87}Rb atoms was created and put in a superposition of states with opposite momenta. The system was then let evolve for variable durations before the momentum distribution was measured. The quite surprising result, shown in Fig. 1.3, was the observation of a non-Gaussian distribution even after thousands of collisions, a clear signal of the lack of thermalization on the experimental time scales. The fact that this system was a very close experimental realization of Lieb-Liniger gas with point-like interaction [77, 78], an integrable system was suggested as the main reason for such a strange behavior, and triggered the subsequent theoretical work on the role of integrability and dimensionality in the dynamics of quantum many-body systems, with a particular interest in their effects in the relaxation towards a stationary state.

Before discussing in more details the nature of the stationary states that can be attained and the differences in the dynamics of integrable and non integrable system, let us clarify from a more formal point of view the issue of the relaxation towards a stationary state for an isolated quantum system. As we briefly mentioned above, asking if the system thermalizes is meaningful only when local degrees of freedom are taken into account. Indeed, the evolution of an isolated quantum system is unitary, thus if we start from a pure state described by a density matrix ρ_0, with the property $\mathrm{Tr}\,[\rho_0^2] = 1$, this can not relax towards a thermal state described by a mixed density matrix rho_{th} with the property $\mathrm{Tr}\,[\rho_{th}^2] < 1$. Indeed, no entropy can be produced during the evolution. Hence, the correct point of view is to focus on the properties of a finite subsystem A described by by the reduced density matrix $\rho_A(t) = \mathrm{Tr}_{\bar{A}}\,[\rho(t)]$, where $\bar{A}$ represents the complement of A, $\rho(t)$ is the evolved density matrix describing the

whole system and $\mathrm{Tr}_{\bar{A}}$ denotes a partial trace performed only over the degrees of freedom of sub-system $\bar{A}$ [45]. The question of the existence of a stationary state can be but put as the question of the existence for any finite subsystem A of a time independent density matrix $\rho_{stat,A}$, obtained as $\rho_{stat,A} = \mathrm{Tr}_{\bar{A}}[\rho_{stat}]$, such that

$$\lim_{t\to\infty} \mathrm{Tr}\left[\rho(t) O_A\right] = \mathrm{Tr}\left[\rho_{stat,A} O_A\right], \tag{1.1}$$

for any local observables O_A, where the subscript A indicate that the observable has support in the subsystem, A. Such a property is guaranteed if

$$\lim_{t\to\infty} \rho_A(t) = \rho_{stat,A}. \tag{1.2}$$

In particular we will say that the system thermalizes if $\rho_{stat} = \rho_{th}$, with

$$\rho_{th} = \frac{1}{Z} e^{-\beta H}, \tag{1.3}$$

where $Z = \mathrm{Tr} e^{-\beta H}$, and the effective temperature is defined in such a way that

$$E = \mathrm{Tr}\left[\rho(t) H\right] = \frac{\mathrm{Tr}\left[e^{-\beta H} H\right]}{Z}. \tag{1.4}$$

1.3.1 Thermalization in non integrable System

For a classical system the concept of thermalization is strictly connected to the one of *ergodicity*. Let us consider a system of N particles in d dimension, described by a point X in a $(2dN)$ dimensional phase space. The system is ergodic if, given an initial condition $X_0 = (\vec{p}_0, \vec{q}_0)$, its trajectory in the phase space covers uniformly the selected hypersurface of constant energy. If such a condition is satisfied, one can replace time averages with phase space averages weighted with the microcanonical ensemble, i.e.

$$\begin{aligned} \langle O \rangle &= \lim_{T\to\infty} \frac{1}{T} \int_0^T dt\, O(\vec{p}(t), q(\vec{t})) = \\ &= \int d^{dN}p\, d^{dN}q\, O(p,q) \delta\left[H(\vec{q},\vec{p}) - H(\vec{q}_0,\vec{p}_0)\right]. \end{aligned} \tag{1.5}$$

However, defining ergodicity for a quantum system is a non trivial task. Indeed, let us consider a system described by an Hamiltonian with eigenstates $|\psi_a\rangle$ and

eigenvalues E_a. The microcanonical density matrix can then be defined by coarse graining the spectrum on energy shells of width δE, large enough to contain a large number of states, but small on a macroscopic scale. Denoting with $\mathcal{H}(\mathcal{E})$ the set of states within a shell with energies $(E, E+\delta E)$,

$$\rho_{mc}(E) = \sum_{a \in \mathcal{H}(E)} \frac{1}{\mathcal{N}(E)} |\psi_a\rangle \langle\psi_a| , \tag{1.6}$$

where $\mathcal{N}(E)$ is the total number of states contained in each shell.
Let us now take a generic initial state lying within a shell, i. e. $|\psi_0\rangle = \sum_{a\in\mathcal{H}(E)} c_a |\psi_a\rangle$, and let us consider what is the long time average of the density matrix. Assuming that the eigenstates are not degenerate we have

$$\lim_{T\to\infty} \frac{1}{T} \int_0^T dt\, |\psi(t)\rangle \langle\psi(t)| = \sum_a |c_a|^2 |\psi_a\rangle \langle\psi_a| \equiv \rho_{diag}, \tag{1.7}$$

where $|\psi(t)\rangle$ is the time evolution of $|\psi_0\rangle$ and ρ_{diag} is the density matrix describing the so-called *diagonal ensemble*. We immediately notice that the diagonal ensemble coincides with the microcanonical one only if all $|c_a|^2$ are equal, a very special situation. Therefore, quantum ergodicity in the strict sense is almost never realized. Our intuition tells us, however, that, unless some very special conditions are met (e.g. integrability, as we will discuss in more detail in the following) a generic quantum system should eventually thermalize, though the mechanism behind such a process is still under debate [95].
A popular scenario at the present time is the so-called *Eigenstate Thermalization Hypothesis* (ETH), put forward by Deutsch and Sdrenicki [36, 119] in the context of quantum chaotic systems. Their idea is that thermalization occurs eigenstate by eigenstate, namely the expectation values of observables over the eigenstates of the Hamiltonian, $\langle\psi_a| O |\psi_a\rangle$, are smooth function over the Energies E_a, being essentially constant on each microcanonical energy shell. This would ensure thermalization for all initial conditions sufficiently narrow in energy. This hypothesis as been recently put under intense scrutiny by different groups in different system, such as hard-core bosons [61,69,99,100,103], spinless fermions [103], the Bose-Hubbard model [11,72], the Hubbard model [40,41,70], spin chains [11, 39, 120], etc.

As pointed out in [12] there are two possible interpretation of the ETH: a weak one, where the fraction of states with non-thermal averages goes to zero in the thermodynamic limit, and a strong one, where such non-thermal states completely disappear in the thermodynamic limit. In the weak version, not every initial condition (even if narrow in energy) will thermalize, because these non-thermal rare states might be heavily weighted. The issue of the rare states and their role in the road towards thermalization has been debated in literature, see for example [15, 102, 109, 110].

These rare states could play an important role in some known examples of non-integrable model displaying lack of thermalization. For instance in [72] the authors numerically found that the dynamics of the Bose-Hubbard model showed an approach to a non-thermal steady state with strong memory of the initial conditions for large values of the final interaction strength. Strict dependence on the initial states was also observed in one dimensional Ising chain where integrability was broken by applying a finite longitudinal magnetic field [4]. However, in this case numerical results were limited to the case of three spins. An alternative explanation is that the numerical simulation only reach the prethermalized regime, which we will discuss later in more details, and thermalization occurs on much longer times scales.

1.3.2 Integrable Systems: GGE Ensemble

Integrable systems are known to lead to a non ergodic behavior, also in the case of classical physics. The reason is the presence of too many integrable of motion other than energy that do not allow a full exploration of the hypersurfaces of constant energy. Even though the generalization of the concept of integrability to the quantum realm is far from being trivial, see for example [24,121], a quantum integrable system usually has an extensive number of local algebraically independent integrals of motion I_n, which commute one with each other and with the Hamiltonian H of the system, i.e.

$$[I_n, I_m] = 0 = [I_n, H]. \tag{1.8}$$

For this reason, in the spirit of the works by Jaynes on the maximum entropy ensemble [64], Rigol et al. proposed that the stationary state of the dynamics of integrable systems should not be thermal, but rather described by the so-called *generalized Gibbs Ensemble* (GGE) [101], whose density matrix is

$$\rho_{GGE} = \frac{1}{Z} e^{-\sum_n \lambda_n I_n}, \tag{1.9}$$

where $Z = \mathrm{Tr} e^{-\sum_n \lambda_n I_n}$ is the generalized partition function, and the Lagrange multipliers are fixed requiring

$$\langle \psi_0 | \, I_n \, | \psi_0 \rangle = \mathrm{Tr} \left[\rho_{GGE} I_n \right], \tag{1.10}$$

with $|\psi_0\rangle$ representing the initial state.

The definition of the GGE ensemble has also been generalized to the case of integrable field theories by Fioretto and Mussardo [47]. Here there is a precise notion of integrability that is based on the requirement that the system has well-define quasiparticle, whose scattering is purely elastic, i.e. there is no particle production or dissipation [86, 121] Let us consider for simplicity a model with only one type of quasiparticles of mass m described by the annihilation operator $A(\theta)$, satisfying the algebra $A(\theta_i)A(\theta_j) = S(\theta_i - \theta_j)A(\theta_j)A(\theta_i)$, where S is the S-matrix of two-particle scattering, and θ denotes the rapidity, which is related to the energy and the momentum of the quasiparticle by the relations $E = m \cosh \theta$ and $p = m \sinh \theta$. Then we have

$$\rho_{GGE} = \frac{e^{-\int d\theta \lambda(\theta) A^\dagger(\theta) A(\theta)}}{Z}. \tag{1.11}$$

In [47] Fioretto and Mussardo were also able to prove that this density matrix correctly describe the asymptotic value of one-point local observables if the initial state belongs to the class of the so-called squeezed states, which have the form

$$|\psi_0\rangle = \mathcal{N} e^{-\int d\theta K(\theta) A^\dagger(\theta) A^\dagger(-\theta)}. \tag{1.12}$$

The validity of the GGE ensemble as a good description of the asymptotic state reached by integrable systems has been heavily tested and established in the case

of theories equivalent to free fermions of free bosons, e.g. [8,17,25,27,29,46,105]. However, the problem is still open in the case of truly interacting integrable theories [53, 82, 97, 130].

An interesting step in this direction has been recently done in [74], where the authors considered a quench in the Lieb-Lininger model, described by the Hamiltonian

$$H = \int dx \left[\partial_x \phi(x)^\dagger \partial_x \phi(x) + c\phi(x)^\dagger \phi(x)^\dagger \phi(x)\phi(x)\right], \tag{1.13}$$

where $\phi(x)$ is a bosonic field satisfying $[\phi(x), \phi^\dagger(y)] = \delta(x-y)$. They prepared the system in the ground state of the theory for $c = 0$ and then quench the interaction to $c = \infty$, where the model can be described in terms of free fermions. Even though the quench is still between two free theories, the relation between the initial and final Hamiltonians is not linear, and remarkably the GGE still describes the steady state of the system, being able to predict the stationary value of the density density correlation function.

However, more recent works questioned the validity of the GGE in interacting systems. Indeed, though a lot of works tackled the issue of the construction of the GGE for generic integrable models and attempted a comparison with numerical simulations concerning the time evolution of such systems [23, 44, 46, 75, 87, 88, 96, 118], in Refs. [97, 130] quenches in the XXZ model from a Majumdar-Ghosh dimer product or a Néel state, are such that the GGE fails to predict the stationary values of certain correlation functions.

1.4 Prethermalization

Even when the system thermalizes, the dynamics of the thermalization can be highly non-trivial, requiring, at least for certain initial conditions, a two steps process, in which the system passes trough an intermediate state that can be very different from the thermal one. This phenomenon is in general called *prethermalization*. This idea was introduced in 2004 by Berges et al. in the context of high energy physics [9], while for of out of equilibrium quantum many-body systems it was first discussed by Moeckel and Kehrein some years

later [84]: they considered a quench in the Hubbard model at half filling for dimensions greater than one, in which the system started in the non-interacting ground state and then a small interaction was switched on.

Focusing the attention on the momentum distribution functions, the authors were able to identify three different regimes: a short-time regime, related to the formation of quasi-particle, in which the discontinuity at the Fermi surface is quickly reduced to a value smaller than one, an intermediate quasi-stationary regime, whose lifetime is inversely proportional to the strength of the final interaction, in which the momentum distribution function stops evolving and stays similar to a Fermi liquid at zero temperature, and finally a long-time thermalization regime. This prediction was later confirmed using dynamical mean field theory (DMFT) numerical simulations by Eckstein, Kollar and Werner [41], which also revealed the presence of a prethermalized regime for large values of the final interaction, a behavior which can be understood considering the integrability of the model in the infinite interaction limit. After that, prethermalization has been studied and discussed in a variety of different models [43, 68, 80, 83, 90, 126, 129].

For the type of quenches considered above, in which the starting point is an integrable Hamiltonian, and the integrability breaking terms in the final Hamiltonian has a small strength, the concept of prethermalization provides a link between the different stationary behavior of integrable and non-integrable systems discussed in the previous section. Indeed, several groups (with some difference between each other in the details of the construction) have pointed out that the prethermalized regime can be described in terms of a "deformed" GGE, in which the integral of motion are perturbatively constructed starting from the ones possessed by the integrable Hamiltonian and are only approximately conserved [43, 57, 71, 90]. From this point of view, the stationary states reached by integrable systems can be thought as prethermalization plateaus that never decay. Also, a similar mechanism might be able to explain why the dynamics of experimental systems, in which integrability is always only approximately valid, can be described in terms of integrable model: what we observe is the prether-

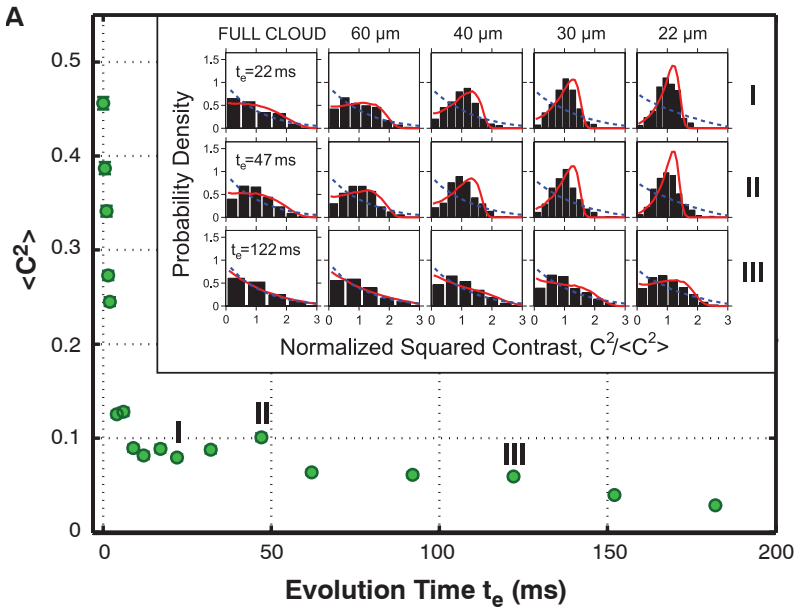

Figure 1.4: *Mean square contrast versus time. After an initial decay a quasi-steady state is approached, which slowly evolves. In the inset experimental full distribution of $C^2/\langle C^2\rangle$ are shown, together with a theoretical equilibrium fit base on Eq. (1.14). Taken from [57].*

malized regime, which is dominated be the physics of the integrable Hamiltonian and non-integrable effects kicks in on much longer time scales.

This has also been partially confirmed by an experiment performed by Schmiedmayer's group in Wien [57, 116]. Here, they started with a 1D Bose gas of ^{87}Rb atoms in the quasi-condensate regime and then rapidly and coherently split it forming two uncoupled 1D Bose gases in a double well potential with almost identical longitudinal phase profiles, in contrast to what happens for two independently created quasi-condensates. The systems was then let evolve for some variable time, after which the gases were released and the interference pattern studied.

Such a pattern is determined by the phase difference $\phi(r)$ between the two quasi-condensate, whose dynamics can be approximately described by the integrable

Tomonaga-Luttinger Hamiltonian [68, 116],

$$H = \frac{\hbar c}{2} \int_{-L/2}^{L/2} dr \left[\frac{K}{\pi} \left(\nabla \phi(r) \right)^2 + \frac{\pi}{K} n^2(r) \right], \tag{1.14}$$

where $K = \pi \xi_h \rho$ is the Luttinger parameter, c is the speed of sound, ξ_h the healing length, ρ the atomic density and L is the length of the system.
The main quantity considered in the experiment to characterize the interference pattern was the integrated interference contrast

$$C^2(L) = \frac{1}{L} \left| \int_{-L/2}^{L/2} dr e^{i\phi(r,t)} \right|^2. \tag{1.15}$$

As shown in Fig. 1.4 its average value shows an initial rapid decay on a time scale $\simeq 10\,\text{ms}$, followed by the emergence of a quasi-steady state slowly evolving on a much slower scale. To probe the nature of such a steady-state the authors analyzed the full distribution function $P(C^2)$, finding a remarkable agreement with the theoretical equilibrium distribution after the initial decay (see the inset of Fig. 1.4), i.e. $t > 12\text{ms}$, so that they were able to extract an effective temperature, whose value was around 14 nK (slowly increasing in time due to the heating of the atom trap), roughly a factor five lower than the temperature of the unsplit system. Thus, the observed state could not be the thermal equilibrium of the entire system.
Looking at the Hamiltonian (1.14) the decay towards a stationary state can be understood as the result of the dephasing between the k modes in terms of which the Hamiltonian is diagonal. By solving the model one finds a temperature that is very close to experimental result. Thus, a prethermalized regime is observed and such a prethermal state is well described as the stationary state of an integrable Hamiltonian. The system is expected to eventually reach thermal equilibrium trough processes not described by Eq. (1.14), such as, for example, three-body scattering, but at time-scales much longer than the dephasing time-scale.
To conclude, at the hearth of the two step thermalization scenario there is the existence of a clear separation of time scales. The first stage is dominated by

the dephasing time, whereas the second stage is dominated by inelastic scattering collisions. At least, this is the picture emerging in the case of the quench starting from an integrable Hamiltonian. The phenomenon of prethermalization, however, seems to be more general, as suggested by the original paper by Berges et al. [9], where a low-energy quark-meson model was considered, or by recent studies via DMFT of quenches between the antiferromagnetic and paramagnetic phases of the Hubbard model [126, 129] and we can fairly state that comprehensive theory is still lacking. It is not clear, for example, what are in general the scales regulating the prethermalization and thermalization stages, and what are the condition for the prethermalization to happen. A possible explanation could be that prethermalization occurs when the dynamics takes the system close to a so-called non-thermal fixed point [10], which in the case of the switching on of a non-integrable term in the Hamiltonian would be simply given by the integrable part, but in general could also occur in non-integrable models.

1.5 Dynamical Phase Transitions

The existence of prethermal states, different from their thermal counterpart, opens the way to the possibility of observing new inherently out of equilibrium critical properties, or dynamical phase transition, generalizing the equilibrium ones between different dynamical regimes, or/and quasi-steady states of different nature. This could in principle allow to observe universal (in the usual sense of statistical mechanics) phenomena out of equilibrium.
The first example of this has been discovered in Ref. [41]. As discussed in the previous section, the authors solve with DMFT the dynamics of the Hubbard model at half-filling,

$$H(t) = \sum_{ij\sigma} V_{ij} c^\dagger_{i\sigma} c^\dagger_{j\sigma} + U \sum_i \left(n_{i,\uparrow} - \frac{1}{2} \right) \left(n_{i,\downarrow} - \frac{1}{2} \right), \tag{1.16}$$

where the $c_{i,\sigma}$'s are fermionic operators satisfying $\left\{ c_{i,\sigma}, c^\dagger_{j,\sigma'} \right\} = \delta_{i,j}\delta_{\sigma,\sigma'}$, $\{c_{i,\sigma}, c_{j,\sigma'}\} = 0$, $n_{i,\sigma} = c^\dagger_{i,\sigma} c_{i,\sigma}$, and the hopping amplitudes V_{ij} corresponding to a semielliptic

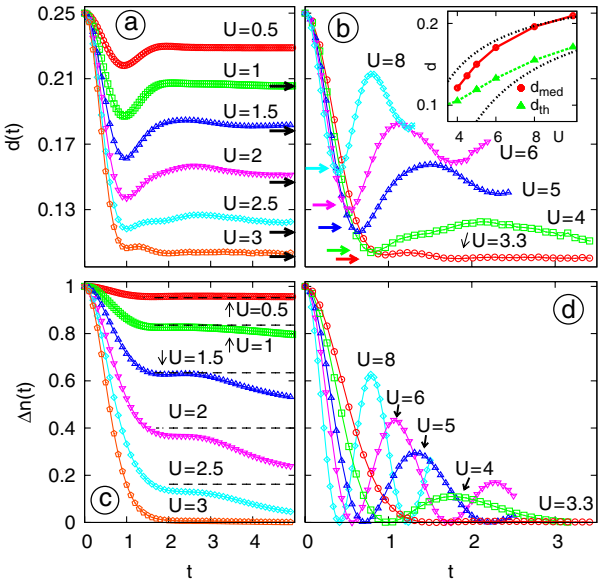

Figure 1.5: *Evolution of the double occupation $d(t)$ and the Fermi surface discontinuity $\Delta n(t)$ for quenches with $U \leq 3$ (left panels) and $U \geq 3.3$ (right panels). Horizontal arrows show the thermal values of the double occupation. Taken from [41].*

density of states $\rho(\epsilon) = \sqrt{4V^2 - \epsilon^2}/(2\pi V)$ were chosen. The system was prepared in the ground state of the noninteracting Hamiltonian $U = 0$ and then a quench to a finite positive value of U was performed.

The existence of two different (prethermalized) regimes separated by a sharp crossover at $U_c \simeq 3.2V$ was established. This can be seen by studying the evolution of the double occupation $d(t) = \langle n_{i\uparrow}(t) n_{i,\downarrow} \rangle$, and the discontinuity in the momentum distribution function at the Fermi energy $\Delta n(t)$. From Fig. 1.5 we can see that in the weak coupling regime, i.e. $U < U_c$ the double occupation relaxes almost to its thermal value, which is indicated by an arrow, while $\Delta n(t)$ stays on a prethermal plateau (its thermal value would be zero) for a time that is the longer the smaller is U and then slowly decays. For strong couplings, instead, both quantities show oscillations, which are not centered around their thermal values. These two different regimes are separated by a small region $3V \lesssim U \lesssim 3.3V$ in which fast thermalization is observed.

A confirmation of such a behavior was then found by Schiró and Fabrizio [111].

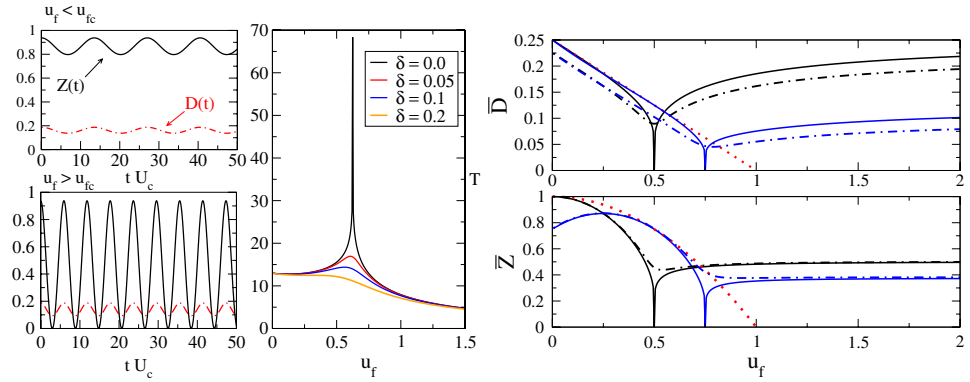

Figure 1.6: *$u_{i,f} = U_{i,f}/U_c$, where U_c equals the equilibrium critical point. (a) Left panel: evolution of the double occupation $D(t)$ and the quasiparticle residue $Z(t)$ from quenches to $u_i = 0.25$ to $u_f = 0.35$ (top panel) and $u_f = 1.25$ (bottom panel). Right panel: period of oscillations for finite doping δ. Note that there is a logarithmic singularity only when $\delta = 0$. (b) Average double occupation $\bar{D}$ and quasiparticle residue $\bar{Z}$ as a function of u_f for fixed $u_i = 0.0, 0.5$ Full lines are zero doping results, while dashed lines are finite doping results. The red points are zero temperature equilibrium results. Taken from [111]*

They considered the same Hubbard Hamiltonian (1.16) with nearest neighbors hopping, and solve the dynamics following a quench of the interaction parameter from U_i to $U_f > U_i$ trough an out of equilibrium Gutzwiller ansatz, limiting themselves to homogeneous paramagnetic wavefunction. Such an approximation is valid in the limit of an infinite coordination lattice. Focusing on the evolution of the double occupation ($D(t)$ in their notation), and the quasiparticle residue ($Z(t)$ in their notation), they also find two different behavior. As shown in Fig. 1.6a for $U_f < U_{f,c}$, whose values depends on the initial interaction U_i, both $D(t)$ and $Z(t)$ displays small oscillations with amplitude and period increasing with the amplitude of the quench ($U_f - U_i$), while for $U_f > U_{f,c}$ the oscillations of $Z(t)$ have a big amplitude with the minimum being equal to zero, and the period and amplitude are now decreasing function of the quench amplitude. These two regimes are separated by a critical point, where the dynamics shows exponential relaxation, while the period of oscillations diverges logarithmically, as can be seen in Fig. 1.6a. Moreover, they considered the long-time averages of both quantities $\bar{D}$ and $\bar{Z}$ showing that they have a singular behavior, vanishing as the inverse of a logarithm when the dynamical transition point is approached. Their behavior is shown if Fig. 1.6b.

One should stress that, being the Gutzwiller ansatz a mean-field approach, no true relaxation can be observed, so that, differently from the DMFT study (which can treat all local fluctuations exactly), oscillations are never dumped, and the transition occurs in the steady-state of the dynamics and not in the prethermal regime. However, we can imagine that when quantum fluctuations are taken into account true relaxation towards a thermal state will eventually happen.

After these findings in the Hubbard model, such a dynamical transition has been observed in a variety of mean-field models [49, 81, 112, 113] and also in the dynamics of the Hubbard model for quenches between the antiferromagnetic and paramagnetic phase studied both by DMFT [126] and by the Gutzwiller ansatz [108]. A full analysis and characterization, however is still lacking, as well as a full understanding of its critical properties and the role of fluctuations.

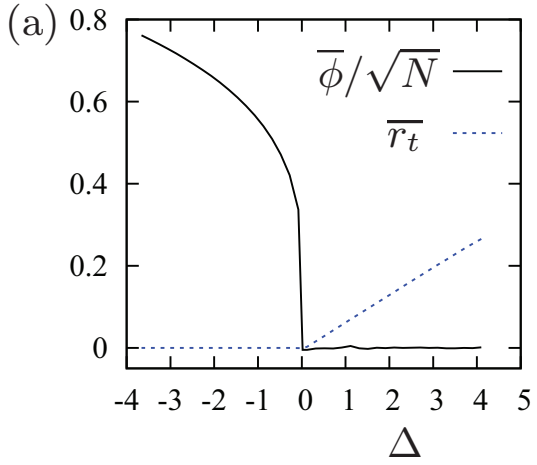

Figure 1.7: *Long time average of the order parameter $\bar{\varphi}/\sqrt{N}$, with N being the number of components of the $O(N)$ model, as a function of the relative distance from the dynamical critical point (in %). Taken from [114].*

A recent attempt to go beyond mean-field has been done by Sciolla and Biroli [114]. They considered an $O(N)$ model at the leading order in the $1/N$ expansion (more detail on the model in chapter 3) and focused on quenches starting from the broken symmetry phase. They found that the model displays true relaxation towards a steady state, which, however, was not the thermal one, because the model still possesses an infinite number of conservation laws that prevents thermalization. They also observed the presence of a dynamical transition with a critical point that depends on the initial point, but is always within the broken symmetry phase. Such a transition is signaled by the vanishing of the asymptotic value (or equivalently of its long-time average) of the order parameter ($\bar{\phi}$) as shown in Fig. 1.7. Remarkably, the order parameter does not vanish in a logarithmic fashion, as it is typical in mean field models, but with a power law, i.e. $\bar{\phi} \sim 1/\Delta^{1/4}$, with Δ measuring the distance of the final parameter of the quench from the critical point. They also reported the existence of a dynamical transition for quenches starting in the paramagnetic phase.

To conclude, we can say that the nature of this transition and the condition for it to be present (e.g., is it necessary that the model as a finite temperature

transition?) are still unclear. A possibility, as in the case of prethermalization, to which it seem to be related, is that is connected to the physics of nonthermal fixed points [10]. However, further studies are needed before anything can be concluded.

1.6 This Thesis

This rest of the thesis is organized in the following way. In Chapter 2 we will first introduce the statistics of the work as a tool to describe the dynamics of quantum many-body systems and then study it for generic protocols in the quantum Ising chain and in the Gaussian field theory. In particular, we will show that its low-energy behavior shows features that are independent from the details of the protocol, therefore "time universal".

In Chapter 3 we will discuss the dynamical phase transition in the $O(N)$ vector model in the limit $N \to \infty$, characterizing its critical properties and showing its strong connection with the statistics of the excitations produced in a double quench studied as a function of the waiting time. Then, we will also study how and if such critical properties are changed a linear ramp in time is performed instead of a sudden quench.

Finally, in Chapter 4 we will discuss the emergence of a non adiabatic behavior in the dynamics of the order parameter in a low-dimensional quantum many-body system subject to a linear ramp of one of its parameter within a gapped phase. This problem will be studied in details in the case of a quantum Ising chain, where the transverse field is changed in time.

Chapter 2

Work distribution for generic protocols

2.1 Statistics of the work and its general features

There are many different ways in which the dynamical response of an isolated quantum many-body systems subject to a variation of one or more parameters of its Hamiltonian according to a generic protocol $\boldsymbol{\lambda}(t)$ can be probed (see section 1.2). From a fundamental point of view, however, every protocol can be thought of as a thermodynamic transformation and can therefore be characterized by the work done on a system [115], the entropy produced and the heat that has been exchanged. Since we are dealing with isolated systems, we will focus on the work W, which characterizes the energy spectrum of the excitations generated during the dynamics and in generic out of equilibrium transformations will be a fluctuating quantity characterized by a probability distribution $P(W)$.

In order to describe such a distribution, we have to make more precise the notion of work done on the system. In general, to determine the value of W in a closed system is enough to measure the energy twice: at the initial time $t = 0$ and at the end of the protocol, i.e. at time $t = \tau$ (or any time afterwards, since the

energy is conserved). The work will be then given by the difference between the two results [19, 123]. So, let us imagine that the systems is initially in a thermal state $\rho_0 = e^{-\beta H[\boldsymbol{\lambda}_i]}/Z$ and let us denote with $|n\rangle_t$ the instantaneous eigenvectors of the Hamiltonian with eigenvalues $E_n(t)$, i.e.,

$$H[\boldsymbol{\lambda}(t)]\,|n(t)\rangle = E_n(t)\,|n\rangle_t\,. \tag{2.1}$$

Then, the probability of the work will in general have the following expression,

$$P(W) = \sum_{n,m} \delta\left[W - E_n(\tau) - E_m(0)\right] p_{n|m}\, p^0_m, \tag{2.2}$$

where

$$p^0_m = g_m e^{-\beta E_m(0)}/Z, \tag{2.3}$$

with g_n being the degeneracy of $|n\rangle_0$, is the probability that the first measurement gives $E_m(0)$ as a result, while

$$p_{n|m} = \mathrm{Tr}\left[\Pi_n(\tau)\rho_m(\tau)\right] \tag{2.4}$$

is the probability that the second measurement gives $E_n(\tau)$ as a result, conditioned over the result of the first measure. Here $\Pi_n(t)$ is the projector on the eigenvectors belonging to the eigenvalue $E_n(t)$, while $\rho_m(\tau)$ is the evolved density matrix after the measurement at $t = 0$, which is equal to $U(\tau)\rho_m U(\tau)^\dagger$, with $U(\tau)$ representing the evolution operators from time $t = 0$ to time $t = \tau$ and $\rho_m = \Pi_m(0)\rho_0\Pi_m(0)$. Such a definition can of course be easily generalized to different initial states by changing the probability p^0_m accordingly.

The probability distribution function (2.2) can be showed to obey a series of fluctuations relations. The most notable example is the Tasaki-Crooks fluctuation theorem [19, 124]. This is a relation between the distribution of the work performed starting from the thermal state corresponding to the initial Hamiltonian $H[\boldsymbol{\lambda_i}]$ at inverse temperature β, and the probability distribution $\tilde{P}(W)$ associated with the inverse protocol $\tilde{\boldsymbol{\lambda}}(t) = \boldsymbol{\lambda}(\tau - t)$ in which the initial state is the thermal state corresponding to the final Hamiltonian $H[\boldsymbol{\lambda_f}]$ at the same inverse temperature. In particular, we have

$$\frac{P(W)}{\tilde{P}(W)} = e^{\beta(W-\Delta F)}, \tag{2.5}$$

where $\Delta F = -\beta \log Z(\boldsymbol{\lambda}_f)/Z(\boldsymbol{\lambda}_i)$ is the free energy difference between the two equilibrium states.
By multiplying both sides of Eq. (2.5) by $\tilde{P}(W)e^{-\beta W}$ and integrating over W, it is possible to obtain the well-known Jarzynski equality [63],

$$\langle e^{-\beta W} \rangle = e^{-\beta \Delta F}. \tag{2.6}$$

These two relations establish a connection between non-equilibrium and equilibrium quantities. For example, Eq. (2.6) tells us that equilibrium free energies can be derived by measuring the nonequilibrium work in many realization of the same protocol, a property that has been used in real experiments [28, 38, 79].
In the following we will always assume that the system is initially prepared in the ground state $|0\rangle_0$ of the initial Hamiltonian $H[\boldsymbol{\lambda}_i]$, so that $p^0_m = \delta_{0,m}$ and expression (2.2) simplifies into

$$P(W) = \sum_n \delta \left[W - E_n(\tau) + E_0(0)\right] |_\tau\langle n|U(\tau)\,|0\rangle_0|^2, \tag{2.7}$$

It is apparent from this expression that the $P(W)$ has a threshold value given by $E_0(\tau) - E_0(0)$, namely the difference between the final and initial ground state energies. From now on we will consider the rescaled variable $W \to W - E_0(\tau) + E_0(0)$, in such a way that $W \geq 0$.
An equivalent statistical description can be given in terms of the moment generating function $G(s)$,

$$G(s) = \langle e^{-sW} \rangle, \tag{2.8}$$

We can distinguish here between two classes of systems: a class A in which the spectrum is bounded and the the work W for large but finite L can not exceed a certain threshold value W_L and a class B in which the spectrum in unbounded and also for finite systems the work can assume arbitrarily large values. Then, in the former class $G(s)$ is defined for all $s \in \mathbb{R}$, with $G(s) \simeq e^{-sL^d W_L}$ for $s \to -\infty$, whereas in the latter class $G(s)$ is defined only for $s > -\bar{s} < 0$ with a generic singularity in the derivative at $-\bar{s}$. The quantum Ising chain and the Gaussian field theory that we will consider in the following belong to class A and B respectively.

Using expression (2.7), we obtain that

$$G(s) = \langle\psi(\tau)|\, e^{-s\tilde{H}[\boldsymbol{\lambda}(\tau)]}\, |\psi(\tau)\rangle\,, \tag{2.9}$$

where $\tilde{H}[\boldsymbol{\lambda}_f] = H[\boldsymbol{\lambda_f}] - E_0(\tau)$ is the rescaled final Hamiltonian and $|\psi(\tau)\rangle = U(\tau)\,|0\rangle_0$ is the evolution up to time τ of the initial state.

Following Refs. [50] [51] we can use the quantum to classical correspondence to interpret the function $G(s)$ for $s > 0$ as the partition function in a $d+1$ dimensional slab, of thickness s of a classical system, with transfer matrix $e^{-\tilde{H}[\boldsymbol{\lambda}_f]}$ and equal boundary conditions described by the state $|\psi(\tau)\rangle$. If we now introduce the cumulant generating function $F(s) = \log G(s)$, we can interpret it (up to a minus sign) as the free energy of such a system. Considering for the moment the case of a global protocol, which in general will inject in the system an extensive amount of energy, it is useful to consider the free-energy density per unit area $f(s) = -L^{-d}F(s)$, which can be decomposed in decreasing powers of s as

$$f(s) = 2f_s + f_c(s). \tag{2.10}$$

The bulk contribution, which would be proportional to s, is here absent because of the rescaling of the variable W performed before, while f_s is the surface free energy associated to the two identical boundaries and $f_c(s)$ is the Casimir effect contribution, describing the interaction between the two boundaries, which goes to zero for large values of s.

We can now discuss some general features of the probability distribution $P(W)$: first of all in any system Eq. 2.7 implies that $P(W)$ has a peak at the origin, with spectral weight $P_0 = e^{-2L^d f_s} = |\langle\psi(\tau)|0\rangle_\tau|^2$. This is just the probability of ending up in the ground state of the final Hamiltonian, a quantity also known as fidelity. In order to exploit the quantum to classical correspondence it is useful to introduce a quantity resembling the free energy, the *normalized logarithmic fidelity* per unit volume, defined as

$$\hat{f}_s = \ln|\langle\psi(\tau)|0\rangle_\tau| L^{-d}\frac{(2\pi)^d}{\Omega_d}, \tag{2.11}$$

where Ω_d is the solid angle in d dimensions.

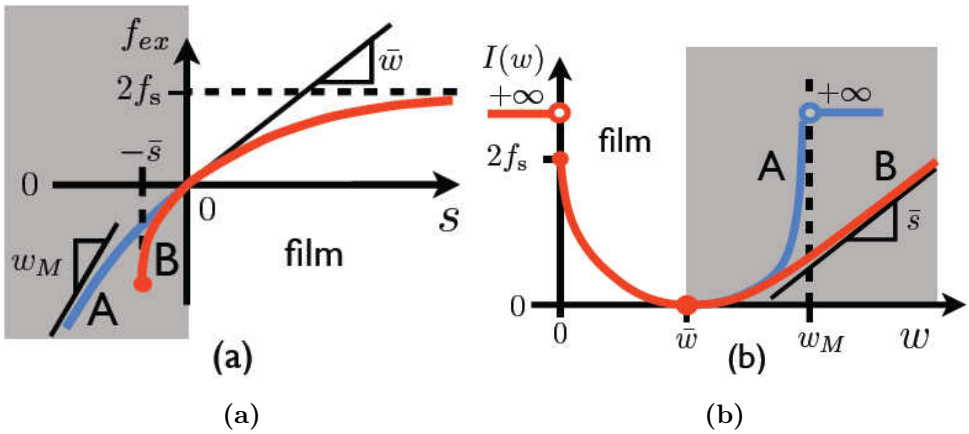

(a) (b)

Figure 2.1: *Schematic representation of (a) $f(s)$ and of the rate function $I(w)$ for systems in class A (blue) and class B (red). The grey area highlights the region where $f(s)$ lacks a thermodynamic interpretation. Taken from [51].*

In addition to this peak, one expects some features starting at $W = \Delta$, where Δ represents the minimum energy gap of the final Hamiltonian. The behavior close to this threshold will be determined by the behavior of f_c for large values of s. In the case of sudden quenches ending in the vicinity of the critical point this features turn out to be a power-law edge singularities related to the so-called *critical Casimir effect* [76] and thus universal in the usual sense of critical phenomena [50, 51], i.e., dependent only on the bulk universality class of the model and on the characteristics of the initial (boundary) state. These singularities, in the case of global protocols, are, however, relevant only in the case of finite size systems, since their weight is exponentially suppressed by the volume.

In order to better see this it is convenient to consider intensive quantities, such as the work density $w = W/L^d$, whose statistics we will denote as $p(w)$. For global protocols the work done on the system is a extensive quantity, therefore as the size of the system increases $p(w)$ will become strongly peaked around its average value $\bar{w}$, with fluctuations scaling as $1/\sqrt{V}$, with V being the volume of the system. Therefore in this case it is interesting to study what are the large

fluctuation of $p(w)$ with respect to the Gaussian distribution. The key quantity to study in this context is the so-called rate function $I(w)$, whose importance is given by the fact that for $L \to \infty$, $p(w) \sim \exp[-L^d I(w)]$ [125]. Since in the limit of large L we can perform the inverse Laplace transform via a saddle-point approximation, the rate function turns out to be given by the Legendre-Fenchel transform of $f(s)$,

$$I(w) = -\inf_s[sw - f(s)], \tag{2.12}$$

with the minimum taken on the region of definition of $G(s)$. Some generic feature of the distribution $p(w)$ can then be inferred. First of all we note that $f(0) = 0$ and $f'(0) = \bar{w}$ and, most importantly $f(s)$ is a concave function of s [125], which approaches $2f_s$ when $s \to \infty$. Fig. 2.1 shows a schematic representation of $f(s)$ and the corresponding $I(w)$ for the the two classes of systems introduced above. The behavior of $I(w)$ near the threshold $w = 0$ is determined by the one of $f(s)$ for $s \to \infty$. In particular $I(0) = 2f_s$, while its approach to this value is determined by $f_c(s)$.

Thanks to the quantum to classical correspondence the function $f_c(s)$ when the final Hamiltonian is near to a critical point are take a universal scaling form, due to the onset of the critical Casimir effect. Therefore, one can conclude that the behavior of the rate function $I(w)$ near the threshold $w = 0$ is universal, so that universal effects can be seen in the large deviations below the average density of the work $\bar{w}$.

Increasing w further away from its average value, the value $s^\star(w)$ at which the minimum of Eq. (2.12) is attained decreasing and so thus the thickness of the associated slab. Therefore, microscopic details are expected to play an increasingly important role, implying a generic lack of universality. Correspondingly also $I(w)$ decreases because $I'(w) = -s^\star(w)$. At the average value $w = \bar{w}$, $s^\star = I(\bar{w}) = 0$, while increasing w the rate function grows again with $s^\star(w) < 0$. Therefore, in the case of $w > \bar{w}$ the rate function is determined by the the function $f(s)$ for $s < 0$, where we can not use the quantum to classical correspondence any more, so it seems that no universal behavior can appear. The qualitative behavior of the rate function in this region depends crucially on

the possibility that the spectrum of the system is bound (class A) or unbound (class B). For systems in class A $I(w)$ diverges approaching $w_N = W_L/L^d$, as required by the fact that $p(w)$ vanishes above this threshold, while in the case B $I(w \to \infty) \simeq \bar{s}w$ and therefore

$$p(w \gg \bar{w}) \sim e^{-L^d \bar{s} w} \tag{2.13}$$

In Ref. [51] it was argued that for systems in the class B an unexpected universal behavior may be possible also in this fully quantum regime. As we will explain in more details later, they explicitly showed that for a quench in a free bosonic theory when the initial mass m_0 approaches the critical point $m_0 rightarrow 0$, the statistics of the density of the work shows a behavior similar to the Bose-Einstein condensation in the grancanonical canonical ensemble, displaying a transition from an exponential to an algebraic behavior.

When local protocols are considered, instead, the situation is different as a result of the fact that in this case the work done is not an extensive quantity. Local quenches are nevertheless interesting to study in the case of gapless systems, where even a local change of the Hamiltonian can have important effects. In particular, if we exclude cyclic protocols, i.e. $\boldsymbol{\lambda}_f = \boldsymbol{\lambda}_i$, we expect $P(W)$ not to have a delta peak at origin, namely the probability to end up in the final ground state will be zero, as consequence of a rather generic Anderson orthogonality catastrophe [3]. In analogy to the turning on of a potential in a Fermi system, we thus expect the presence of an edge singularity starting at $W = 0$ whose specific form will be determined by the large s behavior of $\log G(s)$.

In the following we will compute the statistics of the work for generic protocols and for global and local variations of the system parameters in a Gaussian field theory and in the quantum Ising chain, showing how the general features discussed above emerges in such simple systems. One of the main universal features emerging for abrupt quantum quenches, a power law edge singularity characterizing the low-energy part of $P(W)$, is shown to be hardly sensitive to the details of the protocol considered, being characterized by an exponent that depends only on the initial and final values of the parameter being varied.

Moreover we show that the above-mentioned condensation transition is robust with respect to the choice of the protocol.

2.2 Global protocols in the Gaussian field theory

Let us start by considering the case of a generic protocol in a boson system diagonalizable in independent momentum modes,

$$H_B[m(t)] = \frac{1}{2}\int \frac{d^d k}{(2\pi)^d}\left[\pi_k^2 + \omega_k^2(t)\phi_k^2\right], \tag{2.14}$$

where the integral runs over the first Brillouin $|k| < \pi$, $[\phi_k, \pi_{k'}] = i\delta_{k,k'}$, and we assume a relativistic dispersion relation $\omega_k(t) = \sqrt{k^2 + m^2(t)}$. This simple model captures the physics of a number of physical systems, ranging from ideal harmonic chains to the low-energy properties of interacting fermions and bosons in one dimension [26] and split condensates [58, 59, 68]. We will considering the case of a generic protocol starting from $m(0) = m_i$ and finishing at $m(\tau) = m_f$. We notice that the case of a sudden quench has been solved in Ref. [117].
Since in the Hamiltonian (2.14) the single k modes are independent, the moment generating function factorizes, i.e., $G(s) = \prod_k G_k(s)$, where $G_k(s)$ represents the moment generating function of single mode, which is nothing else than that of an harmonic oscillator with a time-dependent frequency $\omega_k(t)$. Let us therefore quickly consider the problem of computing the moment generating function in such a simple system (see also Ref. [33] for an alternative derivation).

2.2.1 Single harmonic oscillator

Following the discussion above, we will now consider a single harmonic oscillator with generic time-dependent frequency $\omega(t)$, whose Hamiltonian reads

$$H_o(t) = \frac{1}{2}p^2 + \frac{1}{2}\omega^2(t)x^2, \tag{2.15}$$

with $\omega(0) = \omega_i$ and $\omega(\tau) = \omega_f$. The operators x and p are the usual position and momentum operators, satisfying the canonical commutation relation $[x, p] = i$. At each time t we can diagonalize the instantaneous Hamiltonian introducing the bosonic operators

$$\begin{aligned} a_t &= \sqrt{\frac{\omega(t)}{2}}\left(x + \frac{i}{\omega(t)}p\right), \\ a_t^\dagger &= \sqrt{\frac{\omega(t)}{2}}\left(x - \frac{i}{\omega(t)}p\right), \end{aligned} \tag{2.16}$$

which obey the commutation relation $[a_t, a_t^\dagger] = 1$. In terms of such operators the Hamiltonian can be written as

$$H_o(t) = \omega(t)\left(a_t^\dagger a_t + \frac{1}{2}\right). \tag{2.17}$$

As already stated in section 2.1, we assume that the initial state is the ground state of the initial Hamiltonian $H_o(0)$, denoted as $|0\rangle_0$ and defined by the property $a_0 |0\rangle_0 = 0$.

In order to compute the moment generating function $G_o(s)$ using Eq. (2.9), it is convenient to write the evolved state $|\psi(\tau)\rangle$ in terms of the operators $a_\tau^\dagger$ and a_τ diagonalizing the final Hamiltonian $H_o(\tau)$. With this purpose in mind we introduce a time-dependent operator $\tilde{a}(t)$ annihilating the state evolved up to to time t, i.e., $|\psi(t)\rangle = U(t)|0\rangle_0$,

$$\tilde{a}(t)|\psi(t)\rangle = 0. \tag{2.18}$$

The existence of such an operator is guaranteed because we are dealing with a quadratic Hamiltonian, implying that Gaussian states retain their nature during the evolution. Moreover, this operator is characterized by being constant in the Heisenberg representation (as long as we confine ourselves in the subspace spanned by $|\psi(t)\rangle$). Indeed if we take the time derivative of Eq. (2.18) we get

$$\begin{aligned} 0 &= \left(i\frac{\partial}{\partial t}\tilde{a}(t)|\psi(t)\rangle + \tilde{a}(t), H_o(t)\right)|\psi(t)\rangle \\ &= \left(i\frac{\partial}{\partial t}\tilde{a}(t)|\psi(t)\rangle + [\tilde{a}(t), H_o(t)]\right)|\psi(t)\rangle, \end{aligned} \tag{2.19}$$

where we used Eq. (2.18), which, in the subspace required, clearly implies

$$i\frac{d}{dt}\tilde{a}^H(t) = 0, \tag{2.20}$$

where $\tilde{a}^H(t) = U^\dagger(t)\tilde{a}(t)U(t)$ is the operator $\tilde{a}(t)$ in Heisenberg representation (the superscript H will be used in the following always to indicate the Heisenberg evolution of an operator). We can thus drop the time dependence of such an operator in the following.

Remembering that our goal is to write the evolved state $|\psi(\tau)\rangle$ in terms of the operators a_τ and $a_\tau^\dagger$ we now try to find a relation between $\tilde{a}(\tau)$, which annihilates $|\psi(\tau)\rangle$ and the operators $\tilde{a}(t)$ and $\tilde{a}^\dagger(t)$. Let us make the ansatz,

$$a_\tau^H(t) = \alpha(t)\tilde{a}^H + \beta^\star(t)\tilde{a}^{\dagger,H}, \tag{2.21}$$

with α and β being generic complex functions. Let us now try to find an equation determining the coefficients of Eq. (2.21).

In order to do so, we first derive the equation of motion for $a_\tau^H(t)$ and $a_\tau^{\dagger,H}(t)$. The first step is to use the single boson Bogoliubov transformation

$$a_t = \frac{1}{2}\left(\sqrt{\frac{\omega_f}{\omega(t)}} + \sqrt{\frac{\omega(t)}{\omega_f}}\right)a_\tau - \frac{1}{2}\left(\sqrt{\frac{\omega_f}{\omega(t)}} - \sqrt{\frac{\omega(t)}{\omega_f}}\right)a_\tau^\dagger, \tag{2.22}$$

to rewrite the Hamiltonian (2.17) as

$$H_o(t) = \frac{\omega_f^2 + \omega^2(t)}{2\omega_f}a_\tau^\dagger a_\tau + \frac{\omega^2(t) - \omega_1^2}{4\omega_f}\left(a_\tau^2 + {a_\tau^\dagger}^2\right) + \text{const.} \tag{2.23}$$

We can now easily compute the commutator $[a_\tau, H_o(t)]$, obtaining the desired evolution equation

$$i\frac{d}{dt}a_\tau^H(t) = \frac{\omega_f^2 + \omega(t)^2}{2\omega_f}a_\tau^H(t) + \frac{\omega^2(t) - \omega_f^2}{2\omega_f}[a_\tau^\dagger(t)]^H. \tag{2.24}$$

Now by putting these equations into Eq. (2.21) and using the condition (2.18) we can find the desired evolution equation for the coefficients $\alpha(t)$ and $\beta(t)$,

$$i\frac{d}{dt}\alpha(t) = \frac{\omega_f^2 + \omega^2(t)}{2\omega_f}\alpha(t) + \frac{\omega^2(t) - \omega_f^2}{2\omega_f}\beta(t), \tag{2.25a}$$

$$i\frac{d}{dt}\beta(t) = -\frac{\omega_f^2 + \omega^2(t)}{2\omega_f}\beta(t) + \frac{\omega_1^2 - \omega^2(t)}{2\omega_f}\alpha(t). \tag{2.25b}$$

Since an obvious consequence of Eq. (2.20) is $\tilde{a}^H = \tilde{a}(0) = a_0$, the initial conditions for the differential Eqs. (2.25) are given by the coefficients of the Bogoliubov transformation connecting the operators that diagonalize the Hamiltonian at final time $t = \tau$ and at the initial time $t = 0$. These can be read from Eq. (3.31), getting

$$\alpha(0) = \frac{1}{2}\left(\sqrt{\frac{\omega_f}{\omega_i}} + \sqrt{\frac{\omega_i}{\omega_f}}\right),\ \beta(0) = \frac{1}{2}\left(\sqrt{\frac{\omega_f}{\omega_i}} - \sqrt{\frac{\omega_i}{\omega_f}}\right). \tag{2.26}$$

We have now all the ingredients to write the evolved state $|\psi(\tau)\rangle$ in terms of a_τ and $a_\tau^\dagger$.Since this state is annihilated by $\tilde{a}(\tau)$, whose relation with a_τ and $a_\tau^\dagger$ can be read translating Eq. (2.21) at time τ into the Schroedinger picture, that is,

$$a_\tau = \alpha(\tau)\tilde{a}(\tau) + \beta^\star(\tau)\tilde{a}^\dagger(\tau), \tag{2.27}$$

it must be quadratic in terms of a_τ, therefore let us write it as $|\psi(\tau)\rangle = C\exp\left(\rho(a_\tau^\dagger)^2\right)|0\rangle_\tau$, with $|0\rangle_\tau$ representing the final ground state, i.e. $a_\tau|0\rangle_\tau = 0$. The request $\tilde{a}(\tau)|\psi(\tau)\rangle$ implies

$$\begin{aligned} &C\left(\alpha^\star(\tau)a_\tau - \beta^\star(\tau)a_\tau^\dagger\right)\exp\left(\rho(a_\tau^\dagger)^2\right)|0\rangle_\tau = \\ &C\exp\left(\rho(a_\tau^\dagger)^2\right)\left(2\rho\alpha^\star(\tau)a_\tau^\dagger - \beta^\star(\tau)a_\tau^\dagger\right)|0\rangle_\tau = 0, \end{aligned} \tag{2.28}$$

from which we can readily read $\rho = \beta^\star(\tau)/(2\alpha^\star(\tau))$. The value of C is found by requiring the normalization of the state. Indeed, one can easily find that

$$1 = \langle\psi(\tau)|\psi(\tau)\rangle = |C|^2|\alpha(\tau)|, \tag{2.29}$$

implying $C = 1/\sqrt{|\alpha(\tau)|}$. Putting all together, we find

$$|\psi(\tau)\rangle = \frac{1}{\sqrt{|\alpha(\tau)|}}\exp\left(\frac{\beta^\star(\tau)}{2\alpha^\star(\tau)}(a_\tau^\dagger)^2\right)|0\rangle_\tau, \tag{2.30}$$

Since we have now expressed the evolved state in terms of the operators that diagonalize the final Hamiltonian, we can readily compute $G_o(s)$ from Eq. (2.9).

A method for doing so is using the coherent states [117]. Indeed we define the states

$$|z\rangle = e^{za_\tau^\dagger} |0\rangle_\tau , \tag{2.31}$$

with z being a generic complex number, which are unnormalized eigenstates of the operator a_τ with eigenvalue z and satisfy the closure relation

$$\int \frac{dzdz^\star}{2\pi i} e^{-zz^\star} |z\rangle \langle z| = 1. \tag{2.32}$$

Then using the property $e^{-s\tilde{H}_o(\tau)} |z\rangle = |ze^{-s\omega_f}\rangle$ we get

$$G_o(s) = \int \frac{dzdz^\star}{2\pi i} \langle \psi(\tau)|ze^{-s\omega_f}\rangle \langle z|\psi(\tau\rangle e^{-zz^\star}. \tag{2.33}$$

Finally, using

$$\langle z|\psi(\tau)\rangle = \frac{1}{\sqrt{|\alpha(\tau)|}} e^{\frac{\beta(\tau)}{2\alpha(\tau)^\star} z^{\star 2}}, \tag{2.34}$$

and performing the gaussian integral, we obtain

$$G_o(s) = \frac{1}{|\alpha(\tau)|\sqrt{1-|\lambda(\tau)|^2 e^{-2s\omega_1}}}, \tag{2.35}$$

with $\lambda(\tau) = \frac{\beta(\tau)}{\alpha(\tau)}$, which is defined for $s \geq \frac{\ln|\lambda(\tau)|}{\omega_f}$.

2.2.2 Full moment generating function

Using the result of the previous section and remembering that $G(s) = \prod_k G_k(s)$, with $G_k(s) = G_o(s)$, with the substitution $\omega(t) \to \omega_k(t)$, we can write down the full cumulant generating function,

$$\frac{\ln G(s)}{L^d} = -\frac{1}{2} \int \frac{d^d k}{(2\pi)^d} \ln \left[\frac{1-|\lambda_k(\tau)|^2 e^{-2s\omega_k(\tau)}}{1-|\lambda_k(\tau)|^2} \right], \tag{2.36}$$

where λ_k is defined in the previous section for each mode k and the function is defined for $s > \bar{s}_B = \sup_k \frac{\ln|\lambda_k(\tau)|}{\omega_k(\tau)}$. Following section 2.1, we can identify the two contribution $f_c(s) = \frac{1}{2}\int_k \ln[1-|\lambda_k(\tau)|^2] e^{-2s\omega_k(\tau)}$ and $f_s = -\frac{1}{2} f_c(0)$.
We can immediately observe that the structure of the cumulant generating function is always the same with all the dependence on the specific choice of the

protocol encoded in the function $\lambda_k(\tau)$. For a truly adiabatic protocol, since the final state is assumed to be the ground state of the final Hamiltonian, we would have $\lambda_k(\tau) = 0\ \forall k$, such a way that the function $P(W)$ becomes a δ function at the origin as expected. For the opposite limit of a sudden quench, since the state does not change and remains in the initial ground state, we would have $\lambda_k(\tau) = \lambda_k(0)$, whose actual value can be read from Eq. (2.26) for each mode k and is in agreement with previous results [51, 117].

By using Eqs. (2.25), we find that the function $\lambda_k(\tau)$ can in general be determined by solving a parametric in k differential equation of the Riccati type, determining in such a way the full distribution function. Indeed we have

$$i\frac{d}{dt}\lambda_k(t) = -\frac{\omega_k^2(\tau)+\omega_k^2(t)}{\omega_k(\tau)}\lambda_k(t) + \frac{\omega_k^2(\tau)-\omega_k^2(t)}{2\omega_k(\tau)}\left[1+\lambda_k^2(t)\right], \tag{2.37}$$

with initial condition $\lambda_k(0) = \frac{\beta_k(0)}{\alpha_k(0)}$. When $m_f \to 0$ we have that $\omega_k(\tau) \to k$, so the coefficients of Eq. (2.37) become divergent for $k \to 0$. To avoid this it is convenient to make the substitution

$$x_k(t) = \frac{1}{\omega_k(\tau)}\frac{1+\lambda_k(t)}{1-\lambda_k(t)}, \tag{2.38}$$

with the new variable satisfying the elegant Riccati-like equation

$$i\frac{d}{dt}x_k(t) = -\omega_k^2(t)x_k^2(t) + 1, \tag{2.39}$$

with an initial condition, $x_k(0) = 1/\omega_k(0)$, fully determined by the initial parameters.

Let us now compare different protocols starting by considering the behavior of the normalized log-fidelity defined in Eq. (2.11). In particular we choose as examples a linear, a logarithmic, a parabolic, and a quartic protocol, given by

$$m_{\rm lin}(t) = m_i + (m_f - m_i)\frac{t}{\tau}, \tag{2.40a}$$

$$m_{\rm log}(t) = m_i + (m_f - m_i)\frac{\ln(1+6t/\tau)}{\ln 7}, \tag{2.40b}$$

$$m_{\rm par}(t) = m_i + (m_f - m_i)\left(4\frac{t}{\tau} - 3\frac{t^2}{\tau^2}\right), \tag{2.40c}$$

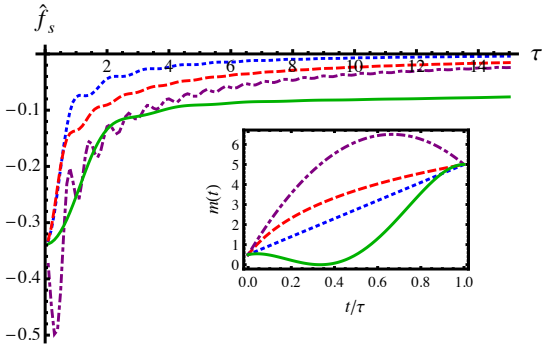

Figure 2.2: *Plot of the normalized log-fidelity $\hat{f}_s$ [see Eq. (2.11) for the definition], for different protocols as a function of the duration τ, with $m_i = 0.5$ and $m_f = 5$. The considered protocols are defined in Eqs. (2.40) and shown in the inset. In particular the dotted (blue) one is $m_{\rm lin}$, the dashed (red) one is $m_{\rm log}$, the dotted-dashed (purple) one is $m_{\rm par}$ and the solid (green) one is $m_{\rm quart}$.*

$$m_{\rm quart}(t) = m_i + (m_f - m_i) \sum_{n=1}^{4} \rho_n (t/\tau)^n, \tag{2.40d}$$

with ρ_n in the last protocol chosen in such a way that the function has a minimum with zero mass at $t/\tau = 1/3$. The actual values of these constants can be found in Appendix 2.B, while the various protocols in the case of $m = 0.5$ and $m_1 = 5$ are plotted in the inset of Fig. 2.2

The results for the normalized log-fidelity for the different protocols introduced above are shown in Fig. 2.2 as a function of the total duration τ, taking $m_i = 0.1$ and $m_f = 5$. From this figure we see that for the linear and logarithmic protocols the log-fidelity is essentially an increasing function of τ tending to zero (implying a fidelity tending to one); for logarithmic protocols it is always lower than for a linear one. In the parabolic case we see oscillations for small τ, when it is possible to have a fidelity lower than in the sudden case, while in the quartic case the fidelity decreases quite rapidly at the beginning, but then reaches a plateau at a value different from zero. This is a consequence of this protocol touching the critical point $m = 0$, where the system is gapless, making an adiabatic behavior impossible even in the large τ limit.

Let us now consider the behavior of the cumulants of the distribution $P(W)$.

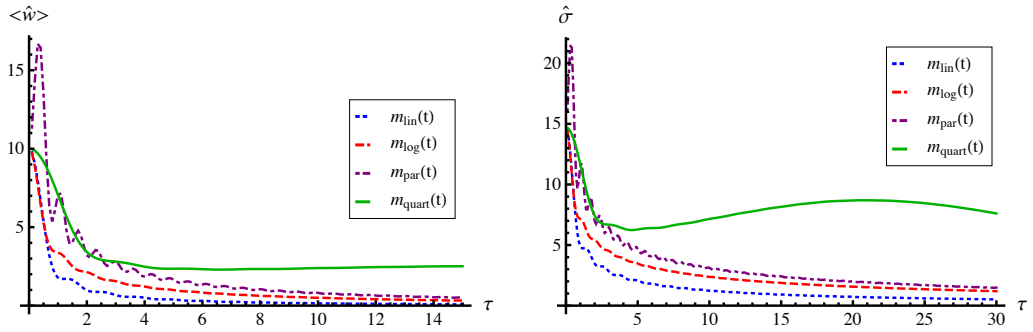

Figure 2.3: *Plot of (a) $\langle \hat{w} \rangle$ and (b) $\hat{\sigma}^2$ [see the definition below Eq. (2.42)] for the different protocols defined in Eqs. 2.40 as a function of the duration τ, with $m_i = 0.5$ and $m_f = 5$.*

They can be computed from Eq. (2.36) using the formula

$$k_n = (-1)^n \frac{\partial^n}{\partial s^n} \ln G(s)_{|s=0}, \tag{2.41}$$

where k_n denotes the n-th cumulant. Explicit expression for the first cumulants are

$$k_1 = \langle W \rangle = L^d \int \frac{d^d k}{(2\pi)^d} \frac{|\lambda_k(\tau)|^2 \omega_k(\tau)}{1 - |\lambda_k(\tau)|^2}, \tag{2.42a}$$

$$k_2 = \sigma^2 = L^d \int \frac{d^d k}{(2\pi)^d} \frac{2|\lambda_k(\tau)|^2 \omega_k^2(\tau)}{[1 - |\lambda_k(\tau)|^2]^2}, \tag{2.42b}$$

$$\frac{\sigma}{\langle W \rangle} \sim L^{-d/2}, \tag{2.42c}$$

$$k_3 = L^d \int \frac{d^d k}{(2\pi)^d} 4 \frac{\omega_k^3(\tau)[|\lambda_k(\tau)|^4 + |\lambda_k(\tau)|^2]}{[1 - |\lambda_k(\tau)|^2]^3}, \tag{2.42d}$$

$$\frac{k_3}{\sigma^3} \sim L^{-d/2}. \tag{2.42e}$$

The first thing we notice is that all the cumulants are extensive, i.e., proportional to the volume L^d, which is a consequence of the function $\ln G(s)$ itself being extensive, as can be clearly seen from Eq. (2.36). For this reason, when the size increases, it is more appropriate to study the probability distribution of the work per unit volume [51] $w = W/L^d$, which has as a moment generating function $\tilde{G}(s) = G(s/L^d)$, implying that the cumulants $\tilde{k}_n$ of this intensive

variable are $\tilde{k}_n = L^{d(1-n)}k_n$. From this we conclude that, in the limit of large L the probability distribution of w will tend to become a Gaussian function with average value k_1 and variance k_2/L^d that tends to zero as $L \to \infty$.

In Fig. 2.3 we plot the behavior of the first two cumulants per unit volume (normalized by a geometric factor) i.e., $\langle \hat{w} \rangle = L^{-d}\langle w \rangle \frac{(2\pi)^d}{\Omega_d}$ and $\hat{\sigma}^2 = L^{-d}\sigma \frac{(2\pi)^d}{\Omega_d}$ for the different protocols defined in (2.40), taking $m_i = 0.5$ and $m_f = 5$. We see that the qualitative behavior of the two cumulants is the same: in the case of the linear and logarithmic protocols they are essentially decreasing functions of τ that tend to zero for τ large and with the logarithmic cumulants always bigger than the linear ones. This is expected, since the larger τ is the more adiabatic the protocol is and the less work is done on the system; in the case of the parabolic protocol there are oscillations for small τ that rapidly decrease in amplitude so that the cumulants are larger than the sudden case only for small duration. We notice also that the value of the cumulants for the parabolic protocol is always larger than the linear and logarithmic ones. Finally, the cumulants for the quartic protocol at the beginning decrease quite fast; then in the case of the average there is essentially a plateau that seems to slightly decrease for large values of τ, while for the variance the plateau is replaced by an increase of the function. The last protocol, except for small τ, always has larger values of both the cumulants. The different qualitative behavior of the quartic protocol has again to be ascribed to the impossibility of achieving an adiabatic behavior.

To end this section we will now turn our attention to the asymptotic behavior of $P(W)$ for small W and prove that (for $m_f \neq 0$)

$$P(W) = e^{-2L^d f_s}\left[\delta(W) + L^d \left(\frac{m_f}{4\pi}\right)^{d/2} \frac{|\lambda_0(\tau)|^2}{2\Gamma(d/2)} \frac{\Theta(W-2m_1)}{(W-2m_f)^{1-d/2}} + \dots\right]. \quad (2.43)$$

As expected, apart from a δ-function peak, there is an edge singularity, which turns out to be fully determined by the asymptotics of $f(s)$ for large s. Apart from the term $2f_s$, which determines an overall constant, this is given just by the asymptotic behavior of $f_c(s)$. In particular, we will now show that the exponent of this singularity is not affected by the choice of a specific protocol.

The first step to obtain Eq. (2.43) is to expand the logarithm as

$$\ln\left[1-|\lambda_k(\tau)|^2 e^{-2s\omega_k(\tau)}\right] = -\sum_{n=1}^{\infty} e^{-2sn\omega_k(\tau)}|\lambda_k(\tau)|^{2n}/n. \tag{2.44}$$

Then, since $|\lambda_k(\tau)|^2 \leq 1$, we can interchange the order of the integration and the sum because of the convergence of the series. For $m_f \neq 0$ we have

$$\begin{aligned} f_c(s) &= -\frac{1}{2}\sum_{n=1}^{\infty}\int_k e^{-2sn\omega_k(\tau)}\frac{|\lambda_k(\tau)|^{2n}}{n} \\ &\simeq -\frac{1}{2}\sum_{n=1}^{\infty} e^{-2snm_f}\frac{|\lambda_0(\tau)|^{2n}}{n}\left(\frac{m_f}{4\pi sn}\right)^{d/2}, \end{aligned} \tag{2.45}$$

where the integrals have been evaluated in the stationary phase approximation. The full series can then be written as (Li denotes the polylogarithm or Jonquiere's function)

$$f_c(s) \simeq -\frac{1}{2}\left(\frac{m_f}{4\pi s}\right)^{d/2} Li_{1+d/2}\left[e^{-2sm_f}|\lambda_0(\tau)|^2\right], \tag{2.46}$$

while the leading asymptotic behavior is given just by the first term

$$f_c(s) \simeq -\frac{e^{-2sm_f}}{2}\left(\frac{m_f}{4\pi s}\right)^{d/2}|\lambda_0(\tau)|^2. \tag{2.47}$$

From this we can extract the form of the edge singularity at the threshold. Indeed, we have that

$$G(s) \simeq e^{-2L^d f_s}\left[1 + L^d\,\frac{e^{-2sm_f}}{2}\left(\frac{m_f}{4\pi s}\right)^{d/2}|\lambda_0(\tau)|^2\right], \tag{2.48}$$

implying Eq. (2.43).

The most interesting feature is that the exponent of the edge singularity is completely determined by the dimensionality, independently of the choice of the protocol, which only affects the coefficient through the absolute value of $\lambda_0(\tau)$. Thus, this is the first example of a quantity that is *"universal" in time* (see section 1.2). Moreover, as we will show in more details in the next section, in the case of a protocol starting from the critical point $m_i = 0$ we have that

$|\lambda_0(\tau)|^2 = 1$ independently of the details of the protocol. We also observe that the edge singularity becomes weaker and weaker as the dimensionality d of the system is increased, turning from a divergence for $d < 2$ to a vanishing distribution for $d > 2$.

In Fig. 2.4 we plot the value of $|\lambda_0(\tau)|^2$ for the protocols defined by Eqs. (2.40) as a function of τ. We see that for the linear, logarithmic, and parabolic protocols it decreases to zero, with the latter showing oscillations for small τ; in the case of the quartic protocol, after an initial decrease, it increases and seems to reach a plateau. This is again a consequence of the fact that the protocol touches the critical point $m = 0$, where the mode 0 is gapless.

When the final mass is zero, i.e., $m_f = 0$, we instead have

$$f_c(s) = \frac{1}{2}\sum_{n=1}^{\infty}\int_k e^{-2sn|k|}\frac{|\lambda_k(\tau)|^{2n}}{n} \simeq -\frac{\Omega_d}{(2\pi)^d}\frac{1}{2}\sum_{n=1}^{\infty}\frac{\Gamma(d)}{(2sn)^d}, \tag{2.49}$$

where we used $|\lambda_0(\tau)|^2 = 1$, which is a simple consequence of Eq. (2.38). The full series is now given by

$$f_c(s) \simeq -\frac{\Omega_d}{(2\pi)^d}\frac{\Gamma(d)}{(2s)^d}\zeta(d), \tag{2.50}$$

with leading asymptotic behavior

$$f_c(s) \simeq -\frac{\Omega_d}{(2\pi)^d}\frac{1}{2}\frac{\Gamma(d)}{(2s)^d}, \tag{2.51}$$

which, similarly to the previous case, gives for the distribution of the work the result

$$P(W) = e^{-2L^d f_s}\Big[\delta(W) + \frac{\Omega_d}{(2\pi)^d}L^d\frac{1}{2^{d+1}W^{d-1}} + \dots\Big]. \tag{2.52}$$

Thus, in this case the edge singularity is exactly at the origin, as expected from the final Hamiltonian being gapless, and both the exponent and the coefficient (apart from the overall factor) are independent of the choice of the protocol, so again *"time universal"*.

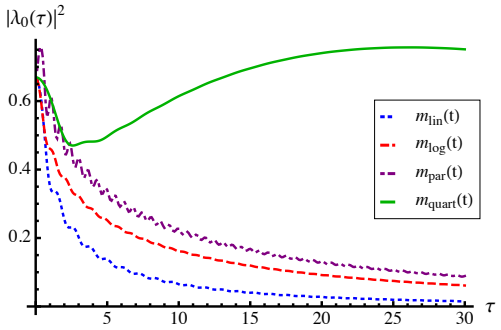

Figure 2.4: *Plot of the coefficient of the edge singularity $|\lambda_0(\tau)|^2$ for the different protocols defined in Eqs. (2.40) with $m_0 = 0.5$ and $m_1 = 5$, as a function of τ.*

2.2.3 Condensation transition

The Gaussian field theory we are considering clearly belongs to class B (see section 2.1) and its function $f(s)$ is defined for $s > -\bar{s}_B$, with

$$-\bar{s}_B = \sup_k \frac{\ln|\lambda_k(\tau)|}{\omega_k(\tau)}, \tag{2.53}$$

as already stated below Eq. (2.36). As we can see from Eq. (2.26), $m_i = 0$ implies $\lambda_k^2(0) = 1 + O(k)$; therefore, for a sudden quench $\bar{s}_B = 0$, implying that $I(w) = 0$ for $w > \bar{w}$ (which is finite for $d > 1$). The vanishing of $I(w)$ means that the decay of $p(w)$ becomes algebraic and as a result the cumulants with $n \geq d$ diverge [51].

We are now interested in understanding the fate of such a transition when a generic protocol is performed. The transition is still present if $\bar{s}_B$ is still zero, which, as can be read from Eq.(2.53), is equivalent to saying that $|\lambda_0(\tau)| = 1$. In order to address this question let us write $\lambda_0(t) = \rho(t)e^{i\theta(t)}$ and use Eq. (2.78) for $k = 0$ to derive the equations for the modulus and the phase. Doing so, we get

$$\frac{d}{dt}\rho(t) = -\frac{m^2(t) - m_f^2}{2m_f}\sin\theta(t)\left(\rho^2(t) - 1\right) \tag{2.54a}$$

$$\frac{d}{dt}\theta(t) = \frac{m_f^2 + m^2(t)}{m_f} + \frac{m^2(t) - m_f^2}{2m_f}\cos\theta(t)\left(\frac{1}{\rho(t)} + \rho(t)\right). \tag{2.54b}$$

We clearly see that $\rho = 1$ is a stationary solution. Therefore, for every protocol starting from $m_i = 0$, since the initial condition is $\rho(0) = 1$ we have that $\lambda_0(\tau) = 1$ and the transition is still present. We, thus, can conclude that is "time universal". We also notice that this transition is analogous to the Bose-Einstein condensation of the ideal Bose gas in the grancanonical canonical ensemble, and it is determined only by the low-energy part of the spectrum, thus being universal in the usual sense of statistical mechanics.

2.3 Global protocols in the Ising model

Let us show that the features described above also pertain to the case of a global protocol in a one-dimensional quantum Ising chain, described by the Hamiltonian

$$H_I[g(t)] = -\frac{1}{2}\sum_{i=1}^{L}\left[\sigma_i^x\sigma_{i+1}^x + g(t)\sigma_i^z\right], \tag{2.55}$$

where σ_i^α represent the Pauli matrices satisfying the usual commutation rules $[\sigma_j^\alpha, \sigma_l^\beta] = \delta_{j,l}\epsilon^{\alpha\beta\gamma}\sigma_j^\gamma$, with $\epsilon^{\alpha\beta\gamma}$ being the completely antisymmetric tensor and we assume periodic boundary conditions $\sigma_{j+L}^\alpha = \sigma_j^\alpha$. We assume that the transverse field $g(t)$ is changed from $g(0) = g_i$ to $g(\tau) = g_f$. This model is a prototypical, exactly solvable example of a quantum phase transition, whose critical point is $g_c = 1$, separating a quantum paramagnetic phase ($g > 1$) from a quantum ferromagnetic one, where the order parameter $\langle\sigma^x\rangle$ is different from zero.

The Hamiltonian (2.55) can be rewritten in terms of spinless fermions, by performing a Jordan-Wigner transformation,

$$\sigma_i^+ = \prod_{j<i}(1 - 2c_j^\dagger c_j)c_i, \tag{2.56a}$$

$$\sigma_j^z = 1 - 2c_j^\dagger c_j, \tag{2.56b}$$

with $\sigma_i^+ = (\sigma_i^x + i\sigma_i^y)/2$ and the introduced fermionic operators satisfy the usual commutation relations $\{c_j, c_l^\dagger\} = \delta_{jl}$ and $\{c_j, c_l\} = 0$, we can write the

Hamiltonian as

$$H_I[g(t)] = P^+ H_I^+[g(t)]P^+ + P^- H_I^-[g(t)]P^-, \tag{2.57}$$

where

$$P^\pm = \frac{1}{2}\left[1 \pm \prod_{j=1}^{L} \sigma_j^z\right] \tag{2.58}$$

are the projectors in the subspace with an even (+) or odd (−) number of fermions and

$$H^\pm[g(t)] = -\frac{1}{2}\sum_{i=1}^{L}\left[c_i^\dagger c_{i+1} + c_i^\dagger c_{i+1}^\dagger + h.c. + g(t)(1 - 2c_i^\dagger c_i)\right], \tag{2.59}$$

with the c_i's obeying antiperiodic boundary conditions $c_{L+1} = -c_1$ in the even sector and periodic boundary conditions $c_{L+1} = c_1$ in the odd one. Since the ground state lies in the even sector for every finite value of L, we will concentrate on the sector described by $H_I[g(t)]^+$, omitting the superscript + in the following. We can now perform a Fourier transform $c_j = \frac{e^{i\pi/4}}{\sqrt{L}}\sum_k e^{ikj}\hat{c}_k$, with k odd multiple of π/L so to implement the antiperiodic boundary conditions, getting

$$H_I[g(t)] = \sum_{k>0}\begin{pmatrix}\hat{c}_k^\dagger & \hat{c}_{-k}\end{pmatrix}\tilde{H}_k(t)\begin{pmatrix}\hat{c}_k \\ \hat{c}_{-k}^\dagger\end{pmatrix}, \tag{2.60}$$

where the matrix $\tilde{H}_k$ is given by

$$\tilde{H}_k(t) = \begin{pmatrix} g(t) - \cos k & -\sin k \\ -\sin k & \cos k - g(t)\end{pmatrix}. \tag{2.61}$$

As in the case of the Gaussian field theory described before, we have reduced the model to a sum over independent (now fermionic) k modes. Thus, also in this case the moment generating function $G(s)$ factorizes and we can first focus on a single k mode.

2.3.1 Single fermionic mode

The procedure to compute the moment generating function for a single mode in the fermionic case closely resemble what we have done in section 2.2.1 for

a single harmonic oscillator. Thus, the first step is to find the operators that diagonalize the instantaneous Hamiltonian, which we call γ_k^t and $(\gamma_k^t)^\dagger$. These are connected to the Jordan-Wigner fermions by the well-known Bogoliubov transformation

$$\begin{pmatrix} \hat{c}_k \\ \hat{c}_{-k}^\dagger \end{pmatrix} = \begin{pmatrix} u_k(t) & -v_k(t) \\ v_k(t) & u_k(t) \end{pmatrix} \begin{pmatrix} \gamma_k^t \\ (\gamma_{-k}^t)^\dagger \end{pmatrix}, \tag{2.62}$$

where $u_k^2(t) + v_k^2(t) = 1$.

The way to choose the coefficients of the transformation is asking that $\begin{pmatrix} u_k(t) & v_k(t) \end{pmatrix}^T$ and $\begin{pmatrix} -v_k(t) & u_k(t) \end{pmatrix}^T$ are the eigenvectors of $\tilde{H}_k$ with eigenvalues $\epsilon_k(t)$ and $-\epsilon_k(t)$, where $\epsilon_k(t) = \sqrt{1 + g^2(t) - 2g(t)\cos k}$. Therefore, we have

$$u_k(t) = \frac{1}{\sqrt{2}} \sqrt{1 + \frac{g(t) - \cos k}{\epsilon_k(t)}}, \tag{2.63a}$$

$$v_k(t) = -\frac{1}{\sqrt{2}} \sqrt{1 - \frac{g(t) - \cos k}{\epsilon_k(t)}}. \tag{2.63b}$$

After having performed the above transformation, the Hamiltonian for the single mode assumes the following diagonal form

$$H_k(t) = \epsilon_k(t) \left[(\gamma_k^t)^\dagger \gamma_k^t + (\gamma_{-k}^t)^\dagger \gamma_{-k}^t - 1 \right]. \tag{2.64}$$

We now define the operators $\tilde{\gamma}_k(t)$ and $\tilde{\gamma}_{-k}(t)$, which are assumed to annihilate the evolved state up to time t, i.e.,

$$\tilde{\gamma}_{\pm k}(t) \left| \psi_k(t) \right\rangle = 0. \tag{2.65}$$

Here we remind that $\left| \psi(t) \right\rangle = U(t) \left| 0 \right\rangle_0$ and $\left| 0 \right\rangle_0$ is the initial ground state defined by the condition $\gamma_{\pm k}^0 \left| 0 \right\rangle_0 = 0$. As in the case of bosons the condition (2.65) implies that

$$i \frac{d}{dt} \tilde{\gamma}_{\pm k}^H(t) = 0, \tag{2.66}$$

in the subspace spanned by $\left| \psi_k(t) \right\rangle$. Therefore, also in this case we will omit the time dependence for such operators.

We now look for the connection between $\tilde{\gamma}_k(t)$ and γ_k^τ, in terms of which the final Hamiltonian is diagonal. The first step in this direction is to find the equation

of motion for the Heisenberg operators $\gamma_k^{\tau,H}(t)$ and $[\gamma_{-k}^{\tau,H}(t)]^\dagger$, for which we need to compute the commutators of these operators with the Hamiltonian $H_k[g(t)]$. Using the Bogoliubov transformation

$$\begin{pmatrix} \gamma_k^t \\ (\gamma_{-k}^t)^\dagger \end{pmatrix} = \begin{pmatrix} \mu_k(t) & \nu_k(t) \\ -\nu_k(t) & \mu_k(t) \end{pmatrix} \begin{pmatrix} \gamma_k^\tau \\ (\gamma_{-k}^\tau)^\dagger \end{pmatrix} \tag{2.67}$$

with

$$\mu_k(t) = u_k(\tau)u_k(t) + v_k(\tau)v_k(t), \tag{2.68a}$$

$$\nu_k(t) = u_k(\tau)v_k(t) - v_k(\tau)u_k(t), \tag{2.68b}$$

we are able to rewrite the Hamiltonian as

$$H_k(t) = \begin{pmatrix} (\gamma_k^\tau)^\dagger & \gamma_{-k}^\tau \end{pmatrix} \begin{pmatrix} r_k(t) & s_k(t) \\ s_k(t) & -r_k(t) \end{pmatrix} \begin{pmatrix} \gamma_k^\tau \\ (\gamma_{-k}^\tau)^\dagger \end{pmatrix}, \tag{2.69}$$

with the coefficients

$$r_k(t) = \frac{g(t)g_f - \cos k[g(t) + g_f] + 1}{\epsilon_k(\tau)}, \tag{2.70a}$$

$$s_k(t) = \frac{\sin k\,[g(t) - g_f]}{\epsilon_k(\tau)}. \tag{2.70b}$$

With the Hamiltonian in this form it is easy to derive the required equations of motion

$$i\frac{d}{dt}\begin{pmatrix} \gamma_k^{\tau,H}(t) \\ [\gamma_{-k}^{\tau,H}(t)]^\dagger \end{pmatrix} = \begin{pmatrix} r_k(t) & s_k(t) \\ s_k(t) & -r_k(t) \end{pmatrix} \begin{pmatrix} \gamma_k^{\tau,H}(t) \\ (\gamma_{-k}^{\tau,H}(t))^\dagger \end{pmatrix}. \tag{2.71}$$

We now make the ansatz

$$\begin{pmatrix} \gamma_k^{\tau,H}(t) \\ [\gamma_{-k}^{\tau,H}(t)]^\dagger \end{pmatrix} = \begin{pmatrix} a_k(t) & -b_k^\star(t) \\ b_k(t) & a_k^\star(t) \end{pmatrix} \begin{pmatrix} \tilde{\gamma}_k^H \\ \tilde{\gamma}_{-k}^{\dagger,H} \end{pmatrix}, \tag{2.72}$$

in such a way that we transform the equations for the operators in equations for the coefficients,

$$i\frac{d}{dt}a_k(t) = r_k(t)a_k(t) + s_k(t)b_k(t), \tag{2.73a}$$

$$i\frac{d}{dt}b_k(t) = -r_k(t)b_k(t) + s_k(t)a_k(t). \tag{2.73b}$$

The initial conditions are given by the coefficients of the Bogoliubov transformation that connects the operators diagonalizing the Hamiltonian the initial and final times, since an obvious consequence of Eq. (2.66) is that $\tilde{\gamma}^H_{\pm k} = \gamma^0_{\pm k}$. Thus from from Eq. (2.67), we get

$$a_k(0) = \mu_k(0), \quad b_k(0) = \nu_k(0). \tag{2.74}$$

The last step is to write the evolved state $|\psi(\tau)\rangle$ in terms of the operators $\gamma^\tau_{\pm k}$. Since such a state is annihilated by $\tilde{\gamma}_{\pm k}(\tau)$, which are linearly related to the the operators diagonalizing the final Hamiltonian (see the translation into Schröedinger picture of Eq. (2.72)), we know that it will have a quadratic expression in $\gamma^\tau_{\pm k}$. By making the same step done in the bosonic case, we indeed find

$$|\psi(\tau)\rangle = \left[a^\star_k(\tau) + b^\star_k(\tau)(\gamma^\tau_{-k})^\dagger(\gamma^\tau_k)^\dagger\right]|0\rangle_\tau\,, \tag{2.75}$$

where $\gamma^\tau_{\pm k}|0\rangle_\tau = 0$. At this point we can readily use Eq. (2.9) to obtain the characteristic function

$$G_k(s) = |a_k(\tau)|^2\left(1 + |y_k(\tau)|^2 e^{-2s\epsilon_k(\tau)}\right), \tag{2.76}$$

with $y_k(\tau) = \frac{b_k(\tau)}{a_k(\tau)}$.

2.3.2 Full moment generating function

Using the results of the previous section we are now able to write down the full cumulant generating function for the Ising chain and for a generic protocol $g(t)$,

$$\frac{\ln G(s)}{L} = \int_0^\pi \frac{dk}{2\pi}\ln\left(\frac{1 + |y_k(\tau)|^2 e^{-2s\epsilon_k(\tau)}}{1 + |y_k(\tau)|^2}\right). \tag{2.77}$$

Following Sec. 2.1, we can identify the two contributions
$f_c(s) = -\int \frac{dk}{2\pi}\ln\left(1 + |y_k(\tau)|^2 e^{-2s\epsilon_k(\tau)}\right)$ and $f_s = -1/2 f_c(0)$.
We notice that also in this case the general structure does not change by changing the protocols, which enters only in the function $y_k(\tau)$. Also here if we

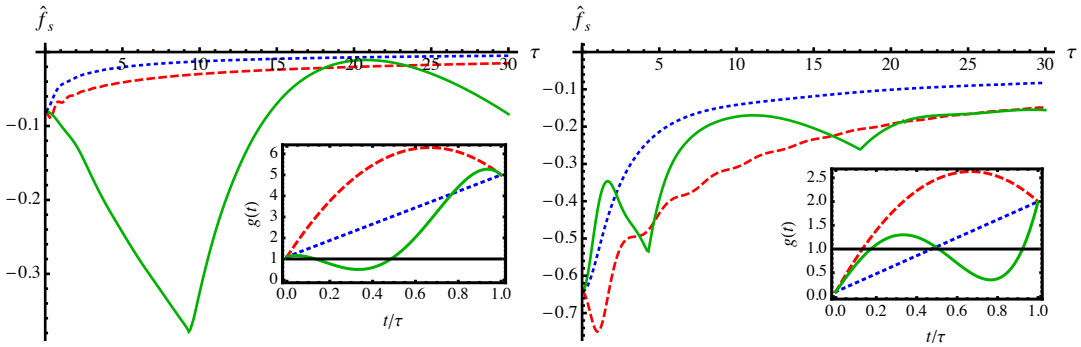

Figure 2.5: *Plot of $\hat{f}_s$ [see Eq. (2.11)] for different protocols as a function of the duration τ. In (a) they start and end in the same phase, with $g_i = 1.1$ and $g_f = 5$, while in (b) they start and end in different phases, with $g_i = 0.1$ and $g_f = 2$. . The considered protocols are defined in Eq. (2.81) and shown in the inset. In particular the dotted (blue) one is $g_{\rm lin}$, the dashed (red) one is $g_{\rm par}$ and the solid (green) one is $g_{\rm quart}$.*

assume an adiabatic protocol, so that the evolved state is the ground state of the final Hamiltonian, we would have $y_k(\tau) = 0$, implying that $P(W)$ consists in a single δ-function peak at the origin, as expected. If, instead, a sudden quench is performed on the system, then the state does not evolve and $y_k(\tau) = y_k(0)$, which can be read off from Eq. (2.68) [51].

In the case of a generic protocol $y_k(\tau)$ can be found, determining in such a way the full distribution function of the work, by solving a Riccati type equation, which can be derived using Eqs. (2.73) and reads

$$i\frac{d}{dt}y_k(t) = -2r_k(t)y_k(t) + s_k(t)\left(1 - y_k(t)^2\right), \tag{2.78}$$

with initial condition $y_k(0) = \frac{b_k(0)}{a_k(0)}$.

Contrary to the case of the free bosons, there are no diverging coefficients in the limit $k \to 0$ for protocols ending in the critical point, i.e., $g(\tau) = 1$, but when the protocol crosses the critical point the initial function $y_k(0)$ diverges as $1/k^2$ for $k \to 0$. To avoid having divergent initial conditions it is possible to define a

new function $z_k(t)$ as

$$z_k(t) = \frac{1 - \text{sign}(g_i - g_f)y_k(t)}{1 + \text{sign}(g_i - g_f)y_k(t)}, \tag{2.79}$$

which also satisfies the Riccati-like equation

$$i\frac{d}{dt}z_k(t) = r_k(t)(1 - z_k^2(t)) + 2s_k(t)\,\text{sign}(g_i - g_f)z_k(t). \tag{2.80}$$

We now start comparing different protocols starting from the discussion of the normalized log-fidelity $\hat{f}_s$. In Fig. 2.5a we show its behavior for different protocols as a function of the duration τ, choosing $g_i = 1.1$ and $g_f = 5$, thus for protocols starting and ending in the paramagnetic phase. The protocols considered are linear, parabolic, and quartic, given by

$$g_{\text{lin}} = g_i + (g_f - g_i)t/\tau, \tag{2.81a}$$

$$g_{\text{par}} = g_i + (g_f - g_i)(4t/\tau - 3t^2/\tau^2), \tag{2.81b}$$

$$g_{\text{quart}} = g_i \sum_{n=1}^{4} \rho_n (t/\tau)^n, \tag{2.81c}$$

with ρ_n in the last protocol chosen in such a way that $g_{\text{quart}}(t)$ is equal to $1/2$ for $t = 1/3$ and g_0 for $t = 1/2$. This protocol crosses the critical point and then returns in the paramagnetic phase. The actual values of the constants can be read in Appendix 2.B and the different protocols are shown in the inset of Fig. 2.5a.

As expected for both the linear and parabolic protocols the log-fidelity is essentially an increasing function of τ tending to zero (corresponding to fidelity going to one) for large τ, with the parabolic protocol always giving a smaller value of the fidelity than the linear one. The quartic protocol has a very different behavior: it increases at the beginning and then decreases, displaying an oscillatory behavior (persistent for larger τ) with an amplitude of the oscillations decreasing as τ increases. The qualitatively different behavior of this protocol has to be ascribed to the fact that it crosses the critical point and spends some time in the ferromagnetic phase before returning in the paramagnetic one.

Fig. 2.5b shows also the behavior of $\hat{f}_s$ as a function of τ for the protocols defined in Eqs. (2.81), but now taking $g_i = 0.1$ and $g_f = 2$, i.e. protocols that start and end in different phases. The coefficients ρ_n are now chosen in such a way that the protocol crosses the critical point three times. We see that for the linear protocol the fidelity is essentially an increasing function of τ with values that are larger than those in the same phase, and with an asymptotic value that appears to be different from zero. The parabolic protocol instead shows oscillations for small values of τ where it is possible to have a fidelity lower than what one gets for a sudden quench. Finally, the quartic protocol shows an oscillatory behavior and gives values of the fidelity always smaller than the sudden quench.

We now turn our attention to the cumulants of the distribution $P(W)$, which can be derived using Eq. (2.41). The first ones are given by

$$k_1 = \langle W \rangle = 2L \int_0^\pi \frac{dk}{2\pi} \frac{\epsilon_k(\tau)|y_k(\tau)|^2}{1+|y_k(\tau)|^2}, \tag{2.82a}$$

$$k_2 = \sigma^2 = L \int_0^\pi \frac{dk}{2\pi} \frac{4\epsilon_k(\tau)^2|y_k(\tau)|^2}{(1+|y_k(\tau)|)^2}, \tag{2.82b}$$

$$\frac{\sigma}{\langle W \rangle} \sim L^{-1/2}, \tag{2.82c}$$

$$k_3 = L \int_0^\pi \frac{dk}{2\pi} \frac{8\epsilon_k(\tau)^3 \left(|y_k(\tau)|^4 - |y_k(\tau)|^2\right)}{\left(1+|y_k(\tau)|^2\right)^3}, \tag{2.82d}$$

$$\frac{k_3}{\sigma^3} \sim L^{-1/2}. \tag{2.82e}$$

The scaling with the size of the system L of both $\ln G(s)$ and the cumulants is the same as in the case of free bosons. Therefore, also in this case, when the size of the system increases, it is convenient to define the intensive variable $w = W/L$, whose probability distribution has cumulants given by $\tilde{k}_n = L^{1-n} k_n$. Therefore, for large L the distribution function $P(w)$ will be Gaussian with a mean equal to k_1 and variance given by k_2/L, which goes to zero for $L \to \infty$.

Figures 2.6 and 2.7 show the behavior of the first two cumulants per unit volume for the protocols introduced previously that start and end in the same phase with $g_0 = 1.1$ and $g_1 = 5$ and for protocols that start and end in different

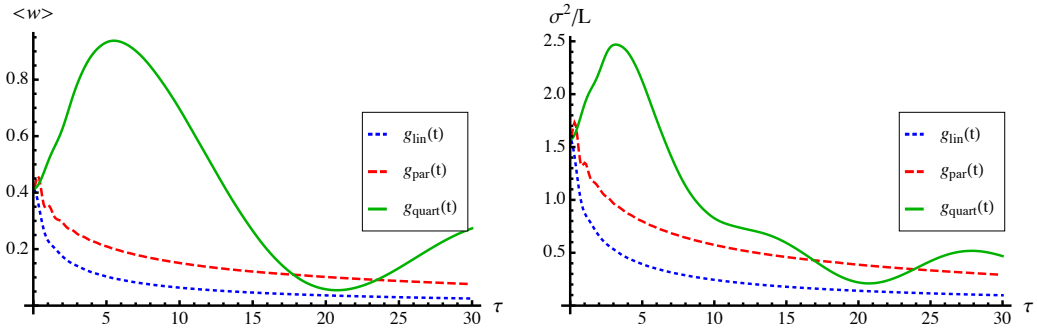

(a) **(b)**

Figure 2.6: *Plot of (a) $\langle w \rangle$ and (b) σ^2/L for the different protocols defined in Eqs. 2.81 as a function of the duration τ, with both $g_i = 1.1$ and $g_f = 5$ in the paramagnetic phase.*

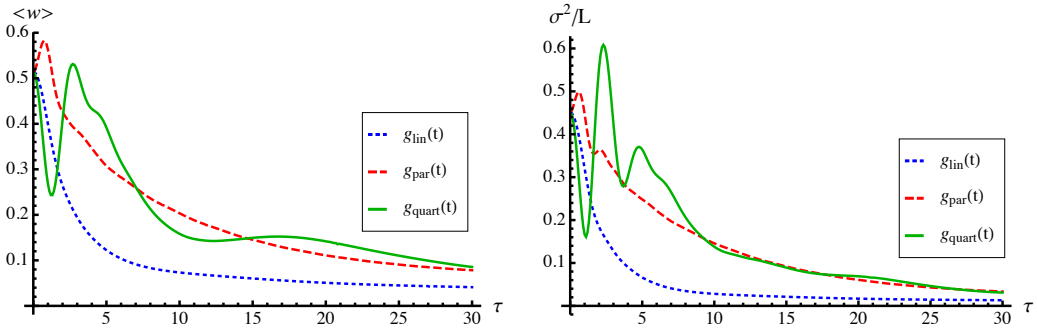

(a) **(b)**

Figure 2.7: *Plot of (a) $\langle w \rangle$ and (b) σ^2/L [see the definition below Eq. (2.42)] for the different protocols defined in Eqs. 2.40 as a function of the duration τ, with $g_i = 0.1$ and $g_f = 2$ in different phases.*

phases with $g_0 = 0.1$ and $g_1 = 2$, respectively [the specific protocols considered are given by Eqs. (2.81)]. In the first case we see that the linear and parabolic protocols have cumulants that are essentially decreasing functions of τ, with the parabolic cumulants always larger than the linear ones, while the quartic protocol shows cumulants with an oscillatory behavior. In the case of protocols starting and ending in different phases we see that the qualitative behavior for the linear protocol is almost the same as before, with the difference that the mean is not going to zero for large τ. This signals the fact that as one crosses the quantum critical point the adiabatic approximation breaks down. In the parabolic case we have oscillations for small τ and values always larger than the linear cumulants. Finally, in the case of the quartic protocol we see oscillations that are not as strong as in the case of protocols starting and ending in the same phase.

We now end this section discussing the behavior of the distribution of the work at low energies, in particular studying how the edge singularity is affected by the specifics of the chosen protocol. For this purpose we will consider the asymptotic behavior of $f_c(s)$, which in the case of a sudden quench has been analyzed in [50], which in turn is determined by the small-k behavior of $y_k(\tau)$ that, as we will now show, is sensitive on whether the ending points of the protocol are in the same phases or in different phases.

Let us start by considering the case of g_i and g_f within the same phase. Then, for a sudden quench $y_k(0)$ is an odd function of k, which has the following behavior for $k \to 0$,

$$y_k(0) = \frac{g_0 - g_1}{2(g_0 - 1)(g_1 - 1)} k + O(k^3). \tag{2.83}$$

We now use Eq. (2.78) to analyze if the small-k behavior of y_k is changed when a more general protocol is considered. For this purpose we expand the function as a power series of k as

$$y_k(t) = c_0(t) + c_1(t)k + c_2(t)k^2 + O(k^3), \tag{2.84}$$

with initial values $c_{2n} = 0 \ \forall n$ and $c_1(0) = \frac{g_0 - g_1}{2(g_0-1)(g_1-1)}$. Then we use the evolution equation and the series expansion of Eq. (2.70) to obtain the equations

for the coefficients $c_n(t)$. For the first terms in the expansion we get

$$i\frac{d}{dt}c_0(t) = 2[1-g(t)]\,\mathrm{sign}(g_f-1)c_0(t), \tag{2.85a}$$

$$i\frac{d}{dt}c_1(t) = \frac{g(t)-g_f}{|1-g_f|}\left(1-c_0^2(t)\right) + 2\left(1-g(t)\right)\,\mathrm{sign}(g_f-1)c_1(t) \tag{2.85b}$$

$$\begin{aligned} i\frac{d}{dt}c_2(t) = {} & 2\,\frac{g_f-g(t)}{|g_f-1|}c_0(t)c_1(t) + \frac{g(t)-g_f^2}{(g_f-1)^2}\,\mathrm{sign}(g_f-1)c_0(t) \\ & + 2\left(1-g(t)\right)\,\mathrm{sign}(g_f-1)c_2(t) \end{aligned} \tag{2.85c}$$

From this we can immediately conclude that $c_0(t) = c_2(t) = 0$. It is actually possible to prove that all the coefficients with even n are zero. We may also explicitly write down the solution for $c_1(t)$, or actually its modulus square, which the one relevant for the edge singularity. Indeed we have $|y_k(\tau)|^2 \sim k^2|c_1(\tau)|^2$, with

$$|c_1(\tau)|^2 = \left(c_1(0) - \int_0^\tau ds \frac{g_f-g(s)}{g_f-1}\sin 2\eta(s)\right)^2 + \left(\int_0^\tau ds\frac{g_f-g(s)}{g_f-1}\cos 2\eta(s)\right)^2, \tag{2.86}$$

with $\eta(s) = \int_0^s [1-g(t)]dt$.

Therefore, for small k we generally have $|y_k(\tau)|^2 \sim k^2$. From this we can extract the asymptotic behavior of $f_c(s)$, which is given by (see appendix 2.C for more details)

$$f_c(s) \simeq -\frac{|c_1(\tau)|^2}{8\sqrt{\pi}}\left(\frac{|1-g_f|}{sg_f}\right)^{3/2} e^{-2s|1-g_f|}, \tag{2.87}$$

Thus, the statistics of the work at low energies is

$$P(W) = e^{-2Lf_S}\left(\delta(W) + L\frac{|c_1(\tau)|^2}{4\pi}\left(\frac{|1-g_f|}{g_f}\right)^{3/2}\frac{\Theta(W-2|1-g_f|)}{(W-2|1-g_f|)^{-1/2}} + \dots\right). \tag{2.88}$$

We notice that the specifics of the protocol appear only in the coefficient $c_1(\tau)$, while the exponent remains unaffected, and thus is robust with respect to the choice of the protocol, i.e.,"time universal". We stress that the derivation above is valid also in the case in which $g(t)$ crosses the critical point at some instant of time, the only requirement being on the initial and final values of the protocol.

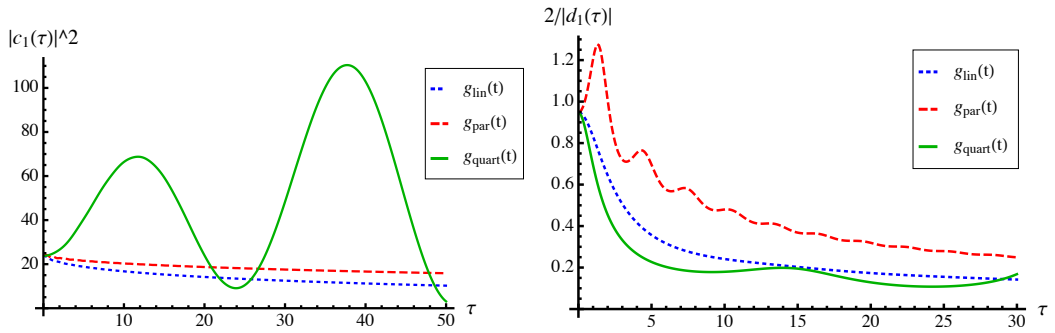

(a) **(b)**

Figure 2.8: *Plot of the coefficient of the edge singularity $|c_1(\tau)|^2$ as a function of τ for the different protocols defined in Eqs. (2.81). In (a) $g_i = 1.1$ and $g_f = 5$ are in the same phase, while in (b) $g_i = 0.1$ and $g_f = 2$ are in different phases.*

In the rather special case of a cyclic protocol, i.e., $g_f = g_i$, there are some minor modifications in the initial conditions, namely, $y_k(0) = 0$, implying that the expansion coefficients of Eq. (2.84) at the initial time are $c_n(0) = 0\ \forall n$. As a result, in Eq. (2.86) we have $c_1(0) = 0$.

In Fig. 2.8a we plot the value of $|c_1(\tau)|^2$ as a function of τ for the protocols defined in Eqs. (2.81) with $g_i = 1.1$ and $g_f = 5$. We see that for the parabolic and linear protocols this is a slowly decreasing function of τ with the values for the first protocol always larger than the others, while in the case of the quartic protocol we see an oscillatory behavior.

We now consider the case in which the protocol chosen start from the critical point $g_i = 1$. In this case the equations for the coefficients of the series expansions (2.84) are still given by Eqs. (2.85), but the initial conditions are different. Indeed we have

$$y_k(0) = \text{sign}(1 - g_f) + \frac{g_f + 1}{2(g_f - 1)} k + O(k^2). \tag{2.89}$$

Therefore the leading behavior for $k \to 0$ is now given by $c_0(\tau)$, whose value is

$$c_0(\tau) = \text{sign}(1 - g_f) e^{2i\,\text{sign}(1-g_f)\int_0^\tau (1-g(s))ds}, \tag{2.90}$$

from which we can immediately see that $|c_0(\tau)| = 1$ independently of the duration of the protocol and the final value of the transverse field g_f. So we conclude that in this case, not only the exponent, but also the coefficient of the edge singularity is robust with respect to the choice of the protocol. Indeed we have (see appendix 2.C for more details)

$$f_c(s) \simeq -\frac{1}{4\sqrt{\pi}} \left(\frac{|1-g_f|}{s g_f} \right)^{1/2} e^{-2s|1-g_f|}, \tag{2.91}$$

implying for the distribution of the work

$$P(W) = e^{-2Lf_s} \Big[\delta(W) + \frac{L}{4\pi} \sqrt{\frac{|1-g_f|}{g_f}} \frac{\Theta(W-2|1-g_f|)}{\sqrt{W-2|1-g_f|}} + \dots \Big]. \tag{2.92}$$

It is now the turn of protocols ending at the critical point $g_f = 1$. In this case the initial condition is given by

$$y_k(0) = \text{ sign}(g_i - 1) - \frac{g_i + 1}{2(g_i - 1)} k + O(k^2), \tag{2.93}$$

which, apart from a minus sign, is the same as Eq. (2.89) with the substitution $g_f \to g_i$. However now also the small-k behavior of $\epsilon_k(\tau)$ and so of $r_k(t)$ and $s_k(t)$ is changed, in such a way that the equations for the coefficient of the expansion (2.84) are modified, becoming (up to order k)

$$i \frac{d}{dt} c_0(t) = (g(t) - 1) \left(1 - c_0^2(t) \right) \tag{2.94a}$$

$$i \frac{d}{dt} c_1(t) = 2 \left(1 - g(t) \right) c_1(t) c_0(t) - \left(g(t) + 1 \right) c_0(t), \tag{2.94b}$$

with initial conditions that can be read from Eq. (2.93). We immediately notice that $c_0 = \pm 1$ is a stationary solution, so also for quenches ending at the critical point both the exponent and the coefficient are both independent of the choice of the protocol, i.e. "time universal". In particular we have (see appendix 2.C)

$$f_c(s) \simeq -\frac{1}{8\pi s}, \tag{2.95}$$

which implies

$$P(W) = e^{-2f_s L} \Big[\delta(W) + L \frac{1}{8\pi} \Theta(W) + \dots \Big]. \tag{2.96}$$

Finally, we consider the case of protocols starting in one phase and ending in the other one. In this case, as anticipated before, the behavior of $y_k(0)$ for small k becomes singular, namely

$$y_k(0) = \frac{2|1-g_i||1-g_f|}{g_i - g_f}\frac{1}{k} + O(k), \tag{2.97}$$

therefore it is more convenient to consider the function z_k defined in Eq.(2.79), whose behavior for $k \to 0$ at time $t = 0$ is instead

$$z_k(0) = -1 + \frac{|g_i - g_f|}{|g_i - 1||g_f - 1|}k + O(k^2). \tag{2.98}$$

Analogously to the previous cases, we expand the function $z_k(t)$ in a power series

$$z_k(t) = d_0(t) + d_1(t)k + d_2(t)k^2 \tag{2.99}$$

and use Eq. (2.80) to determine the evolution of the coefficients, getting

$$i\frac{d}{dt}d_0(t) = (g(t) - 1)\ \mathrm{sign}(g_f - 1)(1 - d_0^2(t)), \tag{2.100a}$$

$$\begin{aligned} i\frac{d}{dt}d_1(t) = &-2\ \mathrm{sign}(g_f - 1)\,(g(t) - 1)\,d_0(t)d_1(t) \\ &+ 2\ \frac{g(t) - g_1}{|1 - g_1|}\,\mathrm{sign}(g_f - g_i)d_0(t) \end{aligned} \tag{2.100b}$$

From this we derive that $d_0(t) = -1\ \forall t$ and

$$d_1(\tau) = e^{2iK(\tau)}\Big[d_1(0) - 2i\int_0^\tau \mathrm{sign}(g_f - g_i)\frac{g_f - g(s)}{|1 - g_f|}e^{-2iK(s)}\Big], \tag{2.101}$$

where $K(t) = \mathrm{sign}(g_f - 1)\eta(t)$, with $\eta(t)$ defined below Eq. (2.86).
Inverting the relation between z_k and y_k, we find

$$y_k(\tau) = -\frac{2}{d_1(\tau)}\frac{1}{k} + O(1), \tag{2.102}$$

so the leading behavior of $y_k(\tau)$ is still of the same type, implying that (see appendix 2.C for more details)

$$f_c(s) \simeq -\frac{1}{4\pi}\left[\frac{4\pi}{|d_1(\tau)|}e^{-s|1-g_1|} + \sqrt{\frac{g_1 s}{|1-g_1|}}\Gamma(-1/2)\frac{4}{|d_1(\tau)|^2}e^{-2s|1-g_1|}\right], \tag{2.103}$$

which for the probability distribution of the work gives,

$$P(W) = e^{-2Lf_s}\Big[\delta(W) + \frac{L}{|d_1(\tau)|}\delta\left(W - |1-g_1|\right) + \frac{L^2}{|d_1(\tau)|^2}\delta\left(W - 2|1-g_1|\right) + \frac{L}{\pi}\frac{1}{|d_1(\tau)|^2}\sqrt{\frac{g_1}{|1-g_1|}}\frac{\Theta(W-2|1-g_1|)}{(W-2|1-g_1|)^{3/2}}\Big]. \tag{2.104}$$

Once again we notice that the choice of the protocol affects only the coefficient of the edge singularity, while the exponent is always the same, thus is "time universal".

In Fig. 2.8b we show the behavior of $2/|d_1(\tau)|$ as a function of τ for the protocols defined in Eqs. (2.81) with $g_i = 0.1$ and $g_f = 2$. We see that in the case of a linear protocol we have a decreasing function of τ, while for the parabolic protocol we see oscillations for small τ that rapidly decrease in amplitude; for the quartic protocol we see an initial quite steep decrease and then small oscillations. The parabolic protocol always gives larger values at least for the time scale considered here.

2.4 Local protocols in the Ising model

In the two previous section we considered global protocols, finding that in the low energy part of the distribution of the work some "time universal" features can be found. However, these are relevant only for systems sizes that are not too big, because the low energy part of $P(W)$ is suppressed exponentially in the size of the system.

Instead, for local protocols the situation is completely different. Indeed, in this case the energy injected in the system is not an extensive quantity, making, in general, the low energy part of the distribution $P(W)$ have a considerable spectral weight also in the thermodynamic limit. The effect of such local protocols are particularly strong at a critical point, where the excitation are gapless, so that also a local change in the Hamiltonian can produce strong effects.

In the following we will study this problem in the case of the Ising chain, for local protocols of the transverse magnetization starting from the critical point.

We will describe the problem in the scaling limit, where the Ising model reduces to the following field theory [107],

$$H\left[m\right]=\int dx\,\frac{1}{2}\left[\left(\psi^{\dagger}(x)\partial_{x}\psi^{\dagger}(x)-\psi(x)\partial_{x}\psi(x)\right)\right.\\ \left.+\frac{m}{2}(\psi^{\dagger}(x)\psi(x)-\psi(x)\psi^{\dagger}(x))\right], \tag{2.105}$$

with $m\sim 1-g$ and $\{\psi(x),\psi^{\dagger}(x')\}=\delta(x-x')$.
Let us now introduce two Majorana fermionic operators,

$$\varphi(x)=\frac{1}{\sqrt{2}}\left(\psi^{\dagger}(x)e^{i\frac{\pi}{4}}+\psi(x)e^{-i\frac{\pi}{4}}\right) \tag{2.106}$$

$$\bar{\varphi}(x)=\frac{1}{\sqrt{2}}\left(\psi^{\dagger}(x)e^{-i\frac{\pi}{4}}+\psi(x)e^{i\frac{\pi}{4}}\right), \tag{2.107}$$

satisfying the commutation relations $\{\varphi(x),\varphi(x')\}=\{\bar{\varphi}(x),\bar{\varphi}(x')\}=\delta(x-x')$, and let us consider, as discussed above, the case of a local quench in the transverse field (or equivalently in the mass), starting from the critical point $m=0$, i.e., $m(t)=m(t)\delta(x)$, with $m(0)=0$, which is then described by the Hamiltonian,

$$H[m(t)]=-\frac{i}{2}\int dx\,[\varphi\partial_{x}\varphi-\bar{\varphi}\partial_{x}\bar{\varphi}]+im(t)\bar{\varphi}\varphi_{|x=0}. \tag{2.108}$$

The first step to solve this model and compute the statistics of the work is duplicating the theory using a trick first introduced by Itzynkson and Zuber [131], i.e., introducing an additional pair of Majorana fermions χ and $\bar{\chi}$ described by the same Hamiltonian (2.108) and anti-commuting with the original ones. From these two pairs of Majorana fermions we can then form two Dirac fermions

$$\psi_{R}=e^{-i\pi/4}\frac{\varphi+i\chi}{\sqrt{2}},\quad \psi_{L}=e^{i\pi/4}\frac{\bar{\varphi}+i\bar{\chi}}{\sqrt{2}}, \tag{2.109}$$

in terms of which the Hamiltonian reads

$$H[m(t)]=\int dx\left[\psi_{R}^{\dagger}(-i\partial_{x})\psi_{R}+\psi_{L}^{\dagger}(i\partial_{x})\psi_{L}\right]+m(t)\left(\psi_{L}^{\dagger}\psi_{R}+\psi_{R}^{\dagger}\psi_{L}\right)_{|x=0}. \tag{2.110}$$

In order to get a nonmixed mass term, we perform a nonlocal transformation [66], defining

$$\begin{aligned}\psi_+(x) &= \frac{(\psi_R(x) + \psi_L(-x))}{\sqrt{2}},\\ \psi_-(x) &= \frac{(\psi_R(x) - \psi_L(-x))}{\sqrt{2}i},\end{aligned} \tag{2.111}$$

so that we finally get

$$H[m(t)] = i\int dx \left[\psi_-^\dagger \partial_x \psi_- - \psi_+^\dagger \partial_x \psi_+\right] + m(t)\left[\psi_+^\dagger \psi_+ - \psi_-^\dagger \psi_-\right]_{|_{x=0}}. \tag{2.112}$$

This transformed Hamiltonian describes two independent chiral modes that, since the Hamiltonian is quadratic, are completely characterized by the single-particle Hamiltonians $H_{+,-} = \mp i\partial_x \pm \delta(x)m(t)$. From this we can immediately write the equations of motion for $\psi_{+,-}$, which read

$$\left[i\partial_t \pm i\partial_x\right]\psi_{+,-}(x,t) = \pm\delta(x)m(t)\psi_{+,-}(x,t), \tag{2.113}$$

whose initial condition is that $\psi_\pm(x,0)$ are free massless fermionic operators. These equations describe the scattering of a chiral field on a time-dependent δ potential: for both $x > 0$ and $x < 0$ the field satisfies the free equation of motion, but after hitting the scatterer [in the region $x > 0$ ($x < 0$) for ψ_+ (ψ_-)], it gets a phase shift determined by the condition

$$\psi_{+,-}(0^\pm, t) = \psi_{+,-}(0^\mp, t)e^{\mp i m(t)}. \tag{2.114}$$

From this we can derive the solution

$$\psi_{+,-}(x,t) = e^{\mp i m(t-|x|)\theta(\pm x)}\psi_{+,-}(x \mp t, 0), \tag{2.115}$$

where

$$\psi_{+,-}(x,0) = \int \frac{dk}{\sqrt{2\pi}}\,\hat{a}_{+,-}(k)e^{-\alpha|k|/2}e^{\pm ikx}, \tag{2.116}$$

with α being the ultraviolet cutoff of the theory, and $\hat{a}_{+,-}$ the fermionic annihilation operators for the mode k.

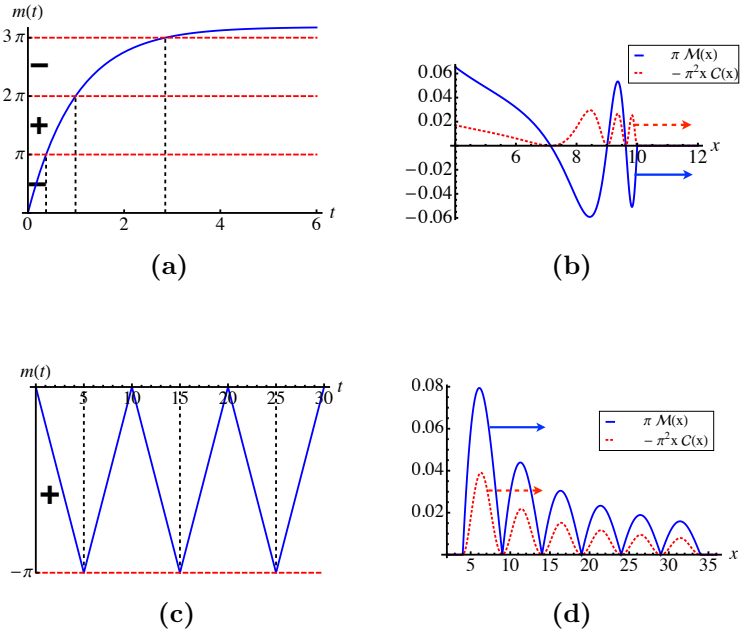

Figure 2.8: *Examples of magnetization and correlations profiles (right) for some specific protocol $m(t)$ (left). In (b) and (d) $t = 10$.*

2.4.1 Transverse Magnetization and its correlations

We are now ready to proceed to the computation of the transverse magnetization produced by the quench $\sigma^z \to 2i\bar{\varphi}(x)\varphi(x) = i\left(\bar{\varphi}(x)\varphi(x) + \bar{\chi}(x)\chi(x)\right)$. We first use Eqs. (2.109) and (2.111) to write it in terms of the Dirac operators $\psi_{+,-}$, getting

$$\begin{aligned}\mathcal{M}(x,t) = \frac{1}{2}\Big[&\psi_+^\dagger(x,t)\psi_+(-x,t) + \psi_+^\dagger(-x,t)\psi_+(x,t) - \psi_-^\dagger(-x,t)\psi_-(x,t) \\ &-\psi_-^\dagger(x,t)\psi_-(-x,t)\Big] - \frac{i}{2}\Big[\psi_+^\dagger(x,t)\psi_-(x,t) - \psi_+^\dagger(-x,t)\psi_-(-x,t) \\ &+\psi_-^\dagger(-x,t)\psi_+(-x,t) - \psi_-^\dagger(x,t)\psi_+(x,t)\Big]\,.\end{aligned} \tag{2.117}$$

We now compute the average of this operator over the initial state, i.e., the Dirac sea in which all the modes $k < 0$ are occupied. We immediately see that the mixed terms in the second row average to zero, while the terms in the first row can be computed using Eq. (2.115) and the mode expansion written below

that equation, getting

$$\langle \psi_+^\dagger(\pm x,t)\psi_+(\mp x,t)\rangle = \frac{e^{\mp im(t-|x|)}}{2\pi(\alpha \mp 2ix)} \tag{2.118a}$$

$$\langle \psi_-^\dagger(\pm x,t)\psi_-(\mp x,t)\rangle = \frac{e^{im(t-|x|)}}{2\pi(\alpha \pm 2ix)}. \tag{2.118b}$$

Putting all the terms together we obtain the final result

$$\langle \mathcal{M}(x,t)\rangle = -\frac{2|x|}{\pi(4x^2+\alpha^2)} \sin\left(m(t-|x|)\right). \tag{2.119}$$

This formula tells us that the local protocol $m(t)$ performed on the system causes the propagation at the velocity of light (which has been taken to be equal to 1) of two identical magnetization profiles to the left and to the right of the origin. The amplitude of these profiles decreases with distance as $1/x$.
Moreover, one can easily extract the qualitative features of the traveling signals. Indeed, the number of zeros is given by the number of times $m(t)$ crosses a value that is a multiple of π and from the properties of the sine one can easily understand if the profile is positive or negative. As an example, in Fig. 2.9a the protocol $m(t) = 10(1-e^{-t})\Theta(t)$ is analyzed. We conclude that the traveling profile will have three zeros, and a positive tail, since it asymptotically ends at a value between 3π and 4π. Figure 2.9b shows that these are indeed the features of the magnetization profile produced. This simple understanding can be used to design protocols $m(t)$ producing a profile with the desired features. As an example, in Fig. 2.8c a protocol that produces six positive wave-packets with the same width is shown.
We can now use the same procedure to compute the connected correlations of the transverse magnetization at equal times $\langle \mathcal{M}(x,t)\mathcal{M}(x',t)\rangle_C$. Using Eq. (2.117) to compute the products of two magnetization operators at different points, one obtains 64 terms, but the average over the initial state makes all the terms in which the number of ψ_+ and ψ_- operators is different vanish, so one is left with 16 relevant terms. At that point one can apply Wick's theorem to decompose the products of four fermionic operators, then has to subtract the product of the average values at x and x' to get the connected correlations, and

finally use Eq. (2.115). More details can be found in Appendix 2.A. The final result of this procedure is

$$\langle \mathcal{M}(x,t)\mathcal{M}(x',t)\rangle_C = \cos\left(m(t-|x|)\right)\cos\left(m(t-|x'|)\right)\left[\frac{1}{2\pi^2\left[\alpha^2+(x-x')^2\right]}\right.$$
$$\left.+\frac{\alpha^2}{2\pi^2(4x^2+\alpha^2)(4x'^2+\alpha^2)}\right]+\sin\left(m(t-|x|)\right)\sin\left(m(t-|x'|)\right)$$
$$\left[\frac{2\Theta(xx')xx'}{\pi^2\left[\alpha^2+(x+x')^2\right]\left[\alpha^2+(x-x')^2\right]}-\frac{2|xx'|}{\pi^2(4x^2+\alpha^2)(4x'^2+\alpha^2)}\right]. \tag{2.120}$$

Since the magnetization profile is symmetric, the correlation between point x and $-x$ is of particular interest. In particular the excess correlation $\mathcal{C}(x,t) = \langle \mathcal{M}(x,t)\mathcal{M}(-x,t)\rangle_C - \langle \mathcal{M}(x,0)\mathcal{M}(-x,0)\rangle_C$ is given by

$$\mathcal{C}(x,t) = \frac{1}{2\pi^2(4x^2+\alpha^2)}\left(\cos\left(2m(t-|x|)\right)-1\right). \tag{2.121}$$

As in the case of the transverse magnetization, one may easily design the protocol $m(t)$ to give a certain desired correlation profile. In particular, the zeros of $\mathcal{C}(x,t)$ are the same as those of the magnetization, as one can also check in Fig.2.9b and 2.8d for specific protocols. More specifically, for every protocol $m(t)$ the excess correlations are always negative and travel through the system at the same speed of the magnetization, decreasing with the distance from the origin as $1/x^2$.

2.4.2 Work distribution

We now turn to the computation of the statistics of the work done by this local protocol. In order to do so we will use a slightly different version of Eq. (2.9) and switch from the moment generating function to the characteristic function by performing the substitution $s \to -i\mu$. Thus we have

$$G(\mu) = {}_0\langle 0|e^{i\mu H^H[m(\tau)]}e^{-i\mu H[m(0)]}\left|0\right\rangle_0, \tag{2.122}$$

where $H^H[m(\tau)] = U^\dagger(\tau)H[m(\tau)]U(\tau)$ is the final Hamiltonian in the Heisenberg picture, while $\left|0\right\rangle_0$ is always the initial ground state. Since we duplicated the theory, we will be actually computing $G^2(\mu)$.

The first step is to bosonize the Hamiltonian (2.112) using the usual formula,

$$\psi_{+,-} = \frac{1}{\sqrt{2\pi\alpha}} e^{\pm i\sqrt{4\pi}\phi_{\pm}(x)}, \tag{2.123}$$

which gives (up to an irrelevant constant)

$$H^H[\bar{m}] = \int dx \left[\partial_x\phi_+(x,\tau) + \frac{\bar{m}}{2\sqrt{\pi}}\delta(x)\right]^2 + \left[\partial_x\phi_-(x,\tau) - \frac{\bar{m}}{2\sqrt{\pi}}\delta(x)\right]^2. \tag{2.124}$$

where $\bar{m} \equiv m(\tau)$, and the bosonic operators $\phi_{+,-}$ are evolved with the full Hamiltonian until the final time τ.
Then, using Eqs. (2.115) and (2.123) we can explicitly compute these evolved bosonic operators, which are given by

$$\phi_{+,-}(x,\tau) = \bar{\phi}_{+,-}(x,\tau) - \frac{m(\tau \mp x)}{\sqrt{4\pi}}\Theta(\pm x), \tag{2.125}$$

where $\bar{\phi}_{+,-}$ are instead bosonic field evolved with the free Hamiltonian. We can then use these expressions to write the Hamiltonian as

$$\begin{aligned} H^H[\bar{m}] = \int dx \left[\partial_x\bar{\phi}_+(x,\tau) - \frac{\Theta(x)}{2\sqrt{\pi}}\partial_x m(\tau - x)\right]^2 \\ + \left[\partial_x\bar{\phi}_-(x,\tau) - \frac{\Theta(-x)}{2\sqrt{\pi}}\partial_x m(\tau + x)\right]^2. \end{aligned} \tag{2.126}$$

We now look for an operator that shifts the derivatives of the fields $\bar{\phi}_{+,-}$ by the terms appearing in the preceding formula. To this aim the ψ_+ and ψ_- operators can be treated independently. Let us then consider the ψ_+ operator and define $\mathcal{U}_+(s) = e^{-is\hat{A}}$, with

$$\hat{A}_+ = \int_0^{+\infty} dy\, \bar{\phi}_+(y,\tau)\partial_y m(\tau - y). \tag{2.127}$$

By using the commutation relation $[\bar{\phi}_+(x,t), \bar{\phi}_+(y,t)] = \frac{i}{4}\,\mathrm{sign}(x-y)$, we can derive the action of this operator on the derivative of the field $\bar{\phi}_+$, which is

$$\mathcal{U}_+^\dagger(s)\partial_x\bar{\phi}_+\mathcal{U}(s) = \partial_x\bar{\phi}_+(x,\tau) + \frac{1}{2}\,\Theta(x)\partial_x m(\tau - x)s, \tag{2.128}$$

so the choice $s = -1/\sqrt{\pi}$ gives the shift we were looking for.

We may now proceed in the same way for the operator ψ_-, so that at the end the unitary operator giving the shift we are looking for both the field $\bar{\phi}_+$ and the field $\bar{\phi}_-$ is $\mathcal{U} = \mathcal{U}_+\mathcal{U}_- = e^{i/\sqrt{\pi}\hat{A}}$ with

$$\hat{A} = \int_0^\infty dy \left(\phi_+(y-\tau,0) + \phi_-(\tau-y,0)\right) \partial_y m(\tau-y). \tag{2.129}$$

Here we used the fact that $\bar{\phi}_{+,-}(y,t) = \phi_{+,-}(y \mp t)$, where from now on the field depending on just one variable is taken at the initial time $t = 0$.
Putting everything together, we have that $H^H[\bar{m}] = \mathcal{U}^\dagger H[m(0)]\mathcal{U}$, which gives us

$$G^2(\mu) = {}_0\langle 0|\mathcal{U}^\dagger\mathcal{U}(\mu)\,|0\rangle_0\,, \tag{2.130}$$

where in $\mathcal{U}(\mu) = e^{i\mu H[m(0)]}\mathcal{U}e^{-i\mu H[m(0)]}$ the bosons fields are evolved with the free Hamiltonian. Rewriting all in terms of the initial fields, we finally get

$$\begin{aligned} G^2(\mu) = \exp\Bigg[\frac{1}{\pi}\int_0^{+\infty} dy \int_0^{+\infty} dy'\, \partial_y m(\tau-y)\partial_{y'} m(\tau-y') \big(\langle\phi_+(y-\tau)\phi_+(y'-\tau-\mu)\rangle \\ + \langle\phi_-(\tau-y)\phi_-(\tau+\mu-y')\rangle - \frac{1}{2}\langle\phi_+(y-\tau)\phi_+(y'-\tau)\rangle \\ - \frac{1}{2}\langle\phi_+(y-\tau-\mu)\phi_+(y'-\tau-\mu)\rangle - \frac{1}{2}\langle\phi_-(\tau-y)\phi_-(\tau-y')\rangle \\ - \frac{1}{2}\langle\phi_-(\tau+\mu-y)\phi_-(\tau-y'+\mu)\rangle\Big)\Bigg]. \end{aligned} \tag{2.131}$$

where $\langle\cdot\rangle = {}_0\langle 0|\cdot|0\rangle_0$.
Now to compute the correlations of the bosonic fields we use their mode expansion

$$\phi_\pm(x) = \pm\int_0^{\pm\infty} dp \frac{e^{-\frac{|\alpha|}{2}p}}{2\pi\sqrt{2|p|}}\left[e^{ipx}\phi(p) + e^{-ipx}\phi^\dagger(p)\right], \tag{2.132}$$

with $\left[\phi(p), \phi^\dagger(p')\right] = 2\pi\delta(p-p')$, from which we obtain

$$\langle\phi_+(y-y'+\mu)\phi_+(0)\rangle - \langle\phi_+(y-y')\phi_+(0)\rangle = \frac{1}{4\pi}\ln\frac{\alpha - i(y-y')}{\alpha - i(y-y'+u)}. \tag{2.133}$$

Finally, considering that $\langle\phi_-(x)\phi_-(y)\rangle = \langle\phi_+(y)\phi_+(x)\rangle$, we obtain the final result $G(\mu) = \exp[F(\mu)]$, with

$$F(\mu) = \frac{1}{4\pi^2}\int_{-\infty}^{\tau} dt \int_{-\infty}^{\tau} dt' \partial_t m(t)\partial_{t'} m(t') \ln\frac{\alpha - i(t-t')}{\alpha - i(t-t'+\mu)}. \tag{2.134}$$

From formula (2.134) we can compute all the cumulants of the distribution of the work using Eq. (2.41). Doing so we get

$$k_n = \frac{1}{4\pi^2 n}\int_{-\infty}^{\tau} dt \int_{-\infty}^{\tau} dt'\, \partial_t m(t)\partial_{t'} m(t')\,\mathrm{Re}\left[\frac{1}{\Big(\alpha - i(t-t')\Big)^n}\right]. \tag{2.135}$$

We immediately notice that, in contrast to what happens in the case of global protocols, and as anticipated before, the cumulants of $P(W)$ are not extensive, i.e. they are not proportional to the volume of the system. As a consequence, we do not have in general that the distribution tends to a Gaussian function in the limit of $L \to \infty$ with higher-order cumulants being suppressed by increasing power of the volume.

We now show that the form of $P(W)$ for small W is independent of the specifics of the protocol performed on the system. For this purpose, as already seen in the previous sections, we have to analyze the asymptotics of $G(\mu)$ for large μ. When $m(\tau) \neq 0$, namely the final local mass is different from zero, we have

$$G(\mu) \simeq e^{\frac{B}{4\pi}}(-i\mu)^{-\frac{\bar{m}}{4\pi^2}}, \tag{2.136}$$

implying

$$P(W) \simeq B w^{\frac{\bar{m}^2}{4\pi^2}-1}, \tag{2.137}$$

with $B = \int_{-\infty}^{\tau} dt \int_{-\infty}^{\tau} dt'\, \partial_t m(t)\partial_{t'} m(t') \ln[\alpha - i(t-t')]$.

Thus $P(W)$ displays an edge singularity with an exponent that depends only on the final value of the local mass but not on the way this value is reached and example of "time universality". For small protocols ($\bar{m} < 2\pi$) there is a power-law divergence, while for large protocols ($\bar{m} > 2\pi$) $P(W)$ vanishes with a cusp. We observe that, as already anticipated in Sec. 2.1 and in contrast to what happens for global protocols, there is no δ peak at the origin, meaning that the probability that the final evolved state is in the ground state of the final Hamiltonian is zero. This is clearly a consequence of the Anderson orthogonality catastrophe [3].

We stress that this result, which may appear natural if one considers monotonic protocols (they all look like sudden quenches when the limit of large μ is taken),

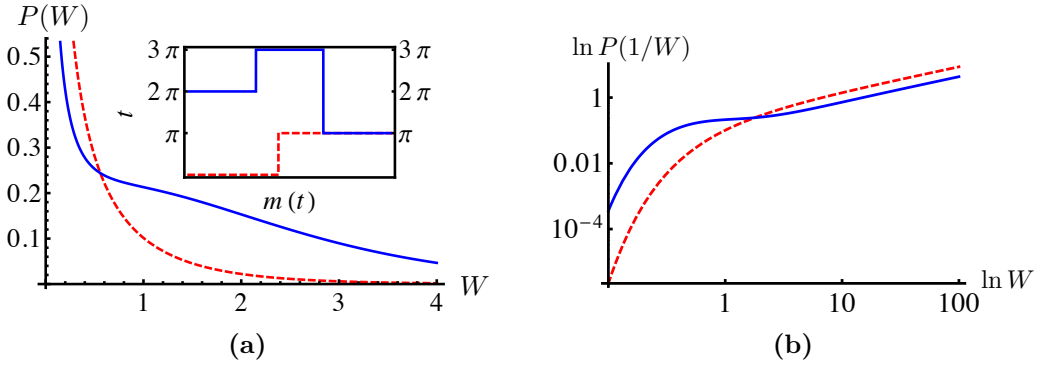

Figure 2.9: *(a) Probability distributions $P(W)$ for a nonmonotonic protocol solid (blue) line, i.e., a series of sudden quenches, and a sudden quench [dashed (red) line] ending at the same value of m and shown in the inset. (b) Logarithmic plot of $P(1/W)$ for the same protocols as before. We set $\alpha = 1$.*

is general: it holds independently of the shape of the protocol, even in the case of nonmonotonic ones or in the case in which the critical point $m = 0$ is crossed. We also note that, while in the case of global protocols (as seen in the previous sections) the spectral weight of the distributions tends to concentrate at a peak at high energies, so that observing the low-energy behavior becomes a rare event when the system size grows, for local protocols the low-energy part still retains a considerable spectral weight, making the power-law behavior likely to be observed. This is a consequence of the fact that, as already observed above, the cumulants of the distribution $P(W)$ are not extensive. The example of Fig. 2.9 clarifies the issue of both nonmonotonicity and observability. In Fig. 2.9a $P(W)$ is shown for a non monotonic protocol and a sudden quench to the same final value of the mass $m(\tau)$ (see the inset). One can see that in both cases the low energy part has a considerable spectral weight. From 2.9b one can see instead that the two protocols at low energy indeed behave as a power law with the same exponent.

The case of cyclic protocol, i.e., $m(\tau) = 0$, is different. In this case the asymptotic behavior of the characteristic function becomes

$$G(u) \simeq e^{\frac{B}{4\pi^2}} e^{C/\mu^2}, \tag{2.138}$$

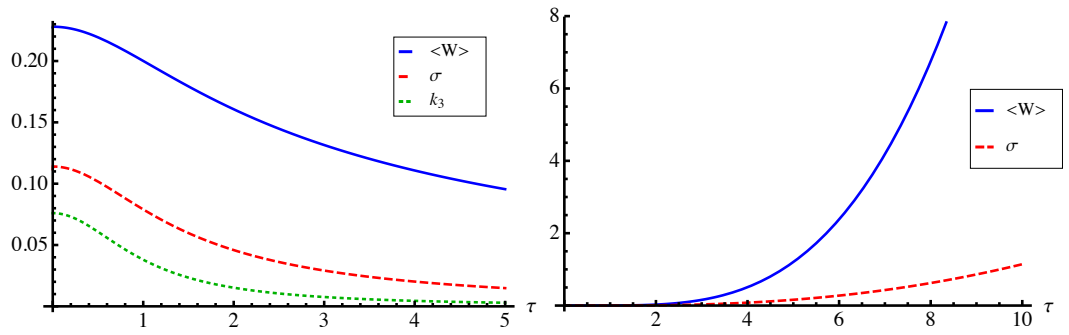

(a) **(b)**

Figure 2.10: *Cumulants for (a) a linear ramp $m(t)$ reaching the final value $\bar{m} = 3$ in a total time τ and (b) parabolic protocol $m(t)$, which returns to $m = 0$ in a total time τ and reaches its maximum value of $\tau^2/4$.. We set $\alpha = 1$.*

with $C = \frac{1}{8\pi^2}\int_{-\infty}^{\tau} dt \int_{-\infty}^{\tau} dt'\, \partial_t m(t)\partial_{t'} m(t')(t - t' + i\alpha)^2$, implying

$$P(W) \simeq e^{\frac{B}{4\pi^2}} \left(\delta(W) + C\, W\right). \tag{2.139}$$

In this case the δ peak is present, since orthogonality catastrophe no longer exists, and still the exponent of the edge singularity is independent of the details of the protocol, even from its final value, since now the regular part of $P(W)$ is always linear.

We conclude this section studying some specific protocols in addition to the ones already considered in Fig. 2.9. Let us start by considering a linear ramp reaching the final value $\bar{m}$. In this case, using formula (2.134) we have that

$$F_{\rm lin}(\mu) = \frac{\bar{m}^2}{\tau^2}\int_0^{\tau} dx_1 \int_0^{\tau} dx_2 \ln\frac{\alpha + i(x_1 - x_2)}{\alpha + i(x_1 - x_2 + u)}. \tag{2.140}$$

The integral can be done explicitly getting

$$\begin{aligned} F_{\rm lin}(\mu) = \frac{\bar{m}^2}{4\pi^2 t_f^2}\Bigg[&\alpha^2 \ln\alpha - (\alpha - i\mu)^2 \ln(\alpha - i\mu) - \frac{(\alpha + i\tau)^2}{2}\ln(\alpha + i\tau) \\ &- \frac{(\alpha - i\tau)^2}{2}\ln(\alpha - i\tau) + \frac{(\alpha - i\mu + i\tau)^2}{2}\ln(\alpha - i\mu + i\tau) \\ &+ \frac{(\alpha - i\mu - i\tau)^2}{2}\ln(\alpha - i\mu - i\tau)\Bigg]. \end{aligned} \tag{2.141}$$

From this one can explicitly check that the asymptotic behavior is the one written above and can get all the cumulants of the distribution. For example, the first three cumulants are given by

$$\langle W\rangle_{\rm lin} = \frac{\bar{m}}{4\pi^2\tau^2}\left[\alpha \ln\frac{\alpha^2}{\alpha^2+\tau^2} + 2\tau \arctan\frac{\tau}{\alpha}\right] \tag{2.142a}$$

$$\sigma^2_{\rm lin} = \frac{\bar{m}^2}{4\pi^2\tau^2}\ln\frac{\sqrt{\alpha^2+\tau^2}}{\alpha} \tag{2.142b}$$

$$k_{3,\rm lin} = \frac{\bar{m}^2}{4\pi^2}\frac{1}{3\alpha(\alpha^2+\tau^2)} \tag{2.142c}$$

In Fig. 2.10a we plot these cumulants as a function of τ for $\bar{m}=3$ and $\alpha=1$. We finally consider an example of a cyclic protocol, namely, a parabolic protocol of total duration τ reaching its maximal amplitude of $k(\tau/2)^2$ at $t=\tau/2$. Using the general formula (2.134) we get

$$F_{\rm par}(\mu) = \frac{k^2}{\pi^2}\int_{-\tau/2}^{\tau/2} dt \int_{-\tau/2}^{\tau/2} dt' t t' \ln\frac{\alpha - i(t-t')}{\alpha - i(t-t'+\mu)}, \tag{2.143}$$

which can be computed to obtain,

$$\begin{aligned} F(\mu) = \frac{k^2}{\pi^2}\Bigg[&\frac{\alpha}{12}(\alpha^3+3\tau^2\alpha+i\tau^3)\,\mathrm{arctanh}\left(\frac{\tau}{2i\alpha-T}\right) - \frac{\alpha}{12}(\alpha^3+3\tau^2\alpha-i\tau^3) \\ &\mathrm{arctanh}\left(\frac{\tau}{2i\alpha+\tau}\right) + \frac{1}{12}\tau^3\alpha\arctan\left(\frac{\tau}{\alpha}\right) + \frac{\alpha^2\tau^2}{24} - \frac{1}{12}(\alpha-i\mu)\left[(\alpha-i\mu)^3\right. \\ &\left.+3\tau^2(\alpha-i\mu)+i\tau^3\right]\,\mathrm{arctanh}\left(\frac{\tau}{2\mu-\tau+2i\alpha}\right) + \frac{1}{12}(\alpha-i\mu)\left[(\alpha-i\mu)^3\right. \\ &\left.+3\tau^2(\alpha-i\mu)-i\tau^3\right]\,\mathrm{arctanh}\left(\frac{\tau}{2i\alpha+\tau+2u}\right) \\ &-\frac{1}{12}\tau^3(\alpha-i\mu)\arctan\left(\frac{\tau}{\alpha-i\mu}\right) - \frac{(\alpha-i\mu)^2}{24}\tau^2\Bigg]. \end{aligned} \tag{2.144}$$

Also in this case one can check that indeed the asymptotic behavior is the same we obtained above and one can compute all the cumulants of the distribution $P(W)$. In particular the first two are given by

$$\langle W\rangle_{\rm par} = \frac{k^2}{6\pi^2}\left[\tau^2\alpha + \tau^3\arctan\left(\frac{\tau}{\alpha}\right) - (3\tau^2\alpha+2\alpha^3)\ln\frac{\sqrt{\alpha^2+\tau^2}}{\alpha}\right], \tag{2.145a}$$

$$\sigma^2_{\rm par} = \frac{k^2}{12\pi^2}\left[(\tau^2+2\alpha^2)\ln\frac{\sqrt{\alpha^2+\tau^2}}{\alpha} - \tau^2\right]. \tag{2.145b}$$

In Fig. 2.10b we show the behavior of these two cumulants as a function of the total time τ for $k = 1$ and $\alpha = 1$.

2.4.3 Generalization to other models

Even tough at the moment we can not mathematically prove that the independence on the details of the protocol, i.e. the "time universality", of the exponent of the edge singularity at low energy in the case of non cyclic protocols is applicable to other models, and so is a general feature for local protocols starting from the critical point, we propose here an heuristic argument in support to such a conclusion.

First, an asymptotic power-law behavior of $G(\mu)$ (and so the absence of a δ peak) has to be expected on the basis of the orthogonality catastrophe, which holds even if the final state is not the ground state of the initial Hamiltonian, since for a local protocol the former differs from the latter only for a finite number of excitations. Then, as explained in Sec. 2.1, $G(\mu)$ can be interpreted as a partition function of a corresponding classical system on a strip of thickness s after the Wick rotation $\mu \to is$. The behavior for large s, which will determine the behavior of $P(W)$ for small W is then expected to be determined by the RG flow of the final state $|\psi(\tau)\rangle$ and the final Hamiltonian $H[m(\tau)]$.

The state should flow back to the initial critical state, since in its evolution only a finite number of excitations has been generated, while the flow of the Hamiltonian will depend on the nature of the defect, which can be marginal, irrelevant, or relevant. Therefore, the flow of the state should ensure the independence from the protocol, while the flow of the Hamiltonian should make the exponent universal in the usual sense of statistical mechanics. Moreover, in the case of a marginal defect (which is the one we explicitly considered here) this exponent should depend on the final strength of the defect (since the flow of the final Hamiltonian does), while in the case of a relevant perturbation we do expect this exponent to be completely independent of the protocol chosen and

equal to $c/8 - 1$, where c is the central charge, coming from the effect of a line of defect in a generic CFT [22]. An indication that this idea may be correct can be observed in the case of sudden quenches (or, equivalently, Fermi edge problem) in a Luttinger liquid [1, 48, 52, 73].

Appendix

2.A Computation of the connected correlations of the transverse magnetization

In this appendix we give additional details about the computation of the connected correlations of the transverse magnetization. As already mentioned, when we multiply two magnetization operators (2.117) at points x and x' we get 64 terms; however we can disregard terms in which the number of creation operators is not equal to the number of annihilation operators for at least one of the two species ψ_+ and ψ_- of chiral fermions. Doing so, we are left with 16 relevant terms

$$\begin{aligned}
&\langle \mathcal{M}(x,t)\mathcal{M}(x',t)\rangle = \frac{1}{4}\Big\langle \psi_+^\dagger(x)\psi_+(-x)\psi_+^\dagger(x')\psi_+(-x') + \psi_+^\dagger(x)\psi_+(-x)\psi_+^\dagger(-x')\psi_+(x') \\
&+ \psi_+^\dagger(-x)\psi_+(x)\psi_+^\dagger(x')\psi_+(-x') + \psi_+^\dagger(-x)\psi_+(x)\psi_+^\dagger(-x')\psi_+(x') + \\
&\psi_-^\dagger(x)\psi_-(-x)\psi_-^\dagger(x')\psi_-(-x') + \psi_-^\dagger(x)\psi_-(-x)\psi_-^\dagger(-x')\psi_-(x') \\
&+ \psi_-^\dagger(-x)\psi_-(x)\psi_-^\dagger(x')\psi_-(-x') + \psi_-^\dagger(-x)\psi_-(x)\psi_-^\dagger(-x')\psi_-(x') \\
&- \psi_+^\dagger(x)\psi_-(x)\psi_-^\dagger(-x')\psi_+(-x') + \psi_+^\dagger(x)\psi_-(x)\psi_-^\dagger(x')\psi_+(x') \\
&+ \psi_+^\dagger(-x)\psi_-(-x)\psi_-^\dagger(-x')\psi_+(-x') - \psi_+^\dagger(-x)\psi_-(-x)\psi_-^\dagger(x')\psi_+(x') \\
&- \psi_-^\dagger(-x)\psi_+(-x)\psi_+^\dagger(x')\psi_-(x') + \psi_-^\dagger(-x)\psi_+(-x)\psi_+^\dagger(-x')\psi_-(-x') \\
&+\psi_-^\dagger(x)\psi_+(x)\psi_+^\dagger(x')\psi_-(x') - \psi_-^\dagger(x)\psi_+(x)\psi_+^\dagger(-x')\psi_-(-x')\Big\rangle .
\end{aligned} \tag{2.146}$$

Here and in the following we will not explicitly write the time dependence of the fermionic operators.

The next step is to decompose the averages of products of four fermionic operators using the Wick theorem and then subtracting the product of the averages of the magnetization at the points x and x' in order to get the connected correlation. If we do so we get

$$\begin{aligned}\langle \mathcal{M}(x,t)\mathcal{M}(x',t)\rangle_C = \frac{1}{4}\Big[&\langle\psi_+^\dagger(x)\psi_+(-x')\rangle\langle\psi_+(-x)\psi_+^\dagger(x')\rangle + \langle\psi_+^\dagger(x)\psi_+(x')\rangle\langle\psi_+(-x)\psi_+^\dagger(-x')\rangle + \\ &\langle\psi_+^\dagger(-x)\psi_+(-x')\rangle\langle\psi_+(x)\psi_+^\dagger(x')\rangle + \langle\psi_+^\dagger(-x)\psi_+(x')\rangle\langle\psi_+(x)\psi_+^\dagger(-x')\rangle + \langle\psi_-^\dagger(x)\psi_-(-x')\rangle \\ &\langle\psi_-(-x)\psi_-^\dagger(x')\rangle + \langle\psi_-^\dagger(x)\psi_-(x')\rangle\langle\psi_-(-x)\psi_-^\dagger(-x')\rangle + \langle\psi_-^\dagger(-x)\psi_-(-x')\rangle\langle\psi_-(x)\psi_-^\dagger(x')\rangle \\ &+ \langle\psi_-^\dagger(-x)\psi_-(x')\rangle\langle\psi_-(x)\psi_-^\dagger(-x')\rangle - \langle\psi_+^\dagger(x)\psi_+(-x')\rangle\langle\psi_-(x)\psi_-^\dagger(-x')\rangle + \langle\psi_+^\dagger(x)\psi_+(x')\rangle \\ &\langle\psi_-(x)\psi_-^\dagger(x')\rangle + \langle\psi_+^\dagger(-x)\psi_+(-x')\rangle\langle\psi_-(-x)\psi_-^\dagger(-x')\rangle - \langle\psi_+^\dagger(-x)\psi_+(x')\rangle\langle\psi_-(-x)\psi_-^\dagger(x')\rangle \\ &- \langle\psi_-^\dagger(-x)\psi_-(x')\rangle\langle\psi_+(-x)\psi_+^\dagger(x')\rangle + \langle\psi_-^\dagger(-x)\psi_-(-x')\rangle\langle\psi_+(-x)\psi_+^\dagger(-x')\rangle + \langle\psi_-^\dagger(x)\psi_-(x')\rangle \\ &\langle\psi_+(x)\psi_+^\dagger(x')\rangle - \langle\psi_-^\dagger(x)\psi_-(-x')\rangle\langle\psi_+(x)\psi_+^\dagger(-x')\rangle + \langle\psi_+^\dagger(x)\psi_+(-x)\rangle\langle\psi_-^\dagger(x')\psi_-(-x')\rangle \\ &+ \langle\psi_+^\dagger(x)\psi_+(-x)\rangle\langle\psi_-^\dagger(-x')\psi_-(x')\rangle + \langle\psi_+^\dagger(-x)\psi_+(x)\rangle\langle\psi_-^\dagger(-x')\psi_-(x')\rangle + \langle\psi_-^\dagger(x)\psi_-(-x)\rangle \\ &\langle\psi_+^\dagger(x')\psi_+(-x')\rangle + \langle\psi_-^\dagger(x)\psi_-(-x)\rangle\langle\psi_+^\dagger(-x')\psi_+(x')\rangle + \langle\psi_-^\dagger(-x)\psi_-(x)\rangle\langle\psi_+^\dagger(x')\psi_+(-x')\rangle \\ &+ \langle\psi_-^\dagger(-x)\psi_-(x)\rangle\langle\psi_+^\dagger(-x')\psi_+(x')\rangle + \langle\psi_+^\dagger(-x)\psi_+(x)\rangle\langle\psi_-^\dagger(x')\psi_-(-x')\rangle\Big].\end{aligned} \tag{2.147}$$

Using Eq. (2.115) and the mode expansion of the fermionic field we can compute the average values of the products of pairs of fermionic operators, which are given by

$$\langle\psi_{+,-}^\dagger(x)\psi_{+,-}(y)\rangle = e^{\pm im(t-|x|)\Theta(\pm x)}e^{\mp im(t-|y|)\Theta(\pm y)}\frac{1}{2\pi\left(\alpha \mp i(x-y)\right)} \tag{2.148a}$$

$$\langle\psi_{+,-}(x)\psi_{+,-}^\dagger(y)\rangle = e^{\pm im(t-|y|)\Theta(\pm y)}e^{\mp im(t-|x|)\Theta(\pm x)}\frac{1}{2\pi\left(\alpha \pm i(x-y)\right)}. \tag{2.148b}$$

With these two expression we can then compute all the terms of Eq. (2.147) and, after some algebra, get the expression (2.120).

2.B Coefficients of the quartic protocol

In this appendix we give the explicit expressions for the coefficients of the quartic protocols considered in the case of the global protocols in the bosons system and in the Ising chain.

In all three cases we wrote the coefficients ρ_n as

$$\rho_4 = e_1/4, \tag{2.149a}$$

$$\rho_3 = -\frac{e_1}{3}(\frac{1}{3} + e_2 + e_3), \tag{2.149b}$$

$$\rho_2 = \frac{e_1}{2}(\frac{e_2}{3} + \frac{e_3}{3} + e_2 e_3), \tag{2.149c}$$

$$\rho_1 = -\frac{e_1 e_2 e_3}{3}, \tag{2.149d}$$

Then, for the bosons we set

$$e_1 = 18 + \frac{486 m_0}{m_i - m_f}, \tag{2.150a}$$

$$\begin{aligned} e_{2/3} =& \frac{1}{1344 m_i - 48 m_f}\Big(580 m_i - 13 m_f \\ & \pm \sqrt{261136 m_i^2 - 9704 m_i m_f + 73 m_f^2}\Big). \end{aligned} \tag{2.150b}$$

In the case of the Ising chain and protocols starting and ending in the same phase we set

$$e_1 = \frac{9(56 g_i - 2 g_f - 27)}{g_i - g_f}, \tag{2.151a}$$

$$\begin{aligned} e_{2/3} =& \frac{1}{48(56 g_i - 27 - 2 g_f)}\Big[1160 g_f - 26 g_f - 567 \\ & \big(251505 + 1044544 g_i^2 + 4 g_f(4779 + 73 g_f) \\ & - 16 g_i(64071 + 2426 g_f)\big)^{1/2}\Big]. \end{aligned} \tag{2.151b}$$

Finally for the case of protocols starting and ending in different phases we set

$$e_1 = \frac{27(8 g_i - 2 g_f - 3)}{2(g_i - g_f)} \tag{2.152a}$$

$$\begin{aligned} e_{2/3} =& \frac{1}{12(8 g_i - 2 g_f - 3)}\Big[14 g_i - 8 g_f - 3 + \big(873 + 4676 g_i^2 \\ & + 32 g_f(18 + g_f) - 4 g_i(1017 + 304 g_f)\Big]^{1/2} \end{aligned} \tag{2.152b}$$

2.C Asymptotic behavior of $f_c(s)$ in the Ising chain

In this appendix we will give additional detail on the computation of the asymptotic behavior in the limit of large s of the function $f_c(s)$ in the Ising chain. The starting formula is Eq. (2.77) from which, as stated above, we derive

$$f_c(s) = -\int_0^\pi \frac{dk}{2\pi} \ln\left(1 + |y_k(\tau)|^2 e^{-2s\epsilon_k(\tau)}\right). \tag{2.153}$$

We now use Mellin transform [91],

$$\log(1+x) = \int_{c-i\infty}^{c+i\infty} \frac{d\mu}{2\pi i} \frac{\pi}{\mu \sin(\pi\mu)} x^{-\mu}, \tag{2.154}$$

where $-1 < c < 0$, to rewrite Eq. (2.153) as

$$f_c(s) = -\int_{c-i\infty}^{c+i\infty} \frac{d\mu}{2\pi i} \frac{\pi}{\mu \sin(\pi\mu)} \int_0^\pi \frac{dk}{2\pi} |y_k(\tau)|^{-2\mu} e^{2\mu\epsilon_k(\tau)s}. \tag{2.155}$$

In the limit of large s the integral over k is dominated by the low k region, so for protocols with $g_f \neq 1$, we have

$$I(k) = \int_0^\pi \frac{dk}{2\pi} |y_k(\tau)|^{-2\mu} e^{2\mu\epsilon_k(\tau)s} \simeq e^{2\mu s|1-g_f|} \int_0^\infty \frac{dk}{2\pi} |y_k(\tau)|^{-2\mu} e^{\frac{g_f}{|1-g_f|}\mu s k^2}. \tag{2.156}$$

Let us now consider the different possible behaviors of $|y_k(\tau)|$ at small k and compute the asymptotics of the previous integral accordingly. For protocols starting and ending in the same phase, we have $|y_k(\tau)|^2 \simeq |c_1(\tau)|^2 k^2$, so that

$$\begin{aligned} I(k) &\simeq \int_0^\pi \frac{dk}{2\pi} |c_1(\tau)|^{-2\mu} k^{-2\mu} e^{2\mu s|1-g_f| + \frac{g_f}{|1-g_f|}\mu s k^2} \\ &\simeq \frac{1}{4\pi} \left(-\frac{\mu s g_f}{|1-g_f|}\right)^{\mu-1/2} \Gamma[1/2-\mu] |c_1(\tau)|^{-2\mu} e^{2\mu s|1-g_f|}, \end{aligned} \tag{2.157}$$

from which

$$f_c(s) = -\frac{1}{4\pi} \int_{c-i\infty}^{c+i\infty} \frac{d\mu}{2\pi i} \frac{\pi}{\mu \sin(\pi\mu)} \left(-\frac{\mu s g_f}{|1-g_f|}\right)^{\mu-1/2} \Gamma(1/2-\mu) |c_1(\tau)|^{-2\mu} e^{2\mu s|1-g_f|}. \tag{2.158}$$

To extract the asymptotic behavior of the previous expression we notice that the integrand has poles for $\mu = -n$, with n positive integer, therefore the dominant contribution will come from the residue computed in $\mu = -1$. This gives as a result Eq. (2.87).

Let us now consider the case of protocols starting from the critical point, where we have $|y_k(\tau)|^2 \simeq 1$, from which

$$I(k) \simeq \int_0^\pi \frac{dk}{2\pi} k^{-2\mu} e^{2\mu s|1-g_f| + \frac{g_f}{|1-g_f|}\mu s k^2} \simeq \frac{e^{2\mu s|1-g_f|}}{2\sqrt{\pi}} \left(-\frac{|1-g_f|}{g_f \mu s}\right)^{1/2}, \quad (2.159)$$

implying

$$f_c(s) = -\frac{1}{4\sqrt{\pi}} \int_{c-i\infty}^{c+i\infty} \frac{d\mu}{2\pi i} \frac{\pi}{\mu \sin(\pi\mu)} \left(-\frac{|1-g_f|}{\mu s g_f}\right)^{1/2} e^{2\mu s|1-g_f|}. \quad (2.160)$$

Also in this case the dominant contribution comes from the residue for $\mu = -1$ and gives as a result Eq. (2.91).

For quenches ending at the critical point we also have $|y_k(\tau)|^2 = 1$, but also the low energy behavior of $\epsilon_k(\tau)$ changes, giving

$$I(k) = \simeq \int_0^\pi \frac{dk}{2\pi} e^{2\mu s k} = -\frac{1}{4\pi\mu s}, \quad (2.161)$$

from which

$$f_c(s) = \frac{1}{4\pi} \int_{c-i\infty}^{c+i\infty} \frac{d\mu}{2\pi i} \frac{\pi}{\mu \sin(\pi\mu)} \frac{1}{2\mu s}, \quad (2.162)$$

whose dominant behavior is again dominate by the residue at $\mu = -1$ that gives Eq. (2.95).

The last case to be examined is when the initial and final point of the protocol are in different phases. When this happens we have $|y_k(\tau)|^2 \simeq \frac{4}{|d_1(\tau)|^2 k^2}$. This implies

$$\begin{aligned} I(k) &\simeq \int_0^\pi \frac{dk}{2\pi} |d_1(\tau)|^{2\mu} 4^{-\mu} k^{2\mu} e^{2\mu s|1-g_f| + \frac{g_f}{|1-g_f|}\mu s k^2} \\ &\simeq \frac{1}{4\pi} \left(-\frac{|1-g_f|}{\mu s g_f}\right)^{\mu+1/2} \Gamma(1/2+\mu) |d_1(\tau)|^{2\mu} 4^{-\mu} e^{2\mu s|1-g_f|}, \end{aligned} \quad (2.163)$$

which requires $\Re\mu > -1/2$ and implies

$$f_c(s) = -\frac{1}{4\pi} \int_{c-i\infty}^{c+i\infty} \frac{d\mu}{2\pi i} \frac{\pi}{\mu \sin(\pi\mu)} \left(-\frac{|1-g_f|}{\mu s g_f}\right)^{\mu+1/2} \Gamma(1/2-\mu) |d_1(\tau)|^{2\mu} 4^{-\mu} e^{2\mu s|1-g_f|}. \quad (2.164)$$

The integrand has now poles for $\mu = -n/2$, with $n \in \mathbb{N}$, i.e. for negative semintegers. This implies the appearance of an additional delta peaks at $W = |1 - g|$ in the distribution of the work. The result of Eq. (2.103 is recovered considering the residues in the first two poles $\mu = -1/2$ and $\mu = -1$.

Chapter 3

Dynamical phase transition in the $O(N)$ vector model ($N \to \infty$)

In this chapter we will discuss the dynamical phase transition in the $O(N)$ vector model at the leading order in the expansion in the $1/N$ expansion (see [85] for a review on the subject), with N being the number of components. The hamiltonian of the model describes an N component real scalar field in generic d spatial dimension with quartic self-interaction,

$$H = \frac{1}{2}\int d^d x \left[\Pi_a \Pi_a + \left(\vec{\nabla}\phi_a\right)\cdot\left(\vec{\nabla}\phi_a\right) + r_0\phi_a\phi_a + \frac{\lambda}{12N}(\phi_a\phi_a)^2\right], \tag{3.1}$$

with

$$[\phi_i(\vec{x}), \Pi_j(\vec{x}')] = i\delta^d(\vec{x}-\vec{x}')\delta_{ij}, \tag{3.2}$$

where i and j denote different components of the field. This model described the critical properties of systems like vapor-liquid, binary mixtures, superfluid Helium or ferromagnetic transitions. In particular, in the case $N = 2$ it describes the properties of a Bose-Hubbard model near the superfluid to Mott insulator transition at constant density [107]. As discussed in section 1.5 the dynamical transition of this model has been numerical studied for $d = 3$ in [114]. However, the nature of such a transition (i.e, it is manly driven by quantum or non equilibrium fluctuations), characterized by a non-analytic behavior of long-time averages of observables, is still unclear. Moreover, since the investigation of this

phenomenon has so far been only theoretical, it would be valuable to find signatures of dynamical transitions that are suitable for experimental studies and that may clearly distinguish them from quantum and/or classical transitions. Here, with these goals in mind, we will characterize the critical properties of the dynamical transition and discuss its detection in the quantum $O(N)$ vector model for quenches starting in the disordered phase and for a generic spatial dimensions, showing that, despite the fact that the system is throughout the dynamics in a pure state, the lower and upper critical dimensions as well as the critical exponents are analogous to those of a finite temperature transition. We will then show that the peculiarities of dynamical transitions (can be detected by studying the *statistics* of the number of excitations generated in a double quench from the disordered phase towards (or below) the dynamical critical point as a function of the time t_W spent in the intermediate phase. The critical properties turn out to be encoded in the fluctuations: while the average number of excitations always saturates to a finite value, the variance (or higher cumulants) shows a qualitatively different behavior as a function of t_W depending on whether the first quench was performed above, below or at the dynamical critical point. Finally we will study how these critical features are affected when, instead of a sudden quench a ramp is performed on the system.

3.1 Equilibrium properties

Let us start by briefly considering the equilibrium properties of the model under study. Using the functional integral formalism [89] we can write its partition function as

$$\mathcal{Z} = \int \mathcal{D}\phi \exp\left\{ -\frac{1}{2}\int_0^\beta d\tau \int d^d x \left[\left(\partial_\tau \phi_a\right)\left(\partial_\tau \phi_a\right) + \left(\vec{\nabla}\phi_a\right)\cdot\left(\vec{\nabla}\phi_a\right) + r_0 \phi_a \phi_a + \frac{\lambda}{12N}(\phi_a\phi_a)^2 \right] \right\}, \tag{3.3}$$

where the field satisfies periodic boundary conditions in τ, i.e. $\phi(\vec{x}, \tau + \beta) = \phi(\vec{x}, \tau)$, and β is the inverse temperature of the system. We can now perform an Hubbard-Stratonovich transformation

$$\exp\left[-\frac{\lambda}{4!N} \int_{\tau,x} (\phi_a \phi_a)^2 \right] \sim \int \mathcal{D}\chi \exp\left\{ \int_{\tau,x} \left[\frac{-3N\chi^2}{2\lambda} + \frac{i}{2}\chi\phi_a\phi_a \right] \right\}, \quad (3.4)$$

where $\int_{\tau,x} = \int_0^\beta d\tau \int d^d x$. The integral over the field ϕ is now gaussian, therefore can be easily performed, giving as a result

$$\mathcal{Z} = \int \mathcal{D}\chi \exp\left[\frac{N}{2} \mathrm{Tr} \log\left[-\nabla^2 + r_0 - i\chi \right] + \int_0^\beta d\tau \int d^d x \frac{3N\chi^2}{2\lambda} \right]. \quad (3.5)$$

Finally, in the limit $N \to \infty$, the integral over χ can be performed using a saddle point approximation, which, assuming it to be uniform, give as a result,

$$\frac{3\beta}{\lambda}\chi - \frac{i}{2} \sum_{\omega_n} \int_k \frac{1}{\omega_n^2 + |\vec{k}|^2 + r_0 - i\chi} = 0, \quad (3.6)$$

where $\omega_n = \frac{2\pi}{\beta} m$, with m integer are the usual Matsubara's frequencies, $\int_k = \int \frac{d^d k}{(2\pi)^d}$, restricted to the region $|\vec{k}| < \Lambda$, with Λ being the ultraviolet cutoff.
We now notice that, with the field χ fixed by the condition (3.6), each component of the field ϕ is decoupled and described by a quadratic Hamiltonian, with an effective mass $r \equiv r_0 - i\chi$. By using the condition (3.6) and performing the sum over Matsubara's frequencies, we can then write down a self-consistent equation determining the value of such an effective mass,

$$r = r_0 + \frac{\lambda}{12} \int_k \frac{\coth\left(\frac{\beta}{2}\sqrt{|\vec{k}|^2 + r} \right)}{\sqrt{k^2 + r}}. \quad (3.7)$$

From this equation we can identify the critical point of the model $r_{0,c}$, which is given by the condition of zero effective mass, i.e., $r = 0$. Indeed, when this condition is verified, the inverse Green's function at $k = 0$ and the susceptibility of the model, are divergent. Thus, we have,

$$r_{0,c} = -\frac{\lambda}{12} \int_k \frac{\coth\left(\frac{\beta|\vec{k}|}{2} \right)}{|\vec{k}|}. \quad (3.8)$$

We immediately notice that when the temperature is non zero $r_{0,c}$ is finite for $d > 2$, while at zero temperature $\beta \to \infty$ it is finite for $d > 1$. Therefore we can identify the lower critical dimension for both the thermal and the quantum (zero temperature) transition, which are respectively $d = 2$ and $d = 1$.
When $r_0 < r_{0,c}$, Eq. (3.7) would predict a negative effective mass, resulting in an unstable theory. This is a signal that the $O(N)$ symmetry, which we have preserved during the whole procedure, is broken, and indeed the problem is solved by assuming that $\langle \phi_{\bar{a}} \rangle \neq 0$ for a certain $\bar{a}$ [85].
Let us now compute the critical exponent ν, describing the divergent behavior of the correlation length ξ, i.e., $\xi \sim (\delta r_0)^{-\nu}$, with $\delta r_0 \equiv r_0 - r_{0,c}$. Combining Eqs. (3.7) and (3.8) and introducing the dimensionless variable $\vec{x} = \vec{k}/\sqrt{r}$, we can write

$$r = \delta r_0 - \frac{\lambda}{12} r^{\frac{d-1}{2}} \int_x \frac{\sqrt{|\vec{x}|^2+1}\coth\left(\frac{\beta\sqrt{r}|\vec{x}|}{2}\right) - |\vec{x}|\coth\left(\frac{\beta\sqrt{r}}{2}\sqrt{|\vec{x}|^2+1}\right)}{|\vec{x}|\sqrt{|\vec{x}|^2+1}}, \quad (3.9)$$

where $\int_x = \int \frac{d^d x}{(2\pi)^d}$, now restricted to the region $|\vec{x}| < \Lambda/\sqrt{r}$.
Let us start analyzing the previous expression in the case of the quantum phase transition at $T = 0$, where we the two hyperbolic cotangents are simply equal to one. In this limit the behavior of the integral for large $|\vec{x}|$ is $1/(2|\vec{x}|^3)$, thus for $d < 3$ the integral is finite in the limit $r \to 0$, implying $r \sim (\delta r_0)^{\frac{1}{d-1}}$, while for $d = 3$ there are logarithmic corrections. Instead, when $d > 3$ the integral diverges, and its asymptotic behavior $(\Lambda/\sqrt{r})^{d-3}$, can be inferred by noticing from the above mentioned behavior of the integrand for large $|\vec{x}|$, which implies that the integral goes like $(r^\star)^{(3-d)/2}$. Therefore, we get a linear relation $r \sim (\delta r_0)$. The behavior of the correlation function can recovered from the relation $\xi^{-1} = \sqrt{r}$, so that we have

$$T = 0 \qquad \begin{array}{ll} \nu = \dfrac{1}{d-1} & 1 < d < 3 \\ \nu = \dfrac{1}{2} & d \geq 3, \end{array} \quad (3.10)$$

from which we conclude that $d = 3$ is the upper critical dimension for the quantum transition.

In the case of the thermal transition, we have to analyze the behavior of the integral in the region $1 \ll x \ll 1/(\beta\sqrt{r})$, which is $1/(\sqrt{r}x^4)$. From this we derive that for $d < 4$, we can take take the upper limit equal to infinity and substitute the integrand with its leading order in the expansion in r, which gives,

$$r \simeq \delta r_0 - \frac{\lambda}{6\beta}\frac{\Omega(d)}{(2\pi)^d} r^{\frac{d-2}{2}} \int_0^\infty dx^{d-3} \frac{1}{x^2+1}, \tag{3.11}$$

therefore the dominant contribution comes from the integral and gives $r \sim (\delta r_0)^{\frac{1}{d-2}}$, while for $d = 4$ there are logarithmic corrections. Finally for $d > 4$ the divergence of the integral with r can be estimated by consider the behavior of the integrand cited above, which gives $r^{(3-d)/2}$, implying the linear relation, $r \sim (\delta r_0)$. Summarizing,

$$T \neq 0 \qquad \begin{array}{ll} \nu = \dfrac{1}{d-2} & 1 < d < 4 \\ \nu = \dfrac{1}{2} & d \geq 4, \end{array} \tag{3.12}$$

which implies that $d = 4$ is the upper critical dimension for the thermal transition.

3.2 Dynamics and dynamical critical properties

Let us now discuss the dynamics of the system. In particular, we will consider the case of a sudden quench of the bare mass r_0, starting from the ground state, from an initial value $r_{0,i}$ in the paramagnetic phase, i.e. $r_{0,i} > r_{0,c}$ to a generic $r_{0,f}$. By performing the same procedure above on the Keldysh partition function [65, 98], one easily sees that also in the case of the dynamics all the components are independent, therefore we will focus on just one component from now on, suppressing the index a, and that we can substitute the full Hamiltonian with an effective quadratic one [30],

$$H_{\text{eff}}(t) = \frac{1}{2}\int d^d x \left[\Pi_a \Pi_a + \left(\vec{\nabla}\phi_a\right)\cdot\left(\vec{\nabla}\phi_a\right) + r(t)\phi_a\phi_a\right] - \frac{3V}{2\lambda}(r(t) - r_{0,f})^2, \tag{3.13}$$

where V is the volume of the system and with a time dependent effective mass,

$$\begin{aligned} r(t) &= r_{0,f} + \frac{\lambda}{6}\langle\phi(\vec{x},t)^2\rangle \\ &= r_{0,f} + \frac{\lambda}{6}\int_k \langle\hat{\phi}_{\vec{k}}(t)\hat{\phi}_{-\vec{k}}(t)\rangle, \end{aligned} \tag{3.14}$$

where $\hat{\phi}_{\vec{k}}(t)$ is the Fourier transform of the field $\phi(\vec{x},t)$.
Expanding the field in terms of the operators $a_{\vec{k}}$ and $a^\dagger_{\vec{k}}$ diagonalizing the initial Hamiltonian, i.e.

$$H_0 = \int_k (|\vec{k}|^2 + r)^{1/2} \left(a^\dagger_{\vec{k}} a_{\vec{k}} + 1/2\right) + \text{const}, \tag{3.15}$$

as

$$\hat{\phi}_{\vec{k}}(t) = f_{\vec{k}}(t) a_{\vec{k}} + f^\star_{\vec{k}}(t) a^\dagger_{-\vec{k}}, \tag{3.16}$$

and imposing the Heisenberg equation of motions

$$\frac{d^2}{dt}\hat{\phi}_{\vec{k}}(t) + \left(k^2 + r(t)\right)\hat{\phi}_{\vec{k}}(t), \tag{3.17}$$

we find that the functions $f_{\vec{k}}(t)$ have to satisfy the equation

$$\frac{d^2 f_{\vec{k}}(t)}{dt^2} + \left(|\vec{k}|^2 + r(t)\right) f_{\vec{k}}(t) = 0, \tag{3.18a}$$

with

$$r(t) = r_{0,f} + \frac{\lambda}{6}\int_k |f_{\vec{k}}(t)|^2. \tag{3.18b}$$

The initial conditions $f_k(0) = \frac{1}{\sqrt{2\omega_{k,i}}}$, $\dot{f}_k(0) = -i\sqrt{\frac{\omega_{k,i}}{2}}$, where $\omega_{k,i} = \sqrt{|\vec{k}|^2 + r_i}$, are fixed by the requirement that $a_{\vec{k}}$ and $a^\dagger_{\vec{k}}$ diagonalize the initial Hamiltonian. Let us start by considering the case of the free theory, i.e. $\lambda = 0$, which implies that the effective mass is equal to the bare mass, namely $r(t) = r_{0,f}$. In this case the solution to Eq. (3.18) can be readily found to be

$$f_{\vec{k}}(t) = \frac{1}{\sqrt{2\omega_{k,i}}}\cos\left(t\sqrt{|\vec{k}|^2 + r_{0,f}}\right) - \frac{i}{\sqrt{|\vec{k}|^2 + r_{0,f}}}\sqrt{\frac{\omega_{k,i}}{2}}\sin\left(t\sqrt{|\vec{k}|^2 + r_{0,f}}\right) \tag{3.19}$$

From this expression one can compute all the quantity of interest. First of all, the equal time two-point correlator of the field can be computed using $\langle \hat{\phi}_{\vec{k}}(t)\hat{\phi}_{-\vec{k}}(t)\rangle = |f_{\vec{k}}(t)|^2$ and obtaining

$$\begin{aligned}\langle \hat{\phi}_{\vec{k}}(t)\hat{\phi}_{-\vec{k}}(t)\rangle = &\frac{2|\vec{k}|^2 + r_{0,i} + r_{0,f}}{4(|\vec{k}|^2 + r_{0,f})\sqrt{|\vec{k}|^2 + r_{0,i}}} + \\ &\frac{r_{0,f} - r_{0,i}}{4(|\vec{k}|^2 + r_{0,f})\sqrt{|\vec{k}|^2 + r_{0,i}}} \cos\left(2t\sqrt{|\vec{k}|^2 + r_{0,f}}\right).\end{aligned} \tag{3.20}$$

In the case of the interacting theory with $\lambda \neq 0$, we have to resort to numerical integration. This shows that for large t the effective mass relaxes towards a stationary state with damped oscillations. To predict this stationary values we make the ansatz that the stationary part of the equal time Green function $\langle \hat{\phi}_{\vec{k}}(t)\hat{\phi}_{-\vec{k}}(t)\rangle$ has the same form as that of the free theory but with renormalized masses. Namely, we take the time average of Eq. (3.20) and make the substitutions $r_{0,i} \to r_i$ and $r_{0,f} \to r^\star$, with $r^\star$ denoting the stationary value of the mass. In this way we obtain a self-consistent equation for $r^\star$,

$$r^\star = r_{0,f} + \frac{\lambda}{24}\int_k \frac{2|\vec{k}|^2 + r_i + r^\star}{(|\vec{k}|^2 + r^\star)\sqrt{|\vec{k}|^2 + r_i}}. \tag{3.21}$$

Fig. 3.1 shows how well this equation predicts the stationary value until the dynamical critical point, identified by the condition $r^\star = 0$, giving

$$r^c_{0,f} = -\frac{\lambda}{24}\int_k \frac{2|\vec{k}|^2 + r_i}{|\vec{k}|^2\sqrt{|\vec{k}|^2 + r_i}}. \tag{3.22}$$

Eq. (3.21) fails when for $r_{0,f} < r^c_{0,f}$,i.e. below the dynamical critical point, where it would predict a negative values for the asymptotic mass, while the numerical simulations show $r^\star = 0$. The figure shows only the cases of $d = 3$ or $d = 4$, since we focused on this cases in more detail, but we checked Eq. (3.21) also in lower and higher dimensions.

From Eq. (3.22) we can immediately notice that $r^c_{0,f}$ is finite for $d > 2$, which allows us to identify $d = 2$ as the lower critical dimension for the dynamical

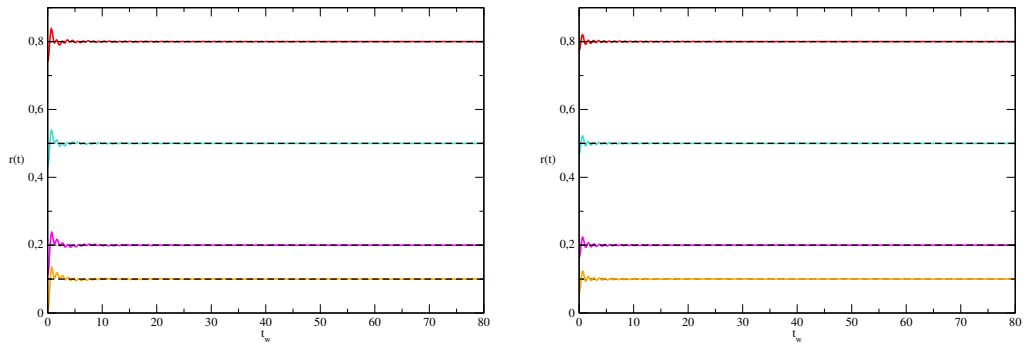

Figure 3.1: *Comparison between $r(t)$ obtained by numerical integration of Eq.(3.18) for quenches to different $r_{0,f} > r^c_{0,f}$ (curves of different colors) and the asymptotic value predicted by Eq. (3.21) (black dashed lines) for $d = 3$ (a) and $d = 4$ (b).*

phase transition. We also notice that $r^c_{0,f} < r_{0,c}$, namely the dynamical critical point is always in the ordered phase.

Analogously to what we have done in the equilibrium case, we can use Eqs. (3.21) and (3.22) to extract the behavior of the asymptotic mass $r^\star$ for small distances of $r_{0,f}$ from the critical point. Indeed let us define $\delta r_{0,f} \equiv r_{0,f} - r^c_{0,f}$ and the dimensionless variable $\vec{y} \equiv \vec{k}/\sqrt{r^\star}$, then for $\delta r_{0,f} > 0$, we have

$$r^\star = \delta r_{0,f} - \frac{\lambda}{24}(r^\star)^{\frac{d-1}{2}} \int_y \frac{\sqrt{|\vec{y}|^2 + r_i/r^\star}}{|\vec{y}|^2(|\vec{y}|^2+1)}, \tag{3.23}$$

with $\int_y = \int \frac{d^d y}{(2\pi)^d}$, now restricted to the region $|\vec{y}| < \Lambda/\sqrt{r^\star}$. Similarly to the case of finite temperature, the asymptotic behavior of the integral for small $r^\star$ is determined by the behavior of the integrand in the region $1 \ll |\vec{y}| \ll \sqrt{r_i/r^\star}$, which is $\sqrt{r_i/r^\star}\frac{1}{|\vec{y}|^4}$. This implies that for $d < 4$ the dominant contribution to the integral can be obtained by putting the upper limit of integration to infinity and taking the leading behavior in $r^\star$ of the integrand, namely

$$\begin{aligned} r^\star &= \delta r_{0,f} - \frac{\lambda\sqrt{r_i}}{24}\frac{\Omega(d)}{(2\pi)^d}(r^\star)^{\frac{d-2}{2}} \int_0^\infty dy\, y^{d-1} \frac{1}{|\vec{y}|^2(|\vec{y}|^2+1)} \\ &= \delta r_{0,f} - \frac{\lambda\sqrt{r_i}}{24}\frac{\Omega(d)}{(2\pi)^d}(r^\star)^{\frac{d-2}{2}} \frac{\pi}{2\sin\left(\frac{\pi(d+2)}{2}\right)}, \end{aligned} \tag{3.24}$$

from which we derive that at the leading order $r^\star \sim (\delta r_{0,f})^{\frac{2}{d-2}}$. For $d = 4$ we will have logarithmic correction to this scaling, while for $d > 4$ the divergence of the integral can be obtained by considering the behavior of the integrand in the region of interest, which we cited above and that tells us that integral goes like $(r^\star)^{(3-d)/2}$, implying the linear relation $r^\star \sim (\delta r_{0,f})^{2/(d-2)}$. Therefore, if we denote with $\xi^\star$, the correlation length in the asymptotic state, described by the stationary part of Eq. (3.20), and with $\nu^\star$ the exponent describing its divergent behavior near the dynamical critical transition, i.e.,

$$(\xi^\star)^{-1} \sim (\delta r_{0,f})^{-\nu^\star} \tag{3.25}$$

and use the relation $\xi^\star \sim \sqrt{r^\star}$, we find

$$\begin{aligned} \nu^\star &= \frac{1}{d-2} \quad 1 < d < 4 \\ \nu^\star &= \frac{1}{2} \qquad\qquad d \geq 4. \end{aligned} \tag{3.26}$$

It is interesting to notice at this point that critical dimensions and the ν exponent of the dynamical critical transition are the same as the thermal transition, even tough the former occurs in a pure state, generated by the unitary dynamics of the model, while the latter occur in a mixed state.

3.3 Statistics of excitations for a double quench

In this section we suggest a new simple protocol to detect the dynamical phase transition. We imagine to start in the disorder phase at a certain $r_{0,i}$, then suddenly change the value of the bare mass r_0 to a smaller value $r_{0,f}$ that can also be in the ordered phase, and let the system evolve. After a waiting time t_w we quench back to the initial $r_{0,i}$ and we count the number of excitations generated in the double quench. As we will show, the statistics of the number of excitations generated bears strong signatures of the dynamical transition.
In the present case the number of excitations is simply given by

$$\hat{N} = \int_k a^\dagger_{\vec{k}} a_{\vec{k}}, \tag{3.27}$$

while in more realistic frameworks, such as Bose-Hubbard systems, the relevant quantity could be the number of doubly occupied and vacant sites in the system, which could be counted with present day technologies. In all cases, the number of defects generated in a double quench is a fluctuating quantity characterized by a probability distribution $P(N, t_w)$. As in the case of the statistics of the work discussed in chapter 2, an equivalent and more convenient from the computational point of view, description can be given in terms of the moment generating function

$$G(s, t_w) = \langle e^{-s\hat{N}} \rangle_{t_w}, \tag{3.28}$$

where the average is taken over the state $|\psi(t_w)\rangle = U(t_w)\,|0\rangle$, that is the evolved state at time t_w.

Since the theory is effectively quadratic and the different k-modes interacts only through the renormalization of the mass $r(t)$, we can focus on a single mode k, because we will have a factorized moment generating function $G(s, t_w) = \prod_k G_k(s, t_w)$, with $G_k(s, t_w)$ representing the generating function for a single mode.

In order to compute $G_k(s, t_w)$ we will first express the evolved state $|\psi(t_w)\rangle_k$ as a function of $a_{\vec{k}}$ and $a^\dagger_{\vec{k}}$. The starting point is the expansion of the evolved field $\hat{\phi}_{\vec{k}}(t_w)$ in the same basis written in Eq. (3.16), which can be translated from Heisenberg to Schroedinger picture by writing

$$\hat{\phi}_{\vec{k}}(0) = f_{\vec{k}}(t)\tilde{a}_{\vec{k}}(t) + f^\star_{\vec{k}}(t)\tilde{a}^\dagger_{-\vec{k}}(t), \tag{3.29a}$$

$$\hat{\Pi}_{\vec{k}}(0) = \dot{f}_{\vec{k}}(t)\tilde{a}_{\vec{k}}(t) + \dot{f}^\star_{\vec{k}}(t)\tilde{a}^\dagger_{-\vec{k}}(t), \tag{3.29b}$$

with the operators $\tilde{a}_{\vec{k}}$ and $\tilde{a}^\dagger_{-\vec{k}}$ defined by the relation $\tilde{a}_{\vec{k}}(t)\,|\psi(t)\rangle = 0$. At the same time, since $a_{\vec{k}}$ and $a^\dagger_{\vec{k}}$ diagonalize the initial Hamiltonian, we know that they are related to the fields at time $t = 0$ in the following way,

$$\hat{\phi}_{\vec{k}}(0) = \frac{1}{\sqrt{2\omega_{k,i}}}\left(a_{\vec{k}} + a^\dagger_{-\vec{k}}\right), \tag{3.30a}$$

$$\hat{\Pi}_{\vec{k}}(0) = i\sqrt{\frac{\omega_{k,i}}{2}}\left(a^\dagger_{-\vec{k}} - a_{\vec{k}}\right). \tag{3.30b}$$

By inverting Eq. (3.29), taking into account that $f_{\vec{k}}(t)\dot{f}^{\star}_{\vec{k}}(t) - \dot{f}_{\vec{k}}(t)f^{\star}_{\vec{k}}(t) = i$, as can easily be inferred from Eq.(3.18a), and inserting the result into Eq. (3.30), one obtains

$$\tilde{a}_{\vec{k}}(t) = \alpha^{\star}_{\vec{k}}(t)a_{\vec{k}} - \beta^{\star}_{\vec{k}}(t)a^{\dagger}_{-\vec{k}}, \tag{3.31}$$

with

$$\alpha_{\vec{k}}(t) = f_{\vec{k}}(t)\sqrt{\frac{\omega_{k,i}}{2}} + i\frac{\dot{f}_{\vec{k}}(t)}{\sqrt{2\omega_{k,i}}}, \tag{3.32a}$$

$$\beta_{\vec{k}}(t) = f_{\vec{k}}(t)\sqrt{\frac{\omega_{k,i}}{2}} - i\frac{\dot{f}_{\vec{k}}(t)}{\sqrt{2\omega_{k,i}}}. \tag{3.32b}$$

From Eq. (3.31) and the requirement that $\tilde{a}_{\vec{k}}(t)$ annihilates the evolved state, similarly to section 2.2.1 one finally finds

$$|\psi(t_w)\rangle_k = \frac{1}{\sqrt{|\alpha_{\vec{k}}(t_w)|}} \exp\left(\frac{\beta^{\star}_{\vec{k}}(t_w)}{2\alpha^{\star}_{\vec{k}}(t_w)} a^{\dagger}_{\vec{k}}a^{\dagger}_{-\vec{k}}\right)|0\rangle\,, \tag{3.33}$$

with $a_{\vec{k}}\,|0\rangle = 0$. Having the expression of the state in terms of $a_{\vec{k}}$ and $a^{\dagger}_{\vec{k}}$, the computation of $G_k(s, t_w)$ can be straightforwardly done (cft. section 2.2.1), obtaining

$$G_k(s, t_w) = \frac{1}{\sqrt{1 + |\rho_k(t_w)|^2(1 - e^{-2s})}}, \tag{3.34}$$

with

$$\rho_k(t_w) = |\beta_{\vec{k}}|^2 = |f_{\vec{k}}(t_w)|^2\frac{\omega_{k,i}}{2} + \frac{|\dot{f}_{\vec{k}}(t_w)|^2}{2\omega_{k,i}} - 1/2. \tag{3.35}$$

Finally using the relation $\log G(s, t_w)/L^d = \int_k \log G_k(s, t_w)$, one gets $G(s, t_w) = \exp(-L^d f(s, t_w))$ with,

$$f(s, t_w) = \frac{1}{2}\int_k \log\left[1 + \rho_k(t_w)\left(1 - e^{-2s}\right)\right], \tag{3.36}$$

defined for $s > -\bar{s} = \frac{1}{2}\sup_k \log\frac{\rho_k(t_w)}{1+\rho_k(t_w)}$, where L is the linear size of the system. The function $\rho_k(t_w)$ that fully determines the statistics of the excitations can in general be obtained from the integration of Eq. (3.18). In the special case of a free theory, i.e. $\lambda = 0$, we can actually analytically find the function ρ_k by using Eq. (3.35). The result is

$$\rho_{k,\text{free}}(t_w) = \frac{(r_{0,f} - r_{0,i})^2}{4(|\vec{k}|^2 + r_{0,f})(|\vec{k}|^2 + r_{0,i})} \sin\left(t_w\sqrt{|\vec{k}|^2 + r_{0,f}}\right)^2. \tag{3.37}$$

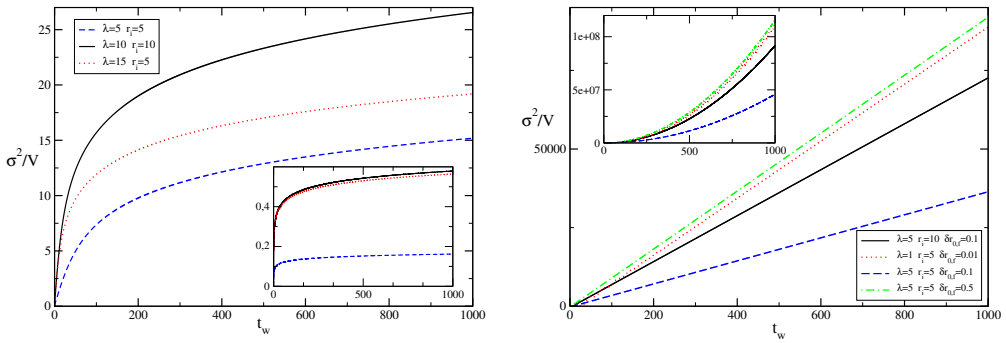

(a) **(b)**

Figure 3.2: *(a) Variance per unit volume σ^2/V, with $V = L^d$, for quenches at the dynamical critical point $r^c_{0,f}$ in $d = 3$ and $d = 4$ (inset) for different values of the interaction λ and different initial effective masses r_i. (b) Variance per unit volume σ^2/V, $V = L^d$, for quenches below the dynamical transition, i.e. $r_{0,f} < r^c_{0,f}$ in $d = 3$ and $d = 4$ (inset) for different values of the interaction λ and different initial effective masses r_i.*

Let us now characterize the dynamical critical behavior of the system by studying all the cumulants k_n's of the distribution of excitations, using the formula $k_n(t_w) = (-1)^n \frac{\partial^n}{\partial s} \log G(s, t_w)|_{s=0}$. Below, we will start by focusing on the first two, i.e. the average and the variance $\sigma^2(t_w)$, and discuss their dependence on the waiting time t_w between the two quenches if the intermediate value $r_{0,f}$ of the bare mass is above, below or at the dynamical critical point, focusing on the cases $d = 3$ and $d = 4$. Their explicit expressions in terms of ρ_k are

$$\frac{\bar{N}(t_w)}{L^d} = \int_k \rho_{\vec{k}}(t_w), \tag{3.38}$$

$$\frac{\sigma^2(t_w)}{L^d} = \int_k 2\rho_{\vec{k}}(t_w) \left(1 + \rho_{\vec{k}}(t_w)\right), \tag{3.39}$$

It is first of all important to notice that the scaling with t_w of the average and of the variance are totally different. While the first does not display striking features, and both in $d = 3$ and in $d = 4$ always tends to a stationary value as a function of t_w, the variance has three qualitatively different behaviors in all

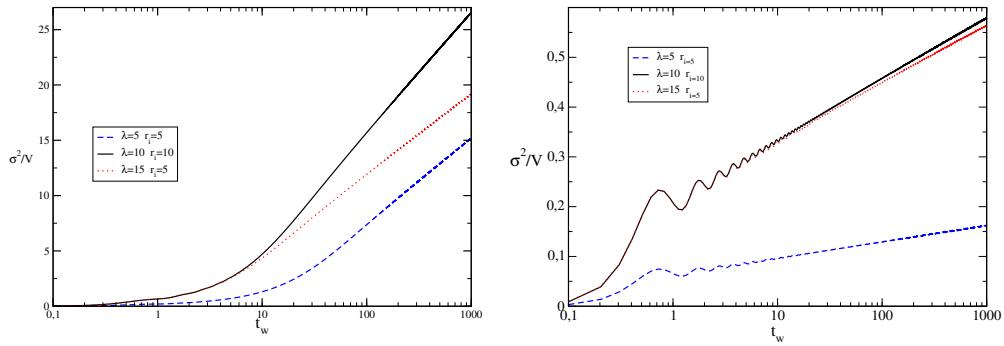

Figure 3.3: *Variance per unit volume σ^2/V, with $V = L^d$, for quenches at the dynamical critical point $r^c_{0,f}$ in $d = 3$ (a) and $d = 4$ (b) for different values of the interaction λ and different initial effective masses r_i in a log-linear scale.*

dimensionalities. If indeed the first quench is at the dynamical critical point, i.e. $r_{0,f} = r^c_{0,f}$, the variance per unit volume appears to grow in a logarithmic fashion as a function of t_w for both $d = 3$ and $d = 4$ (see Figs. 3.2a and 3.3). This should be contrasted with what one would expect for such scaling in a free field theory, where in $d = 3$ the variance would grow in a linear way, while in $d = 4$ we would have a logarithmic growth also in the free case, as can be found be evaluating the long time behavior of Eq. (3.39) using (3.37).

A totally different behavior is observed for quenches below the dynamical critical point, i.e. $r_{0,f} < r^c_{0,f}$: in this case the variance grows as a power law t^α_w with $\alpha = 1$ in three dimensions and $\alpha = 2$ in four dimensions (see Fig. 3.2b and 3.4). In $d = 3$ we find the same behavior we would have for a quench to $r_{0,f} = 0$ in the free theory, while for $d = 4$ the variance grows as t^2_w, which faster than the growth we can have in the free case for $r_{0,f} = 0$, which is logarithmical, as stated above.

Finally in the case of an intermediate value of the bare mass above the dynamical transition, i.e. $r_{0,f} > r^c_{0,f}$, the variance saturates to a finite value as a function of t_w for both $d = 3$ and $d = 4$, as one can see from Fig. 3.5. Notice that for

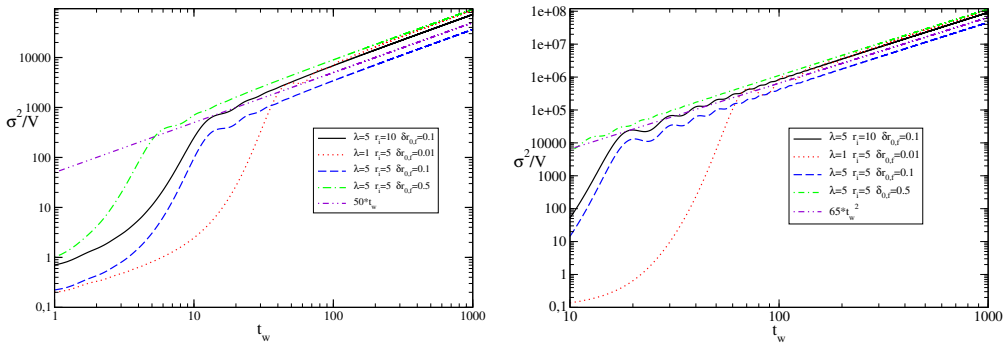

(a) **(b)** log

Figure 3.4: *Variance per unit volume σ^2/V, $V = L^d$, for quenches below the dynamical transition, i.e. $r_{0,f} < r_{0,f}^c$ in $d = 3$ (a) and $d = 4$ (b) for different values of the interaction λ and different initial effective masses r_i in a log-log scale.*

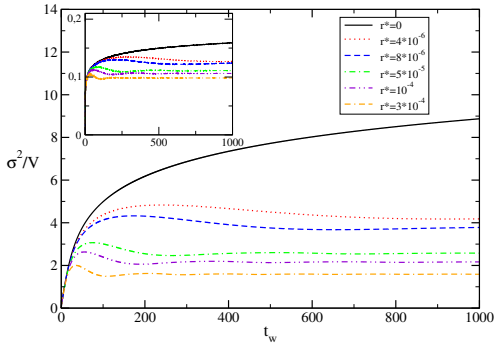

Figure 3.5: *Variance per unit volume σ^2/V, $V = L^d$, for quenches above the dynamical transition, i.e. $r_{0,f} > r_{0,f}^c$ in $d = 3$ and $d = 4$ (inset) for different values of the predicted asymptotic effective parameter $r^\star$ (see Eq. (3.21). We set $\lambda = 10$ and $r_i = 5$.*

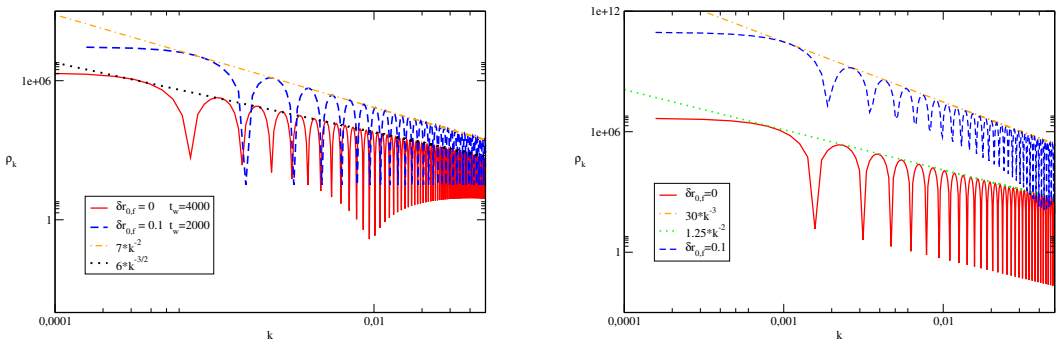

(a) **(b)**

Figure 3.6: *Behavior of ρ_k for (a) $d = 3$ and (b) $d = 4$ as a function of k in a log-log scale for quenches below or at the critical point: $\delta r_{0,f} = r^c_{0,f} - r_{0,f}$ measures the distance from the critical point.*

$r^\star \neq 0$ the curves describing the variance follow the critical line until a certain time that is the longer the smaller $r^\star$, and then deviate and saturate.

The scaling of all the cumulants for large t_w is fully determined by the scaling for small k of $\rho_k(t_w)$. For example, in the free theory and for $r_{0,f} = 0$ we can notice from Eq. (3.37) that when k is small $\rho_{k,\text{free}}$ behaves as $1/k^2$ up to an infrared cutoff provided by the sine which evolves as $1/t_w$. It is then easy to see that the n-th cumulant is given by a weighted sum of the integrals over k of all the integers powers of ρ_k up to n, so that its asymptotic behavior in t_w will be

$$k_n \sim \int_{1/t_w} dk\, k^{d-1-2n} \sim t_w^{2n-d}. \tag{3.40}$$

The same reasoning can be applied also in the case $\lambda \neq 0$, where we numerically determined the low k behavior of ρ_k.

Thus, in the case of a quench to the dynamical critical point in $d = 3$ we expect the scaling $\rho_k \sim 1/k^{3/2}$, which is compatible with the numerical data, as can be seen from Fig. 3.6a. This scaling implies a power law growth for all the higher order cumulants, given by $k_n/V \sim t_w^{3/2n-3}$. In $d = 4$ the data confirm the scaling $\rho_k \sim 1/k^2$ expected from the study of the variance (see Fig. 3.6b) implying for the other cumulants $k_n/V \sim t_w^{2n-4}$. For quenches below the dynamical critical

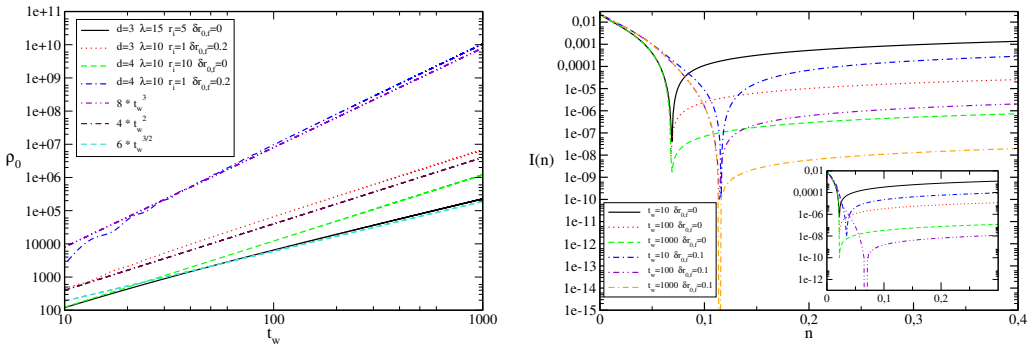

(a) **(b)**

Figure 3.7: *(Color online) (a) Behavior of ρ_0 as a function of t_w for quenches below or at the dynamical critical point in both $d = 3$ and $d = 4$, compared with the expected power law (their coefficient are arbitrary). $\delta r_{0,f} = r^c_{0,f} - r_{0,f}$. (b) Rate function $I(n)$ for quenches at or below the dynamical critical point for $d = 3$ and $d = 4$ (inset) for different waiting times t_w in a linear-log scale. $\delta r_{0,f} = r^c_{0,f} - r_{0,f}$ and we set $\lambda = 15$ and $r_i = 5$.*

point, we see from Fig. 3.6a and 3.6b that the behavior is what we expect from the above discussed growth of the variance, that is $\rho_k \sim 1/k^2$ for $d = 3$ and $\rho_k \sim 1/k^3$ for $d = 4$. Again this implies an even faster power law growth for the higher order cumulants, which is respectively $k_n/V \sim t_w^{2n-3}$ and $k_n/V \sim t_w^{3n-4}$. The small k behavior of $\rho_k(t_w)$ has interesting consequences also on the large deviations statistics of the density of excitations $n = N/L^d$, which are similar to the condensation transition discussed in section 2.2.3. Following the discussion of section 2.1 done in the case of the statistics of the work, we have that in the limit $L \to \infty$ the distribution function of the density of the excitations will behave as $p(n, t_w) \sim \exp(-L^d I(n, t_w))$, where $I(n, t_w)$ is the rate function, which we remind being the Legendre transform of $f(s)$ of Eq. (2.9), namely

$$I(n, t_w) = -\inf_s[sn - f(s, t_w)], \tag{3.41}$$

with $f(s, t_w)$ given by Eq. (3.36).

In particular for $n \gg \langle n \rangle$ we will have $I(n, t_w) \simeq \bar{s}n$, with $\bar{s}$ defined right below Eq. (2.9). From the behavior of ρ_k at small k discussed above, and as confirmed

by Fig. 3.7a, in the case of $r_{0,f} \leq r_{0,f}^c$, we will have

$$\rho_0(t_w) \sim t_w^{-\alpha}, \tag{3.42}$$

with $\alpha = 2$ for quenches at the dynamical critical point in $d = 4$ and below the transition in $d = 3$, $\alpha = 3/2$ for quenches at the critical point in $d = 3$, and $\alpha = 3$ for quenches below the transition in $d = 4$. This in turn implies $\bar{s} \sim t_w^{-\alpha}$, which physically translates in a crossover, whose rapidity is set by α, from an exponential to an algebraic decay above the average value in the limit of large t_w. Fig. 3.7b shows some examples of this behavior.

3.4 Dynamical critical behavior for a ramp

In this section we will consider the dynamics generated by a ramp instead of a sudden quench, concentrating on $d = 3$ and asking what is the fate of the dynamical transition and of its critical properties in this case. Thus, we will imagine to start in the ground state for a certain initial bare mass $r_{0,i}$, which we will still assume to be in the disordered phase ($r_{0,i} > r_{0,c}$), and to change the value of r_0 linearly up to $r_{0,f}$ in a total time τ, namely we will take,

$$r_0(t) = r_{0,i} + (r_{0,f} - r_{0,i}) \frac{t}{\tau} \quad 0 \leq t \leq \tau. \tag{3.43}$$

while for $t > \tau$ we will assume $r_0(t) = r_{0,f}$,
The dynamics will be still generated by the quadratic Hamiltonian of Eq. (3.13) with the substitution $r_{0,f} \to r_0(t)$, and the effective mass given by,

$$r(t) = r_0(t) + \frac{\lambda}{6} \int_k \langle \hat{\phi}_{\vec{k}}(t) \hat{\phi}_{-\vec{k}}(t) \rangle. \tag{3.44}$$

The mode function $f_{\vec{k}}(t)$, defined by expanding the field at time t on the basis diagonalizing the initial Hamiltonian (see Eq. (3.16)), still evolves according to Eq. (3.18a), with $r(t)$ now given by Eq. (3.44).
Also in this case in the special limit of a free theory ($\lambda = 0$) it is possible to

find an analytic expression for $f^0_{\vec{k}}(t)$, which for $0 < t < \tau$ is given by

$$f^0_{\vec{k}}(t) = \frac{\pi}{\sqrt{2}} \frac{\mathrm{Ai}\left(\gamma t - \frac{|\vec{k}|^2 + r_{0,i}}{\gamma^2}\right) \mathrm{Bi}'\left(-\frac{|\vec{k}|^2 + r_{0,i}}{\gamma^2}\right) - \mathrm{Bi}\left(\gamma t - \frac{|\vec{k}|^2 + r_{0,i}}{\gamma^2}\right) \mathrm{Ai}'\left(-\frac{|\vec{k}|^2 + r_{0,i}}{\gamma^2}\right)}{\left(|\vec{k}|^2 + r_{0,i}\right)^{1/4}}$$
$$+ \frac{i\pi}{\sqrt{2}} \left(\frac{\tau}{r_{0,i} - r_{0,f}}\right)^{1/3} \left(|\vec{k}|^2 + r_{0,i}\right)^{1/4} \left[\mathrm{Ai}\left(\gamma t - \frac{|\vec{k}|^2 + r_{0,i}}{\gamma^2}\right) \mathrm{Bi}\left(-\frac{|\vec{k}|^2 + r_{0,i}}{\gamma^2}\right)\right.$$
$$\left. - \mathrm{Bi}\left(\gamma t - \frac{|\vec{k}|^2 + r_{0,i}}{\gamma^2}\right) \mathrm{Ai}\left(-\frac{|\vec{k}|^2 + r_{0,i}}{\gamma^2}\right)\right], \tag{3.45}$$

where $\gamma = \left(\frac{r_{0,i} - r_{0,f}}{\tau}\right)^{1/3}$, and $\mathrm{Ai}(x)$, $\mathrm{Bi}(x)$ denote the Airy functions, while for $t > \tau$

$$f^0_{\vec{k}}(t) = f^0_{\vec{k}}(\tau) \cos\left(t\sqrt{|\vec{k}|^2 + r_{0,f}}\right) + \frac{\dot{f}^0_{\vec{k}}(\tau)}{\sqrt{|\vec{k}|^2 + r_{0,f}}} \sin\left(\sqrt{|\vec{k}|^2 + r_{0,f}}\right), \tag{3.46}$$

where $f^0_{\vec{k}}(\tau)$ has to be read from Eq. (3.45).

When $\lambda \neq 0$ we have to solve the evolution equations numerically. We observe that also in the case of a ramp the effective mass tends to a stationary value at long times, which is positive up to a certain τ-dependent critical point $r^c_{0,f}(\tau)$ and then is always zero for $r_{0,f} < r^c_{0,f}(\tau)$. Some example of the evolution in time of the effective mass are shown in Fig. 3.8a.

To predict the stationary value $r^\star$ we try the same ansatz done in the case of a sudden quench, that is we suppose that the stationary part of the correlation $\langle \hat{\phi}_{\vec{k}}(t) \hat{\phi}_{-\vec{k}}(t) \rangle$ is the same as the free theory with renormalized masses

$$r^\star = r_{0,f} + \frac{\lambda}{12} \int_k \frac{|f^0_{\vec{k},r^\star}(\tau)|^2 \left(|\vec{k}|^2 + r^\star\right) + |\dot{f}^0_{\vec{k},r^\star}(\tau)|^2}{2(|\vec{k}|^2 + r^\star)}, \tag{3.47}$$

where $f^0_{\vec{k},r^\star}(\tau)$ is given by Eq. (3.45) with $r_{0,i} \to r_i$ and $r_{0,f} \to r^\star$. From now on we will explicitly write down the dependence on the asymptotic mass $r^\star$

It turns out that such an ansatz works up to the dynamical critical point only if one also renormalizes the ramp time τ, which, however, cannot be fixed a priori.

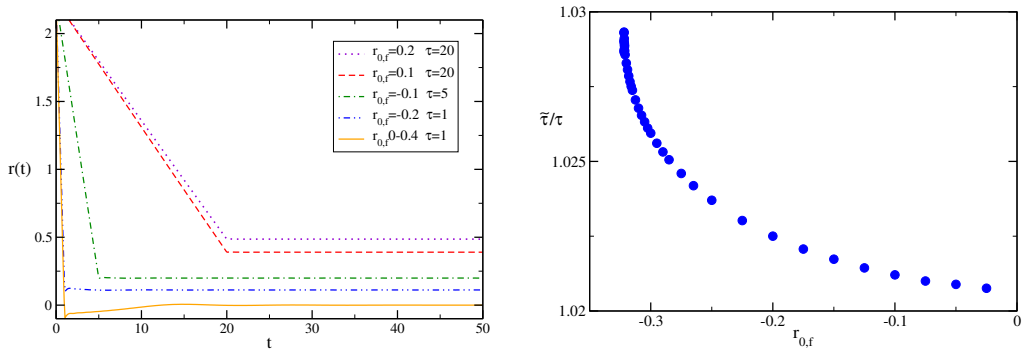

Figure 3.8: *(a) Examples of the evolution of the effective mass $r(t)$ for different values of τ, $r_{0,i}$ and $r_{0,f}$. (b) The ratio $\frac{\tilde{\tau}}{\tau}$ as a function of $r_{0,f}$ for a ramp starting from $r_{0,i} = 5$ and with duration $\tau = 5$.*

Therefore we lose the predictive power that we had in the case of the sudden quench. The effective ramp time $\tilde{\tau}$ can be thus regarded as a nontrivial fitting parameter and turns out to dependent also on the value of $r_{0,f}$, as can be seen from Fig. 3.8b. Nevertheless, the fact that the stationary state can be described as the one of a free theory, even though with an effective parameter $\tilde{\tau}$, allow us to analytically study the critical properties of the transition. We will now assume that the ansatz described above works also for dimensions different from $d = 3$, a fact that seems very reasonable but has still to verified thoroughly.

First of all let us study the lower critical dimension of the dynamical transition in the case of a ramp by analyzing the low k behavior of the integrand of Eq. (3.47), with $r^\star = 0$. For every finite τ the most relevant modes are those with $|\vec{k}| \ll \left(\frac{r_i}{\tau}\right)^{1/3}$, $|\vec{k}| \ll \sqrt{r_i}$, where both $|f^0_{\vec{k},0}(\tilde{\tau})|^2$ and $|\dot{f}^0_{\vec{k},0}(\tilde{\tau})|^2$ tend to a constant (see appendix 3.A for more details), so that the integrand behaves as $1/|\vec{k}|^2$ implying that the critical point is finite for $d > 2$, with $d = 2$ thus being the lower critical dimension for every finite τ.

We observe that when τ increases the region considered above shrinks. Indeed, to understand what happens in the limit $\tau \to \infty$ we have instead to consider the region $\left(\frac{r_i}{\tau}\right)^{1/3} \ll |\vec{k}| \ll \sqrt{r_i}$. Here (see appendix 3.A for more details), we

have

$$|f^0_{\vec{k},0}(\tilde{\tau})|^2 \sim \frac{1}{|\vec{k}|} \quad |\dot{f}^0_{\vec{k},0}(\tilde{\tau})|^2 \sim |\vec{k}|, \tag{3.48}$$

implying that when τ is strictly infinite the lower critical dimension is $d = 1$ as in the case of the quantum transition.

From our ansatz we can also compute the exponent $\nu^\star$ defined in Eq. (3.25). Indeed, by denoting with $\delta r_{0,f}(\tau) = r_{0,f} - r^c_{0,f}(\tau)$, defining the dimensionless variable $\vec{y} = \vec{k}/\sqrt{r^\star}$ and using Eq. (3.47), we can write

$$r^\star = \delta r_{0,f}(\tau) + \frac{\lambda}{12}\,(r^\star)^{\frac{d-2}{2}} \int_y \frac{|\vec{y}|^2 g(|\vec{y}|\sqrt{r^\star}, r^\star) - (|\vec{y}|^2+1)\, g(|\vec{y}|\sqrt{r^\star}, 0)}{|\vec{y}|^2(|\vec{y}|^2+1)}, \tag{3.49}$$

with $\int_y = \int \frac{d^d y}{(2\pi)^d}$, restricted to the region $|\vec{y}| < \Lambda/\sqrt{r^\star}$ and

$$g(|\vec{k}|, r^\star) = |f^0_{\vec{k},r^\star}(\tilde{\tau})|^2 \left(|\vec{k}|^2 + r^\star\right) + |\dot{f}^0_{\vec{k},r^\star}(\tilde{\tau})|^2. \tag{3.50}$$

As we did before in the case of a sudden quench, we have to analyze the behavior of the integrand in the region $1 \ll |\vec{y}| \ll \sqrt{r_i/r^\star}$. Here, it scales as $g(0,0)/|\vec{y}|^4$, thus for $d < 4$ the leading term in the expansion of the integral in powers of $r^\star$ is obtained by substituting the upper limit of integration with infinity and the integrand with its leading order in $r^\star$, namely

$$\begin{aligned} r^\star &= \delta r_{0,f}(\tau) - \frac{\lambda}{12}\frac{\Omega(d)}{(2\pi)^d}\,(r^\star)^{\frac{d-2}{2}} \int_0^\infty dy y^{d-1} \frac{g(0,0)}{y^2(y^2+1)} \\ &= \delta r^\tau_{0,f} - \frac{\lambda}{12}\frac{\Omega(d)}{(2\pi)^d}\,(r^\star)^{\frac{d-2}{2}}\, \frac{\pi g(0,0)}{2\sin\left(\frac{\pi(d+2)}{2}\right)}, \end{aligned} \tag{3.51}$$

from which we derive that also in this case $r^\star \sim (\delta r_{0,f}(\tau))^{\frac{2}{d-2}}$. For $d = 4$ there are logarithmic corrections to this scaling, while for $d > 4$ we can deduce how the integral over y diverges with $r^\star$ by considering the scaling of the integrand in the region $1 \ll |\vec{y}| \ll \sqrt{r_i/r^\star}$ that we mentioned above. Doing so one obtains that the integral scale as $(r^\star)^{\frac{4-d}{2}}$, giving the linear relation $r^\star \sim \delta r_{0,f}(\tau)$. Therefore, we conclude that the $\nu^\star$ exponent is the same as in the transition induced by a sudden quench, i.e.

$$\begin{aligned} \nu^\star &= \frac{1}{d-2} \quad 1 < d < 4 \\ \nu^\star &= \frac{1}{2} \qquad\quad d \geq 4. \end{aligned} \tag{3.52}$$

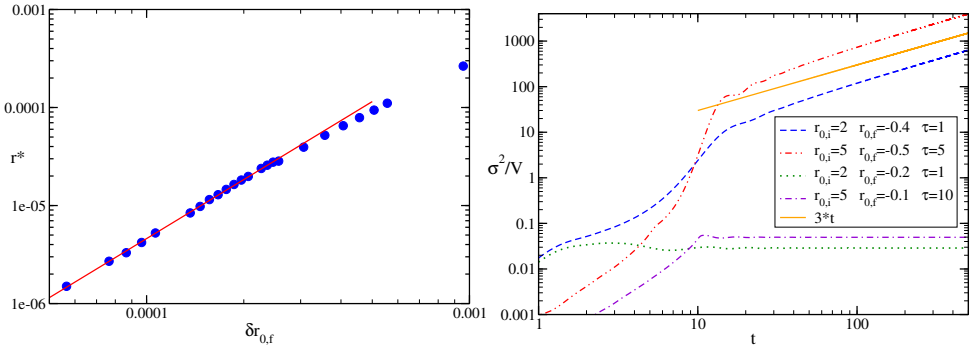

(a) **(b)**

Figure 3.9: *(a) Asymptotic mass $r^\star$ as a function of the distance $\delta r_{0,f}$ from the dynamical critical point in the case $d = 3$, $r_{0,i} = 5$ and $\tau = 5$. The red line is proportional to $(\delta r_{0,f})^2$ and shows excellent agreement with the numerical data, confirming the prediction of Eq. (3.52) (b) Evolution of the variance per unit volume for different ramps. We can clearly distinguish two different qualitative behaviors: linear growth and saturation.*

Fig. 3.9a shows that the numerical data in $d = 3$ agree with the prediction above.

We can also consider the statistics of excitation produced by letting evolve the system after the end of the ramp for a certain waiting time t_w and then suddenly quenching back to the initial $r_{0,i}$. The moment generating function is still given by Eq. (3.36), provided that the function $\rho_{\vec{k}}(t_w)$ is computed using the mode functions $f_{\vec{k}}(t_w)$, obtained using the modified effective mass of Eq. (3.44). Also in this case we observe that the average always saturates for large t_w, while the variance shows non trivial behavior. Indeed, we can still distinguish a regime where it saturates, from a regime where it grows linearly (see Fig. 3.9b), therefore the critical scaling of such a quantity is not modified by the choice of a ramp instead of a sudden quench.

Using the different behavior of the variance as a function of the waiting time t_w we can identify the critical point $r_{0,f}(\tau)$, which, as can be seen in Fig. 3.10, interpolates between the dynamical critical point (3.22) for a sudden quench, corresponding to $\tau = 0$, and the quantum critical point (3.8) (with $\beta \to \infty$) in the limit of large τ. Let us now study how these two limiting values are reached.

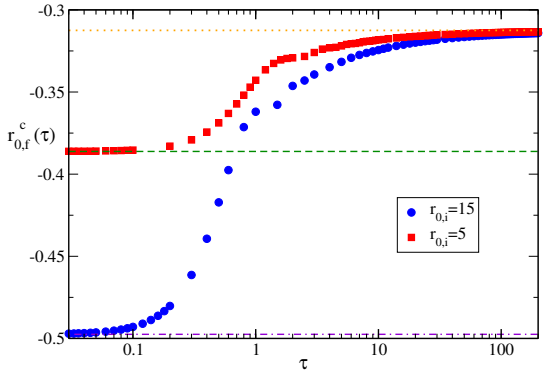

Figure 3.10: *Dynamical critical point $r_{0,f}(\tau)$ as a function of τ for two different initial bare masses $r_{0,i}$. The orange pointed line indicates the quantum critical point to which both curves tend in the limit of large τ. Instead, the green dashed and purple dot-dashed lines shows the dynamical critical point found in the case of a sudden quench and dependent on the initial value of the bare mass $r_{0,i}$.*

By studying the behavior of the effective ramp time $\tilde{\tau}$ as a function of the true ramp time τ at the critical point for a fixed $r_{0,i}$ it turns out that in the limit of small and large τ the two quantities have a linear relation, as can bee see in Figs 3.11a and 3.11b. Moreover, we can also notice that the curves with different $r_{0,i}$ collapse in both limits, implying that the linear relation bears no dependence on the initial state. This allows us to use the free theory result to extract the power law behavior in τ of the critical point when it approaches its two limiting values for $\tau \to 0$ and $\tau \to \infty$.

Let us start with the approach to the quantum critical point that happens at large τ. By using the asymptotic expansion of the Airy functions for large negative arguments (see appendix 3.A), we obtain that for $\tilde{\tau} \gg 1/\sqrt{r_i}$

$$|f^0_{\vec{k}}(\tilde{\tau})|^2 \simeq \frac{\pi}{2r_i^{2/3}}\tilde{\tau}^{1/3}\left[\mathrm{Ai}\left(\frac{-k^2\tilde{\tau}^{2/3}}{r_i^{2/3}}\right)^2 + \mathrm{Bi}\left(\frac{-k^2\tilde{\tau}^{2/3}}{r_i^{2/3}}\right)^2\right], \tag{3.53}$$

$$|\dot{f}^0_{\vec{k}}(\tilde{\tau})|^2 \simeq \frac{\pi}{2\tilde{\tau}^{2/3}}r_i^{1/3}\left[\mathrm{Ai}'\left(\frac{-k^2\tilde{\tau}^{2/3}}{r_i^{2/3}}\right)^2 + \mathrm{Bi}'\left(\frac{-k^2\tilde{\tau}^{2/3}}{r_i^{2/3}}\right)^2\right], \tag{3.54}$$

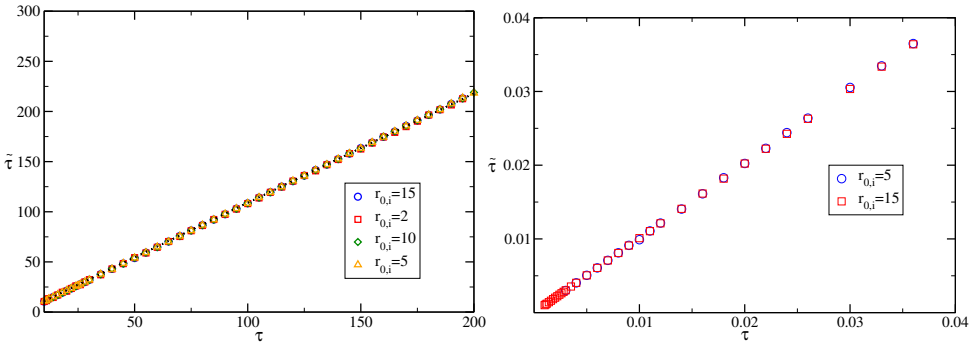

(a) **(b)**

Figure 3.11: *(a) Effective ramp duration $\tilde{\tau}$ as a function of the bare ramp duration τ for large values of τ for different initial bare masses $r_{0,i}$. We can notice that in this regime all the curves collapse on the same line. (b) (a) Effective ramp duration $\tilde{\tau}$ as a function of the bare ramp duration τ for large values of τ for different initial bare masses $r_{0,i}$. We can notice that in this regime the two curves collapse on the same line.*

therefore in this regime we have

$$r_{0,f}^{c}(\tau) = \frac{\lambda}{12}\frac{\Omega(d)}{(2\pi)^d}(I_1 + I_2), \tag{3.55}$$

with

$$I_1(d) = \frac{\pi}{4}\Lambda^d \left(\frac{\tilde{\tau}}{r_i}\right)^{1/3} \int_0^1 dz\, z^{d/2-1} \left[\mathrm{Ai}\left(\frac{-\Lambda^2\tilde{\tau}^{2/3}}{r_i^{2/3}}z\right)^2 + \mathrm{Bi}\left(\frac{-\Lambda^2\tilde{\tau}^{2/3}}{r_i^{2/3}}z\right)^2\right], \tag{3.56}$$

$$I_2(d) = \frac{\pi}{4}\Lambda^{d-2} \left(\frac{r_i}{\tilde{\tau}}\right)^{1/3} \int_0^1 dz\, z^{d/2-2} \left[\mathrm{Ai}'\left(\frac{-\Lambda^2\tilde{\tau}^{2/3}}{r_i^{2/3}}z\right)^2 + \mathrm{Bi}'\left(\frac{-\Lambda^2\tilde{\tau}^{2/3}}{r_i^{2/3}}z\right)^2\right], \tag{3.57}$$

where we introduced the dimensionless variable $z = \frac{|\vec{k}|^2}{\Lambda^2}$. We will now compute the asymptotic behavior of these two integrals in $d = 3$. The integral I_1 can be

computed exactly, getting

$$I_1(3) = \frac{\Lambda^3 \tilde{\tau}^{1/3}}{4 \cdot 35 \cdot 3^{5/6} \sqrt{\pi} \Gamma(-\frac{1}{3})^2 r_i^{1/3}} \left\{ 35 \left[6\sqrt{3}\pi^{3/2} + 2^{1/3} \Gamma\left(-\frac{1}{3}\right)^2 \Gamma\left(\frac{7}{6}\right) \right] \right.$$
$${}_2F_3\left(\frac{1}{6}, \frac{1}{2}; \frac{1}{3}, \frac{2}{3}, \frac{3}{2}; -\frac{4\Lambda^6 \tilde{\tau}^2}{9 r_i^2}\right) + 2 \cdot 3^{1/3} \frac{\Lambda^2 \tilde{\tau}^{2/3}}{r_i^{2/3}} \Gamma\left(-\frac{1}{3}\right)^2 \left[5 \cdot 2^{2/3} \cdot 3^{1/3} \frac{\Lambda^2 \tilde{\tau}^{2/3}}{r_i^{2/3}} \right.$$
$$\left. \left. {}_2F_3\left(\frac{5}{6}, \frac{7}{6}; \frac{4}{3}, \frac{5}{3}, \frac{13}{6}; -\frac{4\Lambda^6 \tilde{\tau}^2}{9 r_i^2}\right) - 14\sqrt{\pi}\, {}_2F_3\left(\frac{1}{2}, \frac{5}{6}; \frac{2}{3}, \frac{4}{3}, \frac{11}{6}; -\frac{4\Lambda^6 \tilde{\tau}^2}{9 r_i^2}\right) \right] \right\}, \tag{3.58}$$

where ${}_2F_3(a, b; c, d, e; x)$ denotes the hypergeometric function. We can now use the asymptotic expansion of the hypergeometric functions for large negative x (see appendix 3.A for more details), obtaining

$$I_1(3) = \frac{\Lambda^2}{4} + \frac{\Gamma\left(-\frac{1}{3}\right)}{3^{4/3} \cdot 2^{11/3}} \left(\frac{r_i}{\tilde{\tau}}\right)^{2/3} + O\left(\left(\frac{r_i}{\Lambda^2 \tilde{\tau}}\right)^{4/3}\right). \tag{3.59}$$

Similarly we can compute the integral I_2, which gives

$$I_2(3) = \frac{-\Lambda}{4 \cdot 270\pi} \left(\frac{r_i}{\tilde{\tau}}\right)^{1/3} \left\{ 270 \cdot 3^{1/3} \Gamma\left(-\frac{1}{3}\right) \Gamma\left(\frac{5}{3}\right) {}_2F_3\left(-\frac{1}{6}, \frac{1}{6}; -\frac{1}{3}, \frac{1}{3}, \frac{7}{6}; -\frac{4\Lambda^6 \tilde{\tau}^2}{9 r_i^2}\right) \right.$$
$$- 5 \cdot 2^{1/3} 3^{1/6} \sqrt{\pi} \frac{\Lambda^8 \tilde{\tau}^{8/3}}{r_i^{8/3}} \Gamma\left(\frac{1}{6}\right) {}_2F_3\left(\frac{7}{6}, \frac{3}{2}; \frac{5}{3}, \frac{7}{3}, \frac{5}{2}; -\frac{4\Lambda^6 \tilde{\tau}^2}{9 r_i^2}\right) + 36 \cdot \sqrt{3}\pi \frac{\Lambda^4 \tilde{\tau}^{4/3}}{r_i^{4/3}}$$
$$\left. {}_2F_3\left(\frac{1}{2}, \frac{5}{6}; \frac{1}{3}, \frac{5}{3}, \frac{11}{6}; -\frac{4\Lambda^6 \tilde{\tau}^2}{9 r_i^2}\right) \right\}, \tag{3.60}$$

from which, expanding the hypergeometric functions (see appendix 3.A for more details), we get

$$I_2(3) = \frac{\Lambda^2}{4} - \frac{\Gamma\left(-\frac{1}{3}\right)}{3^{1/3} \cdot 2^{11/3}} \left(\frac{r_i}{\tilde{\tau}}\right)^{2/3} + O\left(\left(\frac{r_i}{\Lambda^2 \tilde{\tau}}\right)^{4/3}\right). \tag{3.61}$$

Putting all together, we obtain

$$r_{0,f}^c(\tau) = r_{0,c} + \frac{\lambda}{24\pi^2} \frac{\Gamma\left(-\frac{1}{3}\right)}{3^{4/3} \cdot 2^{8/3}} \left(\frac{r_i}{\tilde{\tau}}\right)^{2/3} + O\left(\left(\frac{r_i}{\Lambda^2 \tilde{\tau}}\right)^{4/3}\right), \tag{3.62}$$

where $r_{0,c}$ is the critical point for the quantum transition (see Eq. 3.8 with $\beta \to \infty$). Since, as we stated above, the relation between $\tilde{\tau}$ and τ at the critical

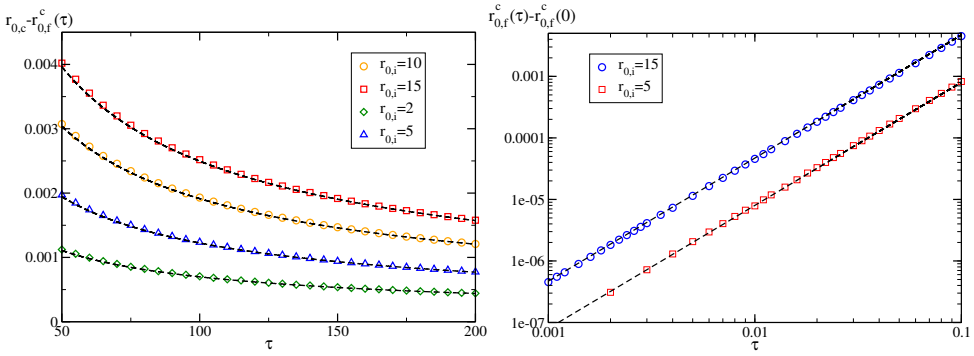

(a) **(b)**

Figure 3.12: *(a) Difference between the quantum critical point $r_{0,c}$ and the τ-dependent critical point $r^c_{0,f}$ as a function of τ for large τ for different initial bare masses $r_{0,i}$. The dashed line are proportional to $\tau^{-2/3}$ and are obtained by fitting the linear relation between $\tilde{\tau}$ and τ that is valid for large τ and putting the result into Eq. (3.62). We can see that the agreement with numerical data is excellent. (b) Log-log plot of the difference between the dynamical critical point for a ramp of duration τ ($r_{0,f}(\tau)$ and a sudden quench ($r^c_{0,f}(0)$) as a function of τ for different initial bare masses $r_{0,i}$. The black dashed lines are proportional to τ^2.*

point is linear for sufficiently large τ, we can conclude that the dynamical critical point approaches the quantum critical point for large τ as $\tau^{-2/3}$.
This is confirmed by the numerical data, as can be seen in Fig. 3.12a. Here the lines are obtained by linearly fitting the relation between τ and $\tilde{\tau}$ for large τ, and then putting the result in Eq. (3.62). We can see that the agreement is excellent.
Finally, let us consider the fate of the dynamical critical point for small values of τ. As can be seen in more details in 3.A, in the limit $\tau \to 0$ we have

$$|f^0_{\vec{k},0}(\tilde{\tau})|^2 \simeq \frac{1}{2\sqrt{|\vec{k}|^2 + r_i}} + \tilde{\tau}^2 \frac{\sqrt{|\vec{k}|^2 + r_i}}{2}, \tag{3.63}$$

$$|\dot{f}^0_{\vec{k},0}(\tilde{\tau})|^2 \simeq \frac{\sqrt{|\vec{k}|^2 + r_i}}{2} + \tilde{\tau}^2 \frac{2|\vec{k}|^2 + r_i}{8\sqrt{|\vec{k}|^2 + r_i}}. \tag{3.64}$$

From this one obtains

$$r^c_{0,f}(\tau) - r^c_{0,f}(0) = -\frac{\lambda}{24}\tilde{\tau}^2 \int_k \frac{4\sqrt{|\vec{k}|^2 + r_i} + 2|\vec{k}|^2 + r_i}{4|\vec{k}|^2}, \tag{3.65}$$

concluding that the deviation from the dynamical critical point found in the case of a sudden quench are quadratic in τ for small τ. This is confirmed by numerical data, as can be seen from Fig. 3.12b.

3.5 Concluding remarks

Summarizing in this chapter we discussed and characterize the dynamical phase transition in the $O(N)$ vector model in the limit of $N \to \infty$. In particular, we were able to identify its lower and upper critical dimensions and to characterize the divergence of the correlation length in the stationary state when the critical point is approached, finding that they are equal to the case of the thermal transition.
Then, we turned our attention to the statistics of the excitations produced by a double quench as a function of the waiting time t_w. We found qualitatively

different behaviors for the variance depending on the first quench being above, at or below the dynamical critical point of the system in $d = 3$ and $d = 4$, arguing that higher order cumulants will also display power laws. This divergence of the cumulants implies a crossover at large t_w from an exponential to an algebraic decay of the probability distribution function of the density of excitations above its average value.

Finally, we discussed the fate of such a dynamical critical point when instead of a sudden quench we perform a linear ramp in time of the bare mass. We found that for every finite τ the transition has the same critical properties of the dynamical phase transition, and only in the limit $\tau \to \infty$ this properties change and become the ones of the quantum phase transition. We also characterized the power-law approach of the critical point as a function of τ to both the quantum critical point (for $\tau \to \infty$) and to the dynamical critical point found for a sudden quench (for $\tau \to 0$).

Appendix

3.A Asymptotic expansions

In this appendix we will give additional details on some asymptotic expansion whose result was stated in section 3.4.

Let us start by reminding the expansion of the Airy functions for both small and large arguments, which will be useful in the following. For small x we have,

$$\mathrm{Ai}(-x) = \frac{1}{3^{2/3}\Gamma\left(\frac{2}{3}\right)} + \frac{x}{3^{1/3}\Gamma\left(\frac{1}{3}\right)} + O(x^3), \tag{3.66a}$$

$$\mathrm{Bi}(-x) = \frac{1}{3^{1/6}\Gamma\left(\frac{2}{3}\right)} - \frac{3^{1/6}x}{\Gamma\left(\frac{1}{3}\right)} + O(x^3), \tag{3.66b}$$

$$\mathrm{Ai}'(-x) = -\frac{1}{3^{1/3}\Gamma\left(\frac{1}{3}\right)} + \frac{x^2}{2\cdot 3^{2/3}\Gamma\left(\frac{2}{3}\right)} + O(x^3), \tag{3.66c}$$

$$\mathrm{Bi}'(-x) = \frac{3^{1/6}}{\Gamma\left(\frac{1}{3}\right)} + \frac{x^2}{3^{5/6}\Gamma\left(\frac{1}{3}\right)} + O(x^3), \tag{3.66d}$$

while for large positive x we have,

$$\mathrm{Ai}(-x) = \frac{1}{\sqrt{\pi}x^{1/4}}\sin\left(\frac{\pi}{4} + \frac{2x^{2/3}}{3}\right) - \frac{5}{48\sqrt{\pi}x^{7/4}}\cos\left(\frac{\pi}{4} + \frac{2x^{2/3}}{3}\right) + O\left((x^{-13/4}\right), \tag{3.67}$$

$$\mathrm{Bi}(-x) = \frac{1}{\sqrt{\pi}x^{1/4}}\cos\left(\frac{\pi}{4} + \frac{2x^{2/3}}{3}\right) + \frac{5}{48\sqrt{\pi}x^{7/4}}\sin\left(\frac{\pi}{4} + \frac{2x^{2/3}}{3}\right) + O\left((x^{-13/4}\right), \tag{3.68}$$

$$\mathrm{Ai}'(-x) = -\frac{x^{1/4}}{\sqrt{\pi}}\cos\left(\frac{\pi}{4} + \frac{2x^{2/3}}{3}\right) + \frac{7}{48\sqrt{\pi}x^{5/4}}\sin\left(\frac{\pi}{4} + \frac{2x^{2/3}}{3}\right) + O\left((x^{-11/4}\right), \tag{3.69}$$

$$\mathrm{Bi}'(-x) = \frac{x^{1/4}}{\sqrt{\pi}} \sin\left(\frac{\pi}{4} + \frac{2x^{2/3}}{3}\right) + \frac{7}{48\sqrt{\pi}x^{5/4}} \cos\left(\frac{\pi}{4} + \frac{2x^{2/3}}{3}\right) + O\left((x^{-11/4}\right), \tag{3.70}$$

Using these, we can first of all show that both $|f^0_{\vec{k},0}(\tau)|$ and $|\dot{f}^0_{\vec{k},0}(\tau)|$ tend to a constant in the limit $|\vec{k}| \ll \sqrt{r_i}, \left(\frac{ri}{\tau}\right)^{1/3}$. To this end let us first of all explicitly write down the expression of $f^0_{\vec{k},r^\star}(\tau)$ and $\dot{f}^0_{\vec{k},r^\star}(\tau)$,

$$\begin{aligned} f^0_{\vec{k},r^\star}(\tau) = {} & \frac{\pi}{\sqrt{2}} \frac{\mathrm{Ai}\left(-\frac{|\vec{k}|^2+r^\star}{\gamma^2}\right) \mathrm{Bi}'\left(-\frac{|\vec{k}|^2+r_{0,i}}{\gamma^2}\right) - \mathrm{Bi}\left(-\frac{|\vec{k}|^2+r^\star}{\gamma^2}\right) \mathrm{Ai}'\left(-\frac{|\vec{k}|^2+r_{0,i}}{\gamma^2}\right)}{\left(|\vec{k}|^2 + r_{0,i}\right)^{1/4}} \\ & + \frac{i\pi}{\sqrt{2}} \left(\frac{\tau}{r_{0,i} - r_{0,f}}\right)^{1/3} \left(|\vec{k}|^2 + r_{0,i}\right)^{1/4} \left[\mathrm{Ai}\left(-\frac{|\vec{k}|^2 + r^\star}{\gamma^2}\right) \mathrm{Bi}\left(-\frac{|\vec{k}|^2 + r_{0,i}}{\gamma^2}\right) \right. \\ & \left. -\mathrm{Bi}\left(-\frac{|\vec{k}|^2 + r^\star}{\gamma^2}\right) \mathrm{Ai}\left(-\frac{|\vec{k}|^2 + r_{0,i}}{\gamma^2}\right)\right], \end{aligned} \tag{3.71}$$

$$\begin{aligned} \dot{f}^0_{\vec{k},r^\star}(\tau) = {} & \frac{i\pi}{\sqrt{2}} \left(\frac{r_{0,i} - r_{0,f}}{\tau}\right)^{1/3} \frac{\mathrm{Ai}'\left(-\frac{|\vec{k}|^2+r^\star}{\gamma^2}\right) \mathrm{Bi}\left(-\frac{|\vec{k}|^2+r_{0,i}}{\gamma^2}\right) - \mathrm{Bi}'\left(-\frac{|\vec{k}|^2+r^\star}{\gamma^2}\right) \mathrm{Ai}\left(-\frac{|\vec{k}|^2+r_{0,i}}{\gamma^2}\right)}{\left(|\vec{k}|^2 + r_{0,i}\right)^{1/4}} \\ & + \frac{\pi}{\sqrt{2}} \left(|\vec{k}|^2 + r_{0,i}\right)^{1/4} \left[\mathrm{Ai}'\left(-\frac{|\vec{k}|^2 + r^\star}{\gamma^2}\right) \mathrm{Bi}\left(-\frac{|\vec{k}|^2 + r_{0,i}}{\gamma^2}\right) \right. \\ & \left. -\mathrm{Bi}'\left(-\frac{|\vec{k}|^2 + r^\star}{\gamma^2}\right) \mathrm{Ai}\left(-\frac{|\vec{k}|^2 + r_{0,i}}{\gamma^2}\right)\right]. \end{aligned} \tag{3.72}$$

From the previous expressions we can conclude that in the region of interest and for $r^\star = 0$, we can substitute all the Airy function in which $r^\star$ enters in the argument with their value in zero, which can be read from Eq. (3.66), and in the ones where $r_{0,i}$ enters the leading order is obtained taking $|\vec{k}| = 0$, and the same applies to the expressions $|\vec{k}|^2 + r_{0,i}$. Thus, we conclude that $f^0_{\vec{k},0}(\tau)$ and $\dot{f}^0_{\vec{k},0}(\tau)$ (and so their absolute values) tend to a constant.

Let now consider the region $\left(\frac{\sqrt{r_i}}{\tau}\right)^{1/3} \ll |\vec{k}| \ll \sqrt{r_i}$. Here for $r^\star = 0$, we have to take the asymptotic expansion for large arguments for the Airy function in

which $r^\star$ enters in the argument, while for the rest the reasoning of before is valid. Thus we see that $f^0_{\vec{k},0}(\tau) \sim 1/\sqrt{|\vec{k}|}$ and $\dot{f}^0_{\vec{k},0}(\tau) \sim \sqrt{|\vec{k}|}$, implying Eq. (3.48).

Then, let us consider the case in which $\tau \gg 1/\sqrt{r_i}$ and $r^\star = 0$. Here, we are allowed to use the asymptotic expansion for large arguments for the Airy functions in which r_i is in in the argument, obtaining,

$$f^0_{\vec{k},r^\star}(\tau) = \frac{\pi}{\sqrt{2} r_i^{1/6}} \tau^{1/6} \left\{ \mathrm{Ai}\left(-\frac{|\vec{k}|^2 \tau^2}{r_i^{2/3}} \right) \left[\sin\left(\frac{\pi}{4} + \frac{2}{3} \frac{(|\vec{k}|^2 + r_i)^{3/2} \tau}{r_i} \right) \right.\right.$$
$$\left. + i \cos\left(\frac{\pi}{4} + \frac{2}{3} \frac{(|\vec{k}|^2 + r_i)^{3/2} \tau}{r_i} \right) \right] + \mathrm{Bi}\left(-\frac{|\vec{k}|^2 \tau^2}{r_i^{2/3}} \right) \left[\cos\left(\frac{\pi}{4} + \frac{2}{3} \frac{(|\vec{k}|^2 + r_i)^{3/2} \tau}{r_i} \right) \right.$$
$$\left.\left. - i \sin\left(\frac{\pi}{4} + \frac{2}{3} \frac{(|\vec{k}|^2 + r_i)^{3/2} \tau}{r_i} \right) \right] \right\}, \tag{3.73a}$$

$$\dot{f}^0_{\vec{k},r^\star}(\tau) = \frac{\pi}{\sqrt{2} \tau^{1/6}} r_i^{1/6} \left\{ \mathrm{Ai}'\left(-\frac{|\vec{k}|^2 \tau^2}{r_i^{2/3}} \right) \left[\sin\left(\frac{\pi}{4} + \frac{2}{3} \frac{(|\vec{k}|^2 + r_i)^{3/2} \tau}{r_i} \right) \right.\right.$$
$$\left. + i \cos\left(\frac{\pi}{4} + \frac{2}{3} \frac{(|\vec{k}|^2 + r_i)^{3/2} \tau}{r_i} \right) \right] + \mathrm{Bi}'\left(-\frac{|\vec{k}|^2 \tau^2}{r_i^{2/3}} \right) \left[\cos\left(\frac{\pi}{4} + \frac{2}{3} \frac{(|\vec{k}|^2 + r_i)^{3/2} \tau}{r_i} \right) \right.$$
$$\left.\left. - i \cos\left(\frac{\pi}{4} + \frac{2}{3} \frac{(|\vec{k}|^2 + r_i)^{3/2} \tau}{r_i} \right) \right] \right\}, \tag{3.73b}$$

from which we can easily recover Eqs. (3.53) and (3.54).

Finally, we report here the asymptotic expansion of the hypergeometric function appearing in Eqs. (3.58) and (3.60) used to obtain the result (3.62),

$${}_2F_3\left(\frac{1}{6}, \frac{1}{2}; \frac{1}{3}, \frac{2}{3}, \frac{3}{2}; -\frac{4\Lambda^6 \tau^2}{9 r_i^2} \right) \simeq \frac{3^{5/6} \sqrt{\pi}}{2^{1/3} \Gamma\left(\frac{1}{6}\right) \Lambda} \left(\frac{r_i}{\tau} \right)^{1/3} - \frac{\sqrt{3} \sqrt{\pi} \Gamma\left(-\frac{1}{3}\right)}{24 \Gamma\left(\frac{1}{6}\right) \Lambda^3} \left(\frac{r_i}{\tau} \right) \tag{3.74a}$$

$${}_2F_3\left(\frac{5}{6}, \frac{7}{6}; \frac{4}{3}, \frac{5}{3}, \frac{13}{6}; -\frac{4\Lambda^6 \tau^2}{9 r_i^2} \right) \simeq \frac{7\sqrt{\pi}}{2^{2/3} 3^{5/6} \Gamma\left(\frac{5}{6}\right) \Lambda^5} \left(\frac{r_i}{\tau} \right)^{5/3} + \frac{7\sqrt{\pi} \Gamma\left(-\frac{1}{3}\right)}{36 2^{1/3} 3^{1/6} \Lambda^7} \left(\frac{r_i}{\tau} \right)^{7/3} \tag{3.74b}$$

$${}_2F_3\left(\frac{1}{2}, \frac{5}{6}; \frac{2}{3}, \frac{4}{3}, \frac{11}{6}; -\frac{4\Lambda^6 \tau^2}{9 r_i^2} \right) \simeq \frac{5}{4\sqrt{3} \Lambda^3} \left(\frac{r_i}{\tau} \right) - \frac{5 \Gamma\left(-\frac{1}{3}\right)}{12 2^{2/3} 3^{5/6} \Lambda^5} \left(\frac{r_i}{\tau} \right)^{5/3} \tag{3.74c}$$

$$ {}_2F_3\left(-\frac{1}{6},\frac{1}{6};-\frac{1}{3},\frac{1}{3},\frac{7}{6};-\frac{4\Lambda^6\tau^2}{9r_i^2}\right) \simeq \frac{\Gamma^3\left(\frac{1}{3}\right)\Lambda}{123^{1/3}\pi\Gamma\left(\frac{4}{3}\right)}\left(\frac{r_i}{\tau}\right)^{-1/3} - \frac{\Gamma^2\left(\frac{1}{3}\right)\Gamma\left(-\frac{1}{3}\right)}{86^{2/3}\pi\Lambda}\left(\frac{r_i}{\tau}\right)^{1/3} \tag{3.74d} $$

$$ {}_2F_3\left(\frac{1}{2},\frac{5}{6};\frac{1}{3},\frac{5}{3},\frac{11}{6};-\frac{4\Lambda^6\tau^2}{9r_i^2}\right) \simeq \frac{5\pi}{\sqrt{3}\Gamma\left(-\frac{1}{6}\right)\Gamma\left(\frac{7}{6}\right)\Lambda^3}\left(\frac{r_i}{\tau}\right) - \frac{5\Gamma\left(-\frac{1}{3}\right)}{2^{5/3}3^{5/6}\Lambda^5}\left(\frac{r_i}{\tau}\right)^{5/3} \tag{3.74e} $$

$$ {}_2F_3\left(\frac{7}{6},\frac{3}{2};\frac{5}{3},\frac{7}{3},\frac{5}{2};-\frac{4\Lambda^6\tau^2}{9r_i^2}\right) \simeq \frac{813^{1/3}\Gamma^2\left(\frac{5}{3}\right)}{4\pi\Lambda^7}\left(\frac{r_i}{\tau}\right)^{7/3} + \frac{81\Gamma\left(-\frac{1}{3}\right)\Gamma^2\left(\frac{5}{3}\right)}{82^{2/3}\Gamma\left(\frac{1}{6}\right)\Gamma\left(\frac{5}{6}\right)\Lambda^9}\left(\frac{r_i}{\tau}\right)^3 \tag{3.74f} $$

Chapter 4

Breakdown of adiabaticity for the order parameter in a low dimensional gapped system

Slow changes of the system parameters, also known under the oxymoron of "slow quenches", are usually studied for systems driven across a quantum critical point, where a generalization of the Kibble-Zurek theory led to the prediction a universal of a universal scaling of the excitation density with the speed at which the critical point is crossed [93, 132] (successively extended also to quenches within gapless phases, [34, 42] where even full violation of adiabaticity may occur. [94]). Specifically, universality is expected whenever the scaling dimension of the fidelity susceptibility [60] (or its generalization for non linear protocols) is negative, and extends to other quantities besides the excitation density, such as the excess energy. All these predictions can be in principle tested experimentally, since the spontaneous generation of defects in the non-equilibrium dynamics has been observed experimentally in spinor condensates. [127]

Intuitive quantum mechanical arguments, rooted ultimately on the adiabatic theorem, suggest that the case of quenches within a gapped phase is much less interesting. Indeed, in this case the scaling dimension of the fidelity susceptibility is always positive, implying that the density of excitations and the excess

energy always tends to zero with the square of the switching rate for linear ramps (generalization to generic power-law ramps is straightforward). This also suggests that other thermodynamics quantities share the same property, [34] i.e. corrections with respect to their equilibrium value are quadratic in the rate. [95] However, intuition indicates a different scenario when considering the order parameter in a phase with spontaneous symmetry breaking. Since even when performing a variation of the Hamiltonian within a gapped phase an extensive amount of energy is injected, one expects to be in a situation similar to the case of finite temperature. In certain instances, for example in low dimensional systems, the effect of temperature is the complete disruption of long range order, [106] an effect which is very far from being a small correction.

In this chapter we will address such an apparent contradiction by studying the dynamics of the order parameter $m^x(t)$ in a one dimensional Quantum Ising chain after a linear variation in time of the transverse field within the ferromagnetic, ordered phase. In particular, we focus on the asymptotic value of the order parameter $m^x(t \to \infty)$ as a function of the duration τ of the linear ramp. We will show that, even though the bigger τ is the closer $m^x(\tau)$ gets to its ground state value m_0^x, nevertheless, however small $|m^x(\tau) - m_0^x|$ is – actually it is proportional to $1/\tau$ – it is enough to completely disrupt the order exponentially fast in the subsequent time evolution, $m^x(t \to \infty) \to 0$. In particular, in the stationary state the inverse correlation length turns out to depend quadratically on the ramp rate for large τ. These quadratic corrections persist also in the limit of small τ, where the reference value is that of the sudden limit $\tau = 0$. For protocols of intermediate durations in turn the inverse correlation length displays an oscillatory behavior. These results show that in low dimensional many-body systems an apparently small correction to adiabaticity can lead to major consequences for certain observables, even in a gapped phase.

4.1 Linear Ramp in the Ising chain: order parameter dynamics

Let us start our analysis by rewriting the Hamiltonian of the model, already introduced in section 2.3,

$$H_I[g(t)] = -\frac{1}{2}\sum_{j=1}^{L}\left(\sigma_j^x\sigma_{j+1}^x + g\sigma_j^z\right), \tag{4.1}$$

where we once again consider periodic boundary conditions $\sigma_{j+L}^{\alpha} = \sigma_j^{\alpha}$, with σ_j^{α} denoting the Pauli matrices, and the function time dependence of the transverse field is

$$g(t) = \begin{cases} g_0 & t \leq 0 \\ g_0 + \dfrac{g_1 - g_0}{\tau}t & 0 \leq t \leq \tau \\ g_1 & t \geq \tau \end{cases}, \tag{4.2}$$

with $g_0, g_1 < 1$ in such a way that the dynamics is restricted in the ferromagnetic phase.

We remind that the model written in terms of spinless fermions, by performing a Jordan-Wigner transformation,

$$\sigma_i^+ = \prod_{j<i}(1 - 2c_j^\dagger c_j)c_i, \tag{4.3a}$$

$$\sigma_j^z = 1 - 2c_j^\dagger c_j, \tag{4.3b}$$

with $\sigma_i^+ = (\sigma_i^x + i\sigma_i^y)/2$, which allows to write the Hamiltonian as

$$H_I[g(t)] = P^+H_I^+[g(t)]P^+ + P^-H_I^-[g(t)]P^-, \tag{4.4}$$

where

$$P^{\pm} = \frac{1}{2}\left[1 \pm \prod_{j=1}^{L}\sigma_j^z\right] \tag{4.5}$$

are the projectors in the subspace with an even (+) or odd (−) number of fermions and

$$H^{\pm}[g(t)] = -\frac{1}{2}\sum_{i=1}^{L}\left[c_i^\dagger c_{i+1} + c_i^\dagger c_{i+1}^\dagger + h.c. + g(t)(1 - 2c_i^\dagger c_i)\right], \tag{4.6}$$

with the c_i's obeying antiperiodic boundary conditions $c_{L+1} = -c_1$ in the even sector and periodic boundary conditions $c_{L+1} = c_1$ in the odd one.

For finite chains the ground state is always in the even sector and the order parameter σ_j^x, which changes the parity of the fermion number, is strictly zero. However, the energy gap between the lowest energy states within each sector, $|\Omega_+\rangle$ and $|\Omega_-\rangle$, vanishes exponentially in the thermodynamic limit and in the ferromagnetic phase, manifestation of spontaneous breaking of the $\mathbb{Z}_2$ symmetry. One can nonetheless recognize spontaneous symmetry breaking even within each separate sector through the long-distance behavior of the correlation function $R_r^x = \langle \Omega_\pm \mid \sigma_j^x \, \sigma_{j+r}^x \mid \Omega_\pm \rangle$, which is independent of j. Indeed, in the ferromagnetic phase, $\lim_{r\to\infty} R_r^x = m_x^2 > 0$, signaling the established long-range order. We shall thence focus on the even sector, where the finite-size ground state lies, and study the time evolution of

$$R_r^x(t) = \lim_{L\to\infty} \langle \psi_+(t) | \, \sigma_j^x \, \sigma_{j+r}^x \, | \psi_+(t) \rangle, \tag{4.7}$$

where $|\psi_+(t)\rangle = \mathcal{U}(t) \, |\Omega_+\rangle$, being $\mathcal{U}(t)$ the evolution operator, and $|\Omega_+\rangle$ the initial state assumed to be the ground state at $g = g_0$.

Then, as we saw previously, the system can be diagonalize by a Fourier transform $c_j = \frac{e^{i\pi/4}}{\sqrt{L}} \sum_k e^{ikj} \hat{c}_k$, with k odd multiple of π/L, followed by a Bogoliubov transformation

$$\begin{pmatrix} \hat{c}_k \\ \hat{c}_{-k}^\dagger \end{pmatrix} = \begin{pmatrix} u_k(t) & -v_k(t) \\ v_k(t) & u_k(t) \end{pmatrix} \begin{pmatrix} \gamma_k^t \\ {\gamma_{-k}^t}^\dagger \end{pmatrix}, \tag{4.8}$$

with coefficients $u_k(t) = \frac{1}{\sqrt{2}} \sqrt{1 + \frac{g(t) - \cos(k)}{\epsilon_k(t)}}$, $v_k(t) = -\frac{1}{\sqrt{2}} \sqrt{1 - \frac{g(t) - \cos(k)}{\epsilon_k(t)}}$, and eigenvalues $\epsilon_k(t) = \sqrt{1 + g^2(t) - 2g(t)\cos(k)}$.

Let us now derive the equation describing the evolution of the system. In this section we will use a slightly different way of describing the dynamics with respect to section 2.3, even if we will follow a very similar route to obtained the desired equations. Indeed, the starting point is again the introduction of the operators $\tilde{\gamma}_{\pm k}(t)$, annihilating the evolved state $|\psi_+(t)\rangle$, i.e. $\tilde{\gamma}_{\pm k}(t) \, |\psi_+(t)\rangle = 0$. As we already know, the Heisenberg version of such an operator (that we again

will denote with $\tilde{\gamma}^H_{\pm k}(t)$) does not dependent on time in the subspace spanned by $|\psi_+(t)\rangle$.

Then, let make the ansatz

$$\begin{pmatrix} \hat{c}_k(t) \\ \hat{c}^\dagger_{-k}(t) \end{pmatrix} = \begin{pmatrix} \alpha_k(t) & -\beta^\star_k(t) \\ \beta_k(t) & \alpha^\star_k(t) \end{pmatrix} \begin{pmatrix} \tilde{\gamma}^H_k \\ \left(\tilde{\gamma}^H_{-k}\right)^\dagger \end{pmatrix}, \tag{4.9}$$

relating the Heisenberg version of the Jordan-Wigner operators (we omit in this case the superscript), with the tilde operators. Finally, to find an equation for the coefficients of our ansatz we use the equation of motion of the Jordan-Wigner operators, which can be easily computed taking commutators with $H_I[g(t)]$,

$$i\frac{\mathrm{d}}{\mathrm{d}t}\begin{pmatrix} \hat{c}_k(t) \\ \hat{c}^\dagger_{-k}(t) \end{pmatrix} = \begin{pmatrix} 2\left(g(t)-\cos(k)\right) & -2\sin(k) \\ -2\sin(k) & -2\left(g(t)-\cos(k)\right) \end{pmatrix} \begin{pmatrix} c_k(t) \\ c^\dagger_{-k}(t) \end{pmatrix}. \tag{4.10}$$

Putting all together we obtain,

$$\begin{cases} i\dfrac{\mathrm{d}}{\mathrm{d}t}\alpha_k(t) = 2\left(g(t)-\cos(k)\right)\alpha_k(t) - 2\sin(k)\beta_k(t), \\ i\dfrac{\mathrm{d}}{\mathrm{d}t}\beta_k(t) = -2\left(g(t)-\cos(k)\right)\beta_k(t) - 2\sin(k)\alpha_k(t), \end{cases} \tag{4.11}$$

with the initial conditions given by the coefficients of the Bogoliubov transformation, because $\tilde{\gamma}_{\pm k}(0) = \gamma^0_\pm$, since the initial state is the ground state of the initial Hamiltonian. By requiring that the state is annihilated by $\tilde{\gamma}_{\pm k}(t)$, we can also obtain the following expression for the evolved state,

$$|\psi_+(t)\rangle = \prod_{k>0}\left(\alpha^\star_k(t) - \beta^\star_k(t)\hat{c}^\dagger_k\hat{c}^\dagger_{-k}\right)|0\rangle\,. \tag{4.12}$$

We note that the coefficient of the ansatz (4.9) satisfy the condition $|\alpha_k(t)|^2 + |\beta_k(t)|^2 = 1$. This implies that the evolution of the system can be described in terms of three real function of k. Indeed we can introduce,

$$f_{1,k}(t) = |\alpha_k(t)|^2 - |\beta_k(t)|^2 \tag{4.13a}$$

$$f_{2,k}(t) = 2\Re\left(\alpha_k(t)\beta^\star_k(t)\right) \tag{4.13b}$$

$$f_{3,k}(t) = 2\Im\left(\alpha_k(t)\beta^\star_k(t)\right), \tag{4.13c}$$

whose evolution equations can be obtained using Eq. (4.11), with the result,

$$\begin{cases} \dfrac{\mathrm{d}}{\mathrm{d}t} f_{1,k}(t) = 4\sin(k) f_{3,k}(t) \\ \dfrac{\mathrm{d}}{\mathrm{d}t} f_{2,k}(t) = 4\left(g(t) - \cos(k)\right) f_{3,k}(t) \\ \dfrac{\mathrm{d}}{\mathrm{d}t} f_{3,k}(t) = -4\left(g(t) - \cos(k)\right) f_{2,k}(t) - 4\sin(k) f_{1,k}(t) \end{cases}, \tag{4.14}$$

with initial conditions,

$$\begin{cases} f_{1,k}(0) = \dfrac{g_0 - \cos(k)}{\epsilon_k^0} \\ f_{2,k}(0) = -\dfrac{\sin(k)}{\epsilon_k^0} \\ f_{3,k}(0) = 0. \end{cases}. \tag{4.15}$$

We observe that the description of the dynamics in terms of the function $f_k(t)$'s is equivalent to a description in terms of the density matrix of the model $\rho_+(t) = |\psi_+(t)\rangle \langle\psi_+(t)|$, which, since the k-modes are decoupled one from each other, takes the form $\rho_+(t) = \bigotimes_{k>0} \rho_{k,+}(t)$. Each matrix $\rho_{k,+}(t)$ is an hermitian 2×2 density matrix with unit trace, so it is a function of only three independent real parameters. Indeed it can be written in term of the functions $f_k(t)$ as

$$\rho_{k,+}(t) = \frac{1}{2} \begin{pmatrix} 1 + f_{k,1}(t) & f_{2,k}(t) + i f_{3,k}(t) \\ f_{2,k}(t) - i f_{3,k}(t) & 1 - f_{k,1}(t) \end{pmatrix}. \tag{4.16}$$

Using the solution of Eqs. (4.14) we can then calculate $R_r^x(t)$, defined in Eq. (4.7). Indeed, by using the Jordan-Wigner transformation (4.3) we can express the correlation function R_r^x as,

$$R_r^x(t) = \langle \Big(c_j^\dagger(t) - c_j(t) \Big) \prod_{j<m<j+r} \left(1 - 2c_m^\dagger(t) c_m(t)\right) \Big(c_{j+r}^\dagger(t) + c_{j+r}(t) \Big) \rangle. \tag{4.17}$$

Then then observing that $\left(1 - 2c_m^\dagger(t) c_m(t)\right) = \left(c_m^\dagger(t) + c_m(t)\right)\left(c_m^\dagger(t) - c_m(t)\right)$, and defining

$$A_j^t = c_j(t) + c_j^\dagger(t) \quad B_j^t = c_j^\dagger(t) - c_j(t), \tag{4.18}$$

satisfying $\left\{A_j^t, B_l^t\right\} = 0\ \forall j, l$, we obtain

$$R_r^x(t) = \langle B_j^t A_{j+1}^t B_{j+1}^t \dots A_{j+r-1}^t B_{j+r-1}^t A_{j+r}^t \rangle_0, \tag{4.19}$$

Using Wick's theorem, Eq. (4.19) can be expressed in terms of the contractions of the A_j's and B_j's, which in terms of the function $f_{1,k}$, $f_{2,k}$ and $f_{3,k}$ read

$$\langle A_j^t A_l^t \rangle_0 = \delta_{jl} - \frac{1}{L}\sum_k e^{ik(j-l)} f_{3,k}(t), \tag{4.20a}$$

$$\langle B_j^t B_l^t \rangle_0 = -\delta_{jl} - \frac{1}{L}\sum_k e^{ik(j-l)} f_{3,k}(t), \tag{4.20b}$$

$$\langle B_j^t A_l^t \rangle_0 = -\frac{1}{L}\sum_k e^{ik(j-l)} (f_{1,k}(t) + i f_{2,k}(t)). \tag{4.20c}$$

Using this equation, we are now ready to compute the evolution of the order parameter. In the next section we will start analyzing the stationary state reached for $t \to \infty$, while in the following one we will give more details about how this stationary state is reached.

4.1.1 Stationary state

For $t > \tau$, $g(t) = g_1$ is constant, so we can readily integrate Eqs. (4.14) in terms of the boundary values $f_{1,k}(\tau)$, $f_{2,k}(\tau)$ and $f_{3,k}(\tau)$, obtaining

$$\begin{aligned} f_{1,k}(t) =& \frac{g_1 - \cos k}{\epsilon_k^1}\left[f_{1,k}(\tau)\frac{g_1 - \cos k}{\epsilon_k^1} - f_{2,k}(\tau)\frac{\sin k}{\epsilon_k^1}\right] + \cos\left(4\epsilon_k^1(t-\tau)\right)\frac{\sin k}{\epsilon_k^1} \\ & \left[f_{1,k}(\tau)\frac{\sin k}{\epsilon_k^1} + f_{2,k}(\tau)\frac{g_1 - \cos k}{\epsilon_k^1}\right] + \sin\left(4\epsilon_k^1(t-\tau)\right)\frac{\sin k}{\epsilon_k^1} f_{3,k}(\tau), \end{aligned} \tag{4.21a}$$

$$\begin{aligned} f_{2,k}(t) =& \frac{\sin k}{\epsilon_k^1}\left[f_{2,k}(\tau)\frac{\sin k}{\epsilon_k^1} - \frac{g_1 - \cos k}{\epsilon_k^1} f_{1,k}(\tau)\right] + \cos\left(4\epsilon_k^1(t-\tau)\right)\frac{g_1 - \cos k}{\epsilon_k^1} \\ & \left[f_{2,k}(\tau)\frac{g_1 - \cos k}{\epsilon_k^1} + \frac{\sin k}{\epsilon_k^1} f_{1,k}(\tau)\right] + \sin\left(4\epsilon_k^1(t-\tau)\right)\frac{g_1 - \cos k}{\epsilon_k^1} f_{3,k}(\tau), \end{aligned} \tag{4.21b}$$

$$f_{3,k}(t) = f_{3,k}(\tau)\cos\left(4\epsilon_k^1(t-\tau)\right) - \sin\left(4\epsilon_k^1(t-\tau)\right)\left[f_{2,k}(\tau)\frac{g_1-\cos k}{\epsilon_k^1} + \frac{\sin k}{\epsilon_k^1}f_{1,k}(\tau)\right], \tag{4.21c}$$

where $\epsilon_k^1 = \epsilon_k(\tau)$.

We note that the solution consists in a stationary part plus oscillatory terms with frequency $4\epsilon_k(\tau)$, which vanish for $t \to \infty$ once integrated over k. We thus find

$$\langle A_j A_l\rangle \to \delta_{jl}, \tag{4.22a}$$

$$\langle B_j B_l\rangle \to -\delta_{jl}, \tag{4.22b}$$

$$\langle B_j A_l\rangle \to C(j-l+1), \tag{4.22c}$$

with

$$C(r) = \int_{-\pi}^{\pi}\frac{dk}{2\pi}\frac{\cos(kr) - g_1\cos(k(r-1))}{1+g_1^2-2g_1\cos k}(1-2n_k), \tag{4.23}$$

where $n_k = \langle {\gamma^\tau}_k^\dagger \gamma_k^\tau\rangle_t$ the occupation numbers in the evolved state, which are actually time-independent for $t > \tau$ and given by

$$1-2n_k = \frac{(g_1-\cos k)f_{1,k}(\tau) - \sin k f_{2,k}(\tau)}{\sqrt{1+g_1^2-2g_1\cos k}}. \tag{4.24}$$

We note that disregarding the oscillatory terms is equivalent to state that the stationary value, being the correlation a local observable, can be computed in the diagonal ensemble, which is completely determined by the occupation numbers n_k.

As in equilibrium, the conditions (4.22) allow to rewrite the correlation R_r^x as a $r \times r$ Toeplitz determinant,

$$R_r^x = \begin{vmatrix} C(0) & C(-1) & \dots & C(-r+1) \\ C(1) & C(0) & \dots & C(-r+2) \\ \vdots & \vdots & \ddots & \vdots \\ C(r-1) & C(r-2) & \dots & C(0) \end{vmatrix}, \tag{4.25}$$

whose asymptotic behavior in the limit $r \to \infty$ has to be determined. To this end ,we first note that $C(r) = \frac{1}{2\pi}\int_{-\pi}^{\pi} dk \tilde{C}(k) e^{-ikr}$, with

$$\tilde{C}(k) = \left(\frac{1-g_1e^{ik}}{1-g_1e^{-ik}}\right)^{1/2}(1-2n_k)\,. \tag{4.26}$$

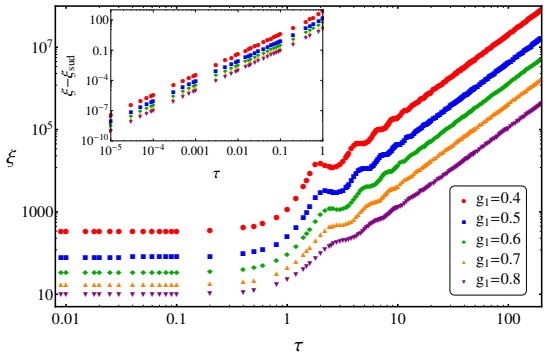

Figure 4.1: *Log-log plot of the correlation length ξ as a function of the duration τ of the linear ramp for initial transverse field $g_0 = 0.3$ and different final values of g_1. ξ_{sud} is the value of the correlation length for a sudden quench from g_0 to g_1.*

In terms of the complex variable $z = e^{ik}$ the function $\tilde{C}(z)$ has zero index around the unit circle and is non vanishing, as long as $n_k < 1/2$, $\forall k$, a condition that has been verified numerically and perturbatively, and is equivalent to say that the effective temperature of all the modes is less than infinity. Under this condition we can apply the strong Szegő lemma [122], which tells us that $R^x_r \sim e^{-r/\xi}$, with the inverse correlation length given by,

$$\xi^{-1} = -\frac{1}{2\pi}\int_{-\pi}^{\pi} dk \log\left(1 - 2n_k\right). \tag{4.27}$$

Therefore, whenever $n_k \neq 0$, the correlation length is finite, implying that R^x_r goes to zero exponentially hence that the order parameter is zero. Such a condition is verified for any finite duration of the linear ramp, implying that adiabaticity is broken for the order parameter. From Eq. (4.27) we observe that a tiny deviation of the occupation numbers with respect to their equilibrium value ($n_k = 0$) translates into a comparably small inverse correlation length. Nonetheless, such small quantitative corrections lead to a completely different behavior of the correlation function R^x_r and of the order parameter.

Figure 4.1 shows the correlation length as a function of τ for different ramps computed by numerically solving Eqs. (4.14) and evaluating Eq. (4.27). We can see that for long durations the correlation length grows quadratically, while for

τ of order one it displays oscillations. The inset of the figure shows that also for small τ the growth of ξ above the sudden-quench value is quadratic. The two limiting cases of slow and sudden quenches can be captured by two different perturbative expansions (more details can be found in the appendices 4.A and 4.B).

For small τ the result of the perturbative expansion of Eqs. (4.14) at the leading order is

$$\begin{aligned}\xi(\tau) = &- \frac{1}{\log\left[\frac{1+g_0g_1+\sqrt{(1-g_1^2)(1-g_0^2)}}{2}\right]} \\ &+ \tau^2 \frac{2(g_1-g_0)^2\left(1+g_0g_1-\sqrt{(1-g_1^2)(1-g_0^2)}\right)}{3(g_0+g_1)^2\log^2\left[\frac{1+g_0g_1+\sqrt{(1-g_1^2)(1-g_0^2)}}{2}\right]} + O(\tau^4),\end{aligned} \tag{4.28}$$

where the first term is the result for a sudden quench (ξ_{sud}). Higher order can be straightforwardly computed. In particular we notice that only even powers of τ are present in the expansion, and all computed corrections are even under $g_0 \leftrightarrow g_1$, i.e. inversion of the ramp. Figure 4.2a shows a comparison between the perturbative and the numerical results, and we can see that the agreement is excellent up to $\tau \simeq 1$ provided corrections up to eighth order are taken into account.

For large τ, instead, one can use the adiabatic perturbation theory described in Ref. [104], which predicts that the occupation numbers n_k for large τ vanish as $1/\tau^2$ in an oscillating fashion. This is actually the source of oscillations observed in ξ. Indeed, by applying the adiabatic perturbation theory one obtains,

$$\begin{aligned}\xi(\tau) = &\frac{64(1-g_0^2)^3(1-g_1^2)^3}{(g_1-g_0)^2\left[(1-g_0^2)^3+(1-g_1^2)^3\right]}\tau^2 + f(\tau)\sqrt{\tau} \\ &+ \Lambda + O(\tau^{-1/2}),\end{aligned} \tag{4.29}$$

where $f(\tau)$ is an oscillating function and Λ is a constant, see the supplemental material. Thus, the relative oscillations of the correlations length goes to zero as $\tau^{-3/2}$. Also in this case all the corrections are invariant under the transformation $g_0 \leftrightarrow g_1$. Figure 4.2b shows a comparison between this adiabatic perturbative

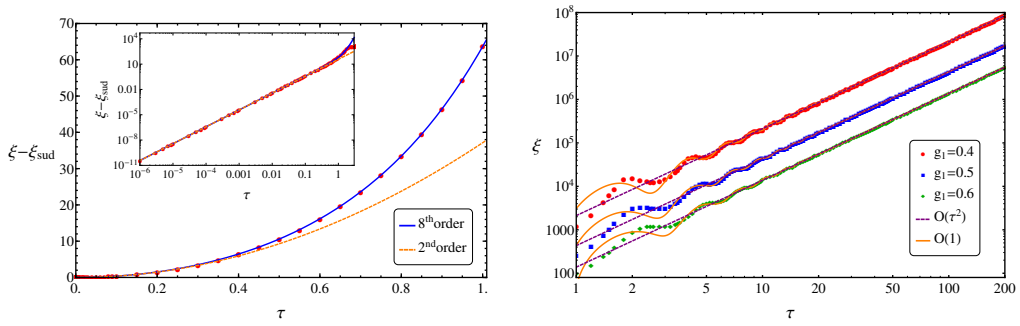

(a) **(b)**

Figure 4.2: *(a) Correlation length ξ as a function of the duration τ for $g_0 = 0.3$ and $g_1 = 0.6$. The numerical results (red circles) are compared with the perturbative expansion for small τ up to second and eight order. The inset shows the same plot in log-log scale. (b)Log-log plot of the correlation length ξ as a function of the duration τ of the linear ramp for initial transverse field $g_0 = 0.3$ and different final values of g_1. Numerical results are compared with the predictions of adiabatic perturbation theory at two different orders.*

expansion and the numerical data. We see that by including correction up to $O(1)$ there is quite a good agreement for $\tau \gtrsim 10$.

4.1.2 Approach to the stationary state

Let us now address the question of how the stationary state described in the previous section is reached. For a generic time t Eqs. (4.22) are no more valid, so that the correlation can not be represented as a Toeplitz determinant. Instead, Eq. (4.19) can be represented as the Pfaffian of a $2r \times 2r$ antisymmetric matrix [16],

$$R_r^x(t) = \mathrm{pf}\left[M(t)\right], \tag{4.30}$$

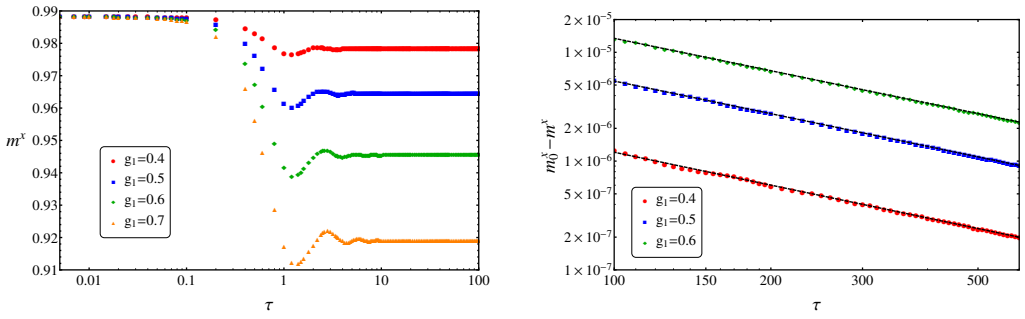

(a) **(b)**

Figure 4.3: *(a) Longitudinal magnetization m^x measured at the end of the ramp as a function of its duration τ for ramps with $g_0 = 0.3$. (b) (b) Difference between the equilibrium value of the longitudinal magnetization m_0^x corresponding to the final value of the transverse field and its value measured at the end of the ramp m^x as a function of its duration τ. The initial transverse field is $g_0 = 0.3$ and the dashed lines are $\sim 1/\tau$ fits.*

where $M(t)$ is given by

$$M(t) = \begin{bmatrix} M_0(t) & M_{-1}(t) & \dots & M_{1-r}(t) \\ M_1(t) & M_0(t) & \dots & M_{2-r}(t) \\ \vdots & \vdots & \ddots & \vdots \\ M_{r-1}(t) & \dots & \dots & M_0(t) \end{bmatrix}, \quad M_l(t) = \begin{pmatrix} -f_l(t) & g_l(t) \\ -g_{-l}(t) & f_l(t) \end{pmatrix}, \tag{4.31}$$

with

$$g_n(t) = \langle B_{j+n-1} A_j \rangle \tag{4.32a}$$

$$f_n(t) = i\langle A_j A_{j+n} \rangle - i\delta_{n,0}. \tag{4.32b}$$

Then we can use the relation between the pfaffian and the determinant $\mathrm{pf}\,[M(t)]^2 = \det[M(t)]$, to write down the order parameter at a genetic time t,

$$m^x(t) = \left(\lim_{r\to\infty} \det[M(t)] \right)^{1/4}. \tag{4.33}$$

By numerically solving Eqs. (4.14) and using formula (4.33), we can compute the valued of the order parameter at a genetic time. Let us start considering what happens at $t = \tau$, that is right after the end of the ramp. As can be

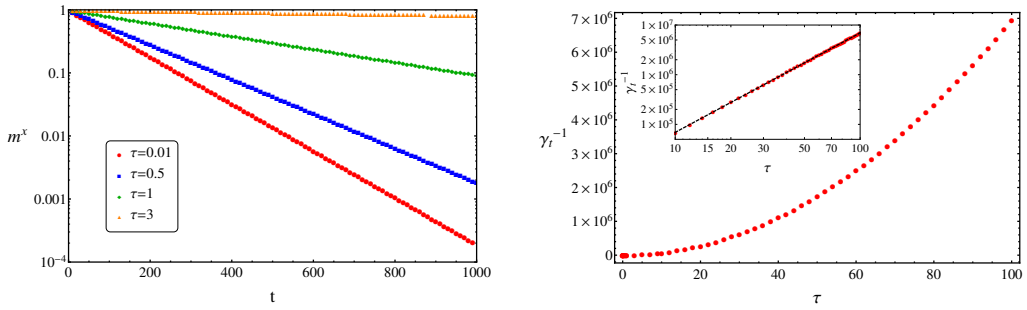

(a) **(b)**

Figure 4.4: *(a) Longitudinal magnetization m^x as a function of the time t elapsed after the end of the ramp in a linear-log scale for different ramp durations τ. The initial and final value of the transverse field are $g_0 = 0.5$ and $g_1 = 0.2$ respectively. (b) Inverse decay rate γ_t^{-1} as a function of the duration of the ramp τ for a ramp with $g_0 = 0.5$ and $g_1 = 0.2$. The inset shows the same plot in log-log scale with the dashed line proportional to τ^2.*

seen from Figs. 4.3a and 4.3b at this point the order parameter is $m^x(\tau) = m_0^x + \delta m^x(\tau)$, where m_0^x is the values that it would have in the ground state of the final Hamiltonian, while $\delta m^x(\tau) \propto 1/\tau$ is a correction. So as expected, the larger is the duration of the ramp τ the nearer is the order parameter to its equilibrium value.

However, the order parameter is not a conserved quantity and unlike classical systems, where the small corrections discussed above would lead to a small precession of the magnetization around its equilibrium value, in quantum low dimensional systems this state is dynamically very fragile, and the subsequent time evolution produces a collapse of the magnetization, as we have found in the previous section.

Indeed, by solving the dynamics for a time t after the end of the ramp we find that the magnetization always decays to zero exponentially in time, as can be seen from Fig. (4.4a), i.e.

$$m_x(t) \sim \exp(-\gamma_t t), \tag{4.34}$$

with a the decay rate γ_t that scales as $1/\tau^2$ as a function of the duration of the ramp as can be seen from Fig. 4.4b.

4.2 Concluding Remarks

Summarizing, we have shown that the stationary value of the order parameter of a one dimensional Quantum Ising model does not behave in an adiabatic way within the ferromagnetic phase however small the switching rate of the transverse field is. This occurs in spite of the fact that the Hamiltonian is gapped, which in principle is the most favorable situation for an adiabatic evolution.
Such a behavior of the order parameter has to be expected whenever the system has a phase transition only at zero temperature and it is driven within the ordered phase. Indeed a finite density of excitations $n_{ex} \sim 1/\tau^2$ will always be generated and in this situation will be always sufficient to destroy order. From this, one can estimate also the behavior of the correlation length, which, following the same reasoning as the Kibble-Zurek argument, will be $\xi \sim 1/n_{ex}^{1/d} \sim \tau^{2/d}$, with d being the dimension of the system. A natural question that comes up is what happens instead in an analogous system where the transition survives at finite temperature. One possibility is that there is a transition in the value of the order parameter as a function of τ, namely for sufficiently slow ramp its asymptotic value is expected to be finite, while it should go to zero for fast ramps. If this is really the case, and in the affirmative case if the value of the order parameter is vanishing or not are interesting question to consider in following studies.

Appendix

4.A Small τ expansion

In this section we show the derivation of the series expansion in powers of τ of the correlation length, valid for small durations of the ramp.
Introducing the variable $s = t/\tau$, which goes from 0 to 1, we write the functions $f_{1,k}$, $f_{2,k}$ and $f_{3,k}$ as power series of τ, i.e.,

$$f_{1,k}(s) = \sum_{n=0}^{\infty} a_k^{(n)}(s)\,\tau^n, \tag{4.35a}$$

$$f_{2,k}(s) = \sum_{n=0}^{\infty} b_k^{(n)}(s)\,\tau^n, \tag{4.35b}$$

$$f_{3,k}(s) = \sum_{n=0}^{\infty} c_k^{(n)}(s)\,\tau^n, \tag{4.35c}$$

with the coefficients satisfying initial conditions $a_k^{(0)}(0) = f_{1,k}(0)$, $b_k^{(0)}(0) = f_{2,k}(0)$, $c_k^{(0)}(0) = 0$, and $a_k^{(n)}(0) = b_k^{(n)}(0) = c_k^{(n)}(0) = 0$, $\forall n > 0$. Inserting the expansions in Eq. (4.14), we can write down explicitly the evolution equations of the coefficients,

$$\frac{da_k^{(n+1)}}{ds} = 4\sin k\, c_k^{(n)}(s), \tag{4.36a}$$

$$\frac{db_k^{(n+1)}}{ds} = 4\,(g_0 - \cos k + \Delta g\, s)\, c_k^{(n)}(s), \tag{4.36b}$$

$$\frac{dc_k^{(n+1)}}{ds} = -4\,(g_0 - \cos k + \Delta g\, s)\, b_k^{(n)}(s) - 4\sin k\, a_k^{(n)}(s), \tag{4.36c}$$

where we have defined $\Delta g = g_1 - g_0$. These equations can be readily integrated, obtaining an iterative procedure to compute $f_{1,k}$, $f_{2,k}$ and $f_{3,k}$ at the desired order in τ. We immediately notice that, since $c_k^{(0)} = 0$, we have $a_k^{(2n+1)} = b_k^{(2n+1)} = c_k^{(2n)} = 0 \quad \forall n$, this in turn implies that the corrections to $1 - 2n_k$, and so to the correlation length, with respect to the sudden quench value are given by even powers of τ.

Let us compute the first non-vanishing correction. From Eq. (4.36c) we derive

$$c_k^{(1)}(s) = \frac{2\Delta g \, \sin k}{\epsilon_k(0)} s^2, \tag{4.37}$$

from which, using Eqs. (4.36a) and (4.36b),

$$a_k^{(2)}(s) = \frac{8\Delta g \, \sin^2 k}{3\epsilon_k(0)} s^3, \tag{4.38}$$

$$b_k^{(2)}(s) = \frac{8\Delta g \, \sin k(g_0 - \cos k)}{3\epsilon_k(0)} s^3 + \frac{2(\Delta g)^2 \sin k}{\epsilon_k(0)} s^4. \tag{4.39}$$

Using Eq.(4.24) we can then obtain

$$\begin{aligned} 1 - 2n_k \quad &= \frac{1 + g_0 g_1 - (g_0 + g_1)\cos k}{\epsilon_k(0)\epsilon_k(1)} \\ &+ \frac{2(\Delta g)^2 \sin^2 k}{3\epsilon_k(0)\epsilon_k(1)} \tau^2 + O(\tau^4). \end{aligned} \tag{4.40}$$

Then, using Eq. (4.27), we can compute the expansion of the inverse of the correlation length up to second order in τ, that is

$$\begin{aligned} \xi^{-1}(\tau) = &- \log\left(\frac{1 + g_0 g_1 + \sqrt{(1 - g_1^2)(1 - g_0^2)}}{2}\right) \\ &- \tau^2 \frac{2(\Delta g)^2 \left(1 + g_0 g_1 - \sqrt{(1 - g_1^2)(1 - g_0^2)}\right)}{3(g_0 + g_1)^2} + O(\tau^4). \end{aligned} \tag{4.41}$$

Finally, by inverting the previous expression, we recover Eq. (4.28).

This procedure can be straightforwardly repeated for computing higher order corrections, and is easily implementable on a computer. We did it up to the eighth order in τ and we notice that all contributions are even if we exchange g_0 and g_1, that is if we either ramp up or down the transverse field.

4.B Large τ expansion

In this section we provide details of the derivation of perturbative expansion in powers of τ of the correlation length, valid for large τ. First, we find an approximate expression of the evolved state by applying the adiabatic perturbation theory (APT) [104]. Then we perform a power series expansion of the occupation numbers $n_k = \langle {\gamma^\tau}_k^\dagger \gamma_k^\tau \rangle_t$ in terms of the small parameter $1/\tau$ and we finally use it to compute the correlation length.

4.B.1 Adiabatic Perturbation Theory

Our problem can be reduced to a two-level problem, greatly simplifying the general results of Ref. [104]. Indeed, because of the momentum conservation, the instantaneous excited states are obtained by applying products ${\gamma^t_{-k}}^\dagger {\gamma^t_k}^\dagger$ to the ground state $|\Omega_+\rangle_t$. Since excitations to different k-modes are independent one from each other, we can consider the problem as a sum of independent two-level systems. Again, it is convenient to use the rescaled time $s = t/\tau$, which goes from 0 to 1. The instantaneous eigenstates of the two-level system are $|-(s)\rangle_k = (u_k(s), v_k(s))^T$ and $|+(s)\rangle_k = (v_k(s), -u_k(s))^T$ with corresponding eigenvalues $E_\pm(s) = \pm 2\epsilon_k(s)$. Using the same notation of Ref. [104], we find that the matrix elements $M_{nm}(s)$ are given by

$$M_{-+}(s) = -M_{+-}(s) = \frac{\Delta g \, \sin k}{2\epsilon_k^2(s)}, \tag{4.42a}$$

$$M_{--}(s) = M_{++}(s) = 0. \tag{4.42b}$$

It follows that the Berry phase $\gamma_n(s)$ and the matrix elements $W_{nm}(s)$ vanish. Moreover, the dynamical phase is such that

$$\omega_k(s) \equiv \omega_+(s) = -\omega_-(s) = \int_0^s ds' \, 2\epsilon_k(s') \tag{4.43}$$

and $\Delta_{+-}(s) = -\Delta_{-+}(s) = 4\epsilon_k(s)$. Since the initial state is the ground state of the two-level system $|-(0)\rangle_k$, the initial condition is given by $b_n(0) = \delta_{n-}$.

We can now calculate explicitly corrections up to second order in the small parameter $1/\tau$. The zeroth order term in the power series expansion of APT is given by the adiabatic approximation,

$$|\psi^{(0)}(s)\rangle_k = e^{i\omega_k(s)\tau}\,|-(s)\rangle_k\,. \tag{4.44}$$

The first order correction to the adiabatic approximation is

$$\begin{aligned}|\psi^{(1)}(s)\rangle_k &= e^{i\omega_k(s)\tau}b^{(1)}_{--}(s)\,|-(s)\rangle_k \\ &+\left(e^{-i\omega_k(s)\tau}b^{(1)}_{++}(s)+e^{i\omega_k(s)\tau}b^{(1)}_{+-}(s)\right)|+(s)\rangle_k\,,\end{aligned} \tag{4.45}$$

while the second order correction is

$$\begin{aligned}|\psi^{(2)}(s)\rangle_k &= \left(e^{-i\omega_k(s)\tau}b^{(2)}_{-+}(s)+e^{i\omega_k(s)\tau}b^{(2)}_{--}(s)\right)|-(s)\rangle_k \\ &+\left(e^{i\omega_k(s)\tau}b^{(2)}_{+-}(s)+e^{-i\omega_k(s)\tau}b^{(2)}_{++}(s)\right)|+(s)\rangle_k\,.\end{aligned} \tag{4.46}$$

The explicit expression of the coefficients is given below. The approximate form of the k-mode evolved state up to second order is

$$|\psi(s)\rangle_k = |\psi^{(0)}(s)\rangle_k + \tau^{-1}|\psi^{(1)}(s)\rangle_k + \tau^{-2}|\psi^{(2)}(s)\rangle_k + O(\tau^{-3}). \tag{4.47}$$

4.B.2 Perturbative Expansion

Using the approximate solution (4.47) and noting that $\gamma^\tau_k\,|-(1)\rangle_k = 0$, which implies that at leading order $n_k(\tau) = 0$, the power series expansion of the occupation numbers up to fourth order in $1/\tau$ is

$$n_k(\tau) = \tau^{-2}n^{(2)}_k(\tau) + \tau^{-3}n^{(3)}_k(\tau) + \tau^{-4}n^{(4)}_k(\tau) + O(\tau^{-5}), \tag{4.48}$$

where

$$\begin{aligned}n^{(2)}_k(\tau) &= \left|b^{(1)}_{++}(1)\right|^2 + \left|b^{(1)}_{+-}(1)\right|^2 \\ &\quad -2\cos\left(\phi_k(\tau)\right)\left(b^{(1)}_{++}(1)b^{(1)}_{+-}(1)\right),\end{aligned} \tag{4.49a}$$

$$\begin{aligned}n^{(3)}_k(\tau) &= 2\sin\left(\phi_k(\tau)\right)\left(ib^{(1)}_{+-}(1)b^{(2)}_{++}(1)\right. \\ &\quad \left.-ib^{(1)}_{++}(1)b^{(2)}_{+-}(1)\right),\end{aligned} \tag{4.49b}$$

$$n_k^{(4)}(\tau) \simeq \left(b_{++}^{(2)}(1)\right)^2 + \left(b_{+-}^{(2)}(1)\right)^2 + 2\cos\left(\phi_k(\tau)\right)\left(b_{++}^{(2)}(1)b_{+-}^{(2)}(1)\right), \tag{4.49c}$$

and

$$b_{++}^{(1)}(1) = \Delta g \frac{i\sin k}{8\epsilon_k^3(0)}, \tag{4.50a}$$

$$b_{+-}^{(1)}(1) = -\Delta g \frac{i\sin k}{8\epsilon_k^3(1)}, \tag{4.50b}$$

$$b_{++}^{(2)}(1) = (\Delta g)^2 \frac{\sin k}{32\epsilon_k^3(0)}\left[\frac{3(g_0-\cos k)}{\epsilon_k^3(0)} + \frac{\sin^2 k}{4}\int_{g_0}^{g_1} dg\left(g^2-2g\cos k+1\right)^{-5/2}\right], \tag{4.50c}$$

$$b_{+-}^{(2)}(1) = -(\Delta g)^2 \frac{\sin k}{32\epsilon_k^3(1)}\left[\frac{3(g_1-\cos k)}{\epsilon_k^3(1)} - \frac{\sin^2 k}{4}\int_{g_0}^{g_1} dg\left(g^2-2g\cos k+1\right)^{-5/2}\right], \tag{4.50d}$$

$$\phi_k(\tau) = \frac{4\tau}{\Delta g}\int_{g_0}^{g_1} dg\sqrt{g^2-2g\cos k+1} \tag{4.50e}$$

We point out that in $n_k^{(4)}(\tau)$ we are neglecting the contribution given by ${}_k\langle\psi^{(1)}(1)|\,\gamma_k^{\tau\dagger}\gamma_k^{\tau}\,|\psi^{(3)}(1)\rangle_k +$ *h.c.*, because it gives higher order corrections to the correlation length. Inserting the expansion (4.48) in Eq. (4.27) and keeping the terms up to fourth order, we obtain

$$\xi^{-1}(\tau) = \frac{1}{\pi}\left\{\tau^{-2}\int_{-\pi}^{\pi} dk\, n_k^{(2)}(\tau) + \tau^{-3}\int_{-\pi}^{\pi} dk\, n_k^{(3)}(\tau) + \tau^{-4}\int_{-\pi}^{\pi} dk\left[n_k^{(4)}(\tau) + \left(n_k^{(2)}(\tau)\right)^2\right]\right\} + O(\tau^{-5}). \tag{4.51}$$

From Eq. (4.51), it is evident that oscillations in the correlation length appear as a consequence of oscillations in the occupation numbers.

Let us compute the integrals in the previous expression using Eqs. (4.49) and (4.50).

$$\begin{aligned} I_1 &= \frac{1}{\pi}\int_{-\pi}^{\pi} dk \left(\left| b_{++}^{(1)}(1) \right|^2 + \left| b_{+-}^{(1)}(1) \right|^2 \right) \\ &= (\Delta g)^2 \, \frac{\left(1-g_0^2\right)^3 + \left(1-g_1^2\right)^3}{64\left(1-g_0^2\right)^3\left(1-g_1^2\right)^3}. \end{aligned} \tag{4.52}$$

$$\begin{aligned} I_2(\tau) &= -\frac{2}{\pi}\int_{-\pi}^{\pi} dk \, \cos\left(\phi_k(\tau)\right) \left(b_{++}^{(1)}(1) b_{+-}^{(1)}(1) \right) \\ &= -\frac{(\Delta g)^2}{16\pi} \Re \left[\int_{-\pi}^{\pi} dk \frac{\sin^2 k}{\left(\epsilon_k(0)\epsilon_k(1)\right)^3} e^{i\phi_k(\tau)} \right]. \end{aligned} \tag{4.53}$$

The contribution of the integral (4.53) can be evaluated applying the stationary phase approximation. Since in the power series expansion (4.51) we are keeping only terms up to fourth order, we can neglect all the contributions of $I_2(\tau)$ higher than the second order in $1/\tau$. We finally obtain

$$\begin{aligned} I_2(\tau) &= -\tau^{-3/2} \frac{(\Delta g)^2}{64\sqrt{\pi}} \left[\frac{A_2}{C_2^{3/2}} \cos\left(C_0\tau + \frac{3\pi}{4} \right) \right. \\ &\left. + \frac{B_2}{|D_2|^{3/2}} \cos\left(D_0\tau - \frac{3\pi}{4} \right) \right] + O\left(\tau^{-5/2}\right), \end{aligned} \tag{4.54}$$

where

$$\begin{aligned} A_2 &= \frac{1}{(1-g_0)^3(1-g_1)^3}, \\ C_0 &= 2\left(2-g_0-g_1\right), \\ C_2 &= \frac{2}{\Delta g}\left[\log\left(\frac{1-g_0}{1-g_1} \right) - \Delta g \right], \\ B_2 &= \frac{1}{(1+g_0)^3(1+g_1)^3}, \\ D_0 &= 2\left(2+g_0+g_1\right), \\ D_2 &= -\frac{2}{\Delta g}\left[\log\left(\frac{1+g_0}{1+g_1} \right) + \Delta g \right]. \end{aligned} \tag{4.55}$$

All the other integrals containing an oscillatory part can be calculated using the stationary phase approximation. However, they give higher order corrections to

the expansion (4.51), so their contribution is negligible. So, the only integrals that we have to take into account are

$$I_3 = \frac{1}{\pi}\int_{-\pi}^{\pi} dk \left[\left(b_{++}^{(2)}(1)\right)^2 + \left(b_{+-}^{(2)}(1)\right)^2\right], \tag{4.56}$$

which has been evaluated numerically, and

$$\begin{aligned} I_4 &= \frac{1}{\pi}\int_{-\pi}^{\pi} dk \left[\left|b_{++}^{(1)}(1)\right|^2 + \left|b_{+-}^{(1)}(1)\right|^2\right]^2 \\ &= \frac{3\left(\Delta g\right)^4}{16384}\left[\frac{1+g_0^2}{\left(1-g_0^2\right)^7} + \frac{1+g_1^2}{\left(1-g_1^2\right)^7}\right. \\ &\left. + \frac{2\left(1+g_0 g_1\right)}{\left(1-g_0^2\right)\left(1-g_1^2\right)\left(1-g_0 g_1\right)^5}\right]. \end{aligned} \tag{4.57}$$

Replacing the contribution of integrals I_1, I_2, I_3 and I_4 in Eq. (4.51), we get an expansion of $\xi^{-1}(\tau)$ in powers of $1/\tau$:

$$\xi^{-1}(\tau) = a_2\tau^{-2} + a_3(\tau)\tau^{-7/2} + a_4\tau^{-4} + O\left(\tau^{-9/2}\right), \tag{4.58}$$

with $a_2 = I_1$, $a_3(\tau) = I_2(\tau)\tau^{3/2}$, and $a_4 = I_3 + I_4$. Inverting this power series, we obtain the result of Eq. (4.29)

$$\xi(\tau) = \frac{1}{a_2}\tau^2 + f(\tau)\sqrt{\tau} + \Lambda + O\left(\tau^{-1/2}\right). \tag{4.59}$$

with $f(\tau) = -a_3(\tau)/a_2^2$ and $\Lambda = -a_4/a_2^2$. Again, all the terms of the expansion are invariant if we exchange g_0 and g_1.

Bibliography

[1] I. Affleck and A. Ludwig. *The fermi edge singularity and boundary condition changing operatos.* J. Phys. A: Math. Gen., **27**, 5375 (1994).

[2] M. Anderson, J. Ensher, M. Matthews, C. Wieman, and E. Cornell. *Observation of bose-einstein condensation in a dilute atomic vapor.* Science, **269**, 198 (1995).

[3] P. Anderson. *Infrared catastrophe in fermi gases with local scattering potentials.* Phys. Rev. Lett., **18**, 1049 (1967).

[4] M. Banuls, J. Cirac, and M. Hastings. *Strong and weak thermalization of infinite nonintegrable quantum systems.* Phys. Rev. Lett., **106**, 050405 (2011).

[5] E. Barouch, B. M. McCoy, and M. Dresden. *Statistical mechanics of the xy model. i.* Phys. Rev. A, **2**, 1075 (1970).

[6] E. Barouch and B. McCoy. *Statistical mechanics of the xy model. ii. spin-correlation functions.* Phys. Rev. A, **3**, 786 (1971).

[7] E. Barouch and B. McCoy. *Statistical mechanics of the xy model. iii.* Phys. Rev. A, **3**, 2137 (1971).

[8] T. Barthel and U. Schollwöck. *Dephasing and the steady state in quantum many-particle systems.* Phys. Rev. Lett., **100**, 100601 (2008).

[9] J. Berges, S. Borsányi, and C. Wetterich. *Prethermalization.* Phys. Rev. Lett., **93**, 142002 (2004).

[10] J. Berges, A. Rothkopf, and J. Schmidt. *Nonthermal fixed points: Effective weak coupling for strongly correlated systems far from equilibrium.* Phys. Rev. Lett., **101**, 041603 (2008).

[11] W. Beugeling, R. Moessner, and M. Haque. *Finite-size scaling of eigenstate thermalization.* Phys. Rev. E, **89**, 042112 (2014).

[12] G. Biroli, C. Kollath, and A. M. Lauchli. *Effect of rare fluctuations on the thermalization of isolated quantum systems.* Phys. Rev. Lett., **105**, 250401 (2010).

[13] I. Bloch, J. Dalibard, and W. Zwerger. *Many-body physics with ultracold gases.* Rev. Mod. Phys., **80**, 885 (2008).

[14] C. Bradley, C. Sacketta, J. Tollett, and R. Hulet. *Evidence of bose-einstein condensation in an atomic gas with attractive interactions.* Phys. Rev. Lett., **75**, 1687 (1995).

[15] G. Brandino, A. D. Luca, R. Konik, and G. Mussardo. *Quench dynamics in randomly generated extended quantum models.* Phys. Rev. B, **85**, 214435 (2012).

[16] P. Calabrese, F. Essler, and M. Fagotti. *Quantum quench in the transverse field ising chain: I. time evolution of order parameter correlators.* J. Stat. Mech, **2012**, P07016 (2012).

[17] P. Calabrese, F. Essler, and M. Fagotti. *Quantum quenches in the transverse field ising chain: Ii. stationary state properties.* J. Stat. Mech, **2012**, P07022 (2012).

[18] P. Calabrese and J. Cardy. *Time dependence of correlation functions following a quantum quench.* Phys. Rev. Lett., **96**, 136801Apr 2006.

[19] M. Campisi, P. Hänggi, and P. Talkner. *Colloquium : Quantum fluctuation relations: Foundations and applications.* Rev. Mod. Phys., **83**, 771 (2011).

[20] T. Caneva, T. Calarco, R. Fazio, G. Santoro, and S. Montangero. *Speeding up critical system dynamics through optimized evolution.* Phys. Rev. A, **84**, 012312 (2011).

[21] T. Caneva, T. Calarco, and S. Montangero. *Chopped random-basis quantum optimization.* Phys. Rev. A, **84**, 022326 (2011).

[22] J. Cardy. *Measuring entanglement using quantum quenches.* Phys. Rev. Lett., **106**, 150404 (2011).

[23] J. Caux and R. Konik. *Constructing the generalized gibbs ensemble after a quantum quench.* Phys. Rev. Lett., **109**, 175301 (2012).

[24] J. Caux and J. Mossel. *Remarks on the notion of quantum integrability.* J. Stat. Mech, **2011**, P02023 (2011).

[25] M. A. Cazalilla. *Effect of suddenly turning on interactions in the luttinger model.* Phys. Rev. Lett., **97**, 156403 (2006).

[26] M. A. Cazalilla, R. Citro, T. Giamarchi, E. Orignac, and M. Rigol. *One dimensional bosons: From condensed matter systems to ultracold gases.* Rev. Mod. Phys., **83**, 1405 (2011).

[27] M. A. Cazalilla, A. Iucci, and M. Chung. *Thermalization and quantum correlations in exactly solvable models.* Phys. Rev. E, **85**, 011133 (2012).

[28] D. Collin, F. Ritort, C. Jarzynski, S. B. Smith, I. Tinoco, and C. Bustamante. *Verification of the crooks fluctuation theorem and recovery of rna folding free energies.* Nature, **437**, 231 (2005).

[29] M. Collura, S. Sotiriadis, and P. Calabrese. *Equilibration of a tonks-girardeau gas following a trap release.* Phys. Rev. Lett., **110**, 245301 (2013).

[30] F. Cooper, S. Habib, Y. Kluger, and E. Mottola. *Nonequilibrium dynamics of symmetry breaking in $\lambda\phi^4$ theory.* Phys. Rev. D, **55**, 6471 (1997).

[31] P. Courteille, R. Freeland, D. Heinzen, F. van Abeelen, and B. Verhaar. *Observation of a feshbach resonance in cold atom scattering.* Phys. Rev. Lett., **81**, 69 (1998).

[32] K. Davis, M. Miewes, M. Andrews, N. van Druten, D. Durfee, D. Kurn, and W. Ketterle. *Bose-einstein condensation in a gas of sodium atoms.* Phys. Rev. Lett., **75**, 3969 (1995).

[33] S. Deffner and E. Lutz. *Nonequilibrium work distribution of a quantum harmonic oscillator.* Phys. Rev. E, **77**, 021128 (2008).

[34] C. De Grandi and A. Polkovnikov. *Adiabatic perturbation theory: from Landau-Zener problem to quenching through a quantum critical point*, chapter , pages . Springer, Heidelberg, (2010).

[35] B. DeMarco and D. Jin. *Onset of fermi degeneracy in a trapped atomic gas.* Science, **185**, 1703 (1999).

[36] J. Deutsch. *Quantum statistical mechanics in a closed system.* Phys. Rev. A, **43**, 2046 (1991).

[37] P. Doria, T. Calarco, and S. Montangero. *Optimal control technique for many-body quantum dynamics.* Phys. Rev. Lett., **106**, 190501 (2011).

[38] F. Douarche, S. Ciliberto, A. Petrosyan, and I. Rabbiosi. *An experimental test of the jarzynski equality in a mechanical experiment.* Europhys. Lett., **70**, 593 (2005).

[39] S. Dubey, L. S. adn J. Finn, S. Vinjanampathy, and K. Jacobs. *Approach to typicality in many-body quantum systems.* Phys. Rev. E, **85**, 011141 (2012).

[40] M. Eckstein and M. Kollar. *Nonthermal steady states after an interaction quench in the falicov-kimball model.* Phys. Rev. Lett., **100**, 120404 (2008).

[41] M. Eckstein, M. Kollar, and P. Werner. *Thermalization after an interaction quench in the hubbard model.* Phys. Rev. Lett., **103**, 056403 (2009).

[42] M. Eckstein and M. Kollar. *Near-adiabatic parameter changes in correlated systems: influence of the ramp protocol on the excitation energy.* New J. of Phys., **12**, 055012 (2010).

[43] F. Essler, S. Kehrein, S. Manmana, and N. Robinson. *Quench dynamics in a model with tuneable integrability breaking.* Phys. Rev. B, **89**, 165104 (2014).

[44] M. Fagotti, M. Collura, F. Essler, and P. Calabrese. *Relaxation after quantum quenches in the spin $\frac{1}{2}$ heisenberg xxz chain.* Phys. Rev. B, **89**, 125101 (2014).

[45] M. Fagotti and F. Essler. *Reduced density matrix after a quantum quench.* Phys. Rev. B, **87**, 245107 (2013).

[46] M. Fagotti and F. Essler. *Stationary behaviour of observables after a quantum quench in the spin-$\frac{1}{2}$ heisenberg xxz chain.* J. Stat. Mech, **2013**, P07012 (2013).

[47] D. Fioretto and G. Mussardo. *Quantum quenches in integrable field theories.* New. J. Phys., **12**, 055015 (2009).

[48] A. Furusaki. *Local perturbation in a tomonaga-luttinger liquid at $g = \frac{1}{2}$: Orthogonality catastrophe, fermi-edge singularity, and local density of states.* Phys. Rev. B, **56**, 9352 (1997).

[49] A. Gambassi and P. Calabrese. *Quantum quenches as classical critical films.* Europhys. Lett., **95**, 66007September 2011.

[50] A. Gambassi and A. Silva. *Statistics of the work in quantum quenches, universality and the critical casimir effect.* arXiv: 1106.2671 (2011).

[51] A. Gambassi and A. Silva. *Large deviations and universality in quantum quenches.* Phys. Rev. Lett., **109**, 250602 (2012).

[52] A. Gogolin. *Local time-dependent perturbation in luttinger liquid.* Phys. Rev. Lett., **71**, 2995 (1993).

[53] G. Goldstein and N. Andrei. *Failure of the gge hypothesis for integrable models with bound states.* arxiv: 1405.4224 (2014).

[54] M. Greiner, O. Mandel, T. Esslinger, T. W. Hänsch, and I. Bloch. *Quantum phase transition from a superfluid to a mott insulator in a gas of ultracold atoms.* Nature, **415**, 39 (2002).

[55] M. Greiner, O. Mandel, T. W. Hansch, and I. Bloch. *Collapse and revival of the matter wave field of a bose-einstein condensate.* Nature, **419**, 51 (2002).

[56] R. Grimm, M. Weidemuller, and Y. Ovchinnikov. *Optical dipole trap for neutral atoms.* Adv. At. Mol. Opt. Phys., **42**, 95 (2000).

[57] M. Gring, M. Kuhnert, T. Langen, T. Kitagawa, B. Rauer, M. Schreitl, I. Mazets, D. A. Smith, E. Demler, and J. Schmiedmayer. *Relaxation and prethermalization in an isolated quantum system.* Science, **337**, 1318 (2012).

[58] V. Gritsev, E. Demler, E. Lukin, and A. Polkovnikov. *Spectroscopy of collective excitations in interacting low-dimensional many-body systems using quench dynamics.* Phys. Rev. Lett., **99**, 200404 (2007).

[59] V. Gritsev, A. Polkovnikov, and E. Demler. *Linear response theory for a pair of coupled one-dimensional condensates of interacting atoms.* Phys. Rev. B, **75**, 174511 (2007).

[60] S.-J. Gu and H.-Q. Lin. *Scaling dimension of fidelity susceptibility in quantum phase transitions.* Europhys. Lett., **87**, 10003 (2009).

[61] T. Ikeda, Y. Watanabe, and M. Ueda. *Eigenstate randomization hypothesis: Why does the long-time average equal the microcanonical average?* Phys. Rev. E, **84**, 021130 (2011).

[62] S. Inouye, M. R. Andrews, J. Stenger, H.-J. Miesner, D. Stamper-Kurn, and W. Ketterle. *Observation of feshbach resonances in a bose–einstein condensate*. Nature, **392**, 151 (1998).

[63] C. Jarzynski. *Nonequilibrium equality for free energy differences*. Phys. Rev. Lett., **78**, 2690 (1997).

[64] E. T. Jaynes. *Information theory and statistical mechanics*. Phys. Rev., **106**, 620 (1957).

[65] A. Kamenevn. *Field Theory of Non-Equilbirum Systems*. Cambridge University Press (2011).

[66] C. L. Kane, K. A. Matveev, and L. I. Glazman. *Fermi-edge singularities and backscattering in a weakly interacting one-dimensional electron gas*. Phys. Rev. B, **49**, 2253 (1994).

[67] T. Kinoshita, T. Wenger, and D. S. Weiss. *A quantum newton's cradle*. Nature, **440**, 900 (2006).

[68] T. Kitagawa, A. Imambekov, J. Schmiedmayer, and E. Demler. *The dynamics and prethermalization of one-dimensional quantum systems probed through the full distributions of quantum noise*. New J. Phys., **13**, 073018 (2011).

[69] S. Klebnikov and M. Kruczenski. *Thermalization of isolated quantum systems*. arxiv: 1312.4612 (2013).

[70] M. Kollar and M. Eckstein. *Relaxation of a one-dimensional mott insulator after an interaction quench*. Phys. Rev. A, **78**, 013626 (2008).

[71] M. Kollar, F. A. Wolf, and M. Eckstein. *Generalized gibbs ensemble prediction of prethermalization plateaus and their relation to nonthermal steady states in integrable systems*. Phys. Rev. B, **84**, 054304 (2011).

[72] C. Kollath, A. M. Läuchli, and E. Altman. *Quench dynamics and non-equilibrium phase diagram of the bose-hubbard model.* Phys. Rev. Lett., **98**, 180601 (2007).

[73] A. Komnik, R. Egger, and A. Gogolin. *Exact fermi-edge singularity exponent in a luttinger liquid.* Phys. Rev. B, **56**, 1153 (1997).

[74] M. Kormos, M. Collura, and P. Calabrese. *Analytic results for a quantum quench from free to hard-core one-dimensional bosons.* Phys. Rev. A, **89**, 013609 (2014).

[75] M. Kormos, A. Shashi, Y. Chou, J. Caux, and A. Imambekov. *Interaction quenches in the one-dimensional bose gas.* Phys. Rev. B, **88**, 205131 (2013).

[76] M. Krech. *The Casimir Effect in Critical Systems.* World Scientific, Singapore (1994).

[77] E. H. Lieb. *Exact analysis of an interacting bose gas. ii. the excitation spectrum.* Phys. Rev., **130**, 1616 (1963).

[78] E. H. Lieb and W. Liniger. *Exact analysis of an interacting bose gas. i. the general solution and the ground state.* Phys. Rev., **130**, 1605 (1963).

[79] J. Liphardt, S. Dumont, S. B. Smith, I. Tinoco, and C. Bustamante. *Equilibrium information from nonequilibrium measurements in an experimental test of jarzynski's equality.* Science, **296**, 1832 (2002).

[80] M. Marcuzzi, J. Marino, A. Gambassi, and A. Silva. *Pre-thermalization in a non-integrable quantum spin chain after a quench.* Phys. Rev. Lett., **111**, 197203 (2013).

[81] G. Mazza and M. Fabrizio. *Dynamical quantum phase transitions and broken-symmetry edges in the many-body eigenvalue spectrum.* Phys. Rev. B, **86**, 184303 (2012).

[82] M. Mierzejewski, P. Prelovsek, and T. Prosen. *Breakdown of the generalized gibbs ensemble for current-generating quenches.* arxiv: 1405.2557 (2014).

[83] A. Mitra. *Correlation functions in the prethermalized regime after a quantum quench of a spin chain.* Phys. Rev. B, **87**, 205109 (2013).

[84] M. Moeckel and S. Kehrein. *Interaction quench in the hubbard model.* Phys. Rev. Lett., **100**, 175702 (2008).

[85] M. Moshe and J. Zinn-Justin. *Quantum field theory in the large n limit: a review.* Phys. Rep., **385**, 69 (2003).

[86] G. Mussardo. *Statistical Field Theory. An Introduction to Exactly Solved Models in Statistical Physics.* Oxford University Press (2009).

[87] G. Mussardo. *Infinite-time average of local fields in an integrable quantum field theory after a quantum quench.* Phys. Rev. Lett., **111**, 100401 (2013).

[88] J. D. Nardis, B. Wouters, M. Brockmann, and J. Caux. *Solution for an interaction quench in the lieb-liniger bose gas.* Phys. Rev. A, **89**, 033601 (2014).

[89] J. W. Negele and H. Orland. *Quantum Many-Particle Systems.* Westview Press (1998).

[90] N. Nessi, A. Iucci, and M. A. Cazalilla. *Quantum quench and prethermalization dynamics in a two-dimensional fermi gas with long-range interactions.* arxiv: 1401.1986 (2014).

[91] R. Paris and D. Jaminski. *Asymptotics and Mellin-Barnes Integrals.* Cambridge University Press (2001).

[92] P. Pfeuty. *The one-dimensional ising model with a transverse field.* Ann. Phys., **57**, 79 (1970).

[93] A. Polkovnikov. *Universal adiabatic dynamics in the vicinity of a quantum critical point.* Phys. Rev. B, **72**, 161201(R) (2005).

[94] A. Polkovnikov and V. Gritsev. *Breakdown of the adiabatic limit in low-dimensional gapless systems.* Nat. Phys., **4**, 477 (2008).

[95] A. Polkovnikov, K. Sengupta, A. Silva, and M. Vengalattore. *Colloquium : Nonequilibrium dynamics of closed interacting quantum systems.* Rev. Mod. Phys., **83**, 863 (2011).

[96] B. Pozsgay. *The generalized gibbs ensemble for heisenberg spin chains.* J. Stat. Mech, **2013**, P07003 (2013).

[97] B. Pozsgay, M. Mestyan, M. Werner, M. Kormos, G. Zarand, and G. Takacs. *Correlations after quantum quenches in the xxz spin chain: Failure of the generalized gibbs ensemble.* arxiv: 1405.2843 (2014).

[98] J. Rammer. *Quantum Field Theory of Non-equilibrium States.* Cambridge University Press (2007).

[99] M. Rigol. *Breakdown of thermalization in finite one-dimensional systems.* arXiv:0904.3746 (2009).

[100] M. Rigol, V. Dunjko, and M. Olshanii. *Thermalization and its mechanism for generic isolated quantum systems.* Nature, **452**, 854 (2008).

[101] M. Rigol, V. Dunjko, V. Yurovsky, and M. Olshanii. *Relaxation in a completely integrable many-body quantum system: An ab initio study of the dynamics of the highly excited states of 1d lattice hard-core bosons.* Phys. Rev. Lett., **98**, 050405 (2007).

[102] M. Rigol and L. F. Santos. *Quantum chaos and thermalization in gapped systems after a quench.* arXiv:1003.1403 (2010).

[103] M. Rigol and M. Srednicki. *Alternatives to eigenstate thermalization.* Phys. Rev. Lett., **108**, 110601 (2012).

[104] G. Rigolin, G. Ortiz, and V. H. Ponce. *Beyond the quantum adiabatic approximation: Adiabatic perturbation theory.* Phys. Rev. A, **78**, 052508 (2008).

[105] D. Rossini, A. Silva, G. Mussardo, and G. E. Santoro. *Effective thermal dynamics following a quantum quench in a spin chain.* Phys. Rev. Lett., **102**, 127204 (2009).

[106] A. Sachdev and A. Young. *Low temperature relaxational dynamics of the ising chain in a transverse field.* Phys. Rev. Lett., **78**, 2220 (1997).

[107] S. Sachdev. *Quantum Phase Transitions.* Cambridge University Press (1999).

[108] M. Sandri and M. Fabrizio. *Nonequilibrium dynamics in the antiferromagnetic hubbard model.* Phys. Rev. B, **88**, 165113 (2013).

[109] L. F. Santos and M. Rigol. *Onset of quantum chaos in one-dimensional bosonic and fermionic systems and its relation to thermalization.* Phys. Rev. E, **81**, 036206 (2010).

[110] L. F. Santos and M. Rigol. *Localization and the effects of symmetries in the thermalization properties of 1d quantum systems.* Phys. Rev. E, **82**, 031130 (2010).

[111] M. Schiró and M. Fabrizio. *Time-dependent mean field theory for quench dynamics in correlated electron systems.* Phys. Rev. Lett., **105**, 076401 (2010).

[112] B. Sciolla and G. Biroli. *Quantum quenches and off-equilibrium dynamical transition in the infinite-dimensional bose-hubbard model.* Phys. Rev. Lett., **105**, 220401 (2010).

[113] B. Sciolla and G. Biroli. *Dynamical transitions and quantum quenches in mean-field models.* J. Stat. Mech, **2011**, P11003 (2011).

[114] B. Sciolla and G. Biroli. *Quantum quenches, dynamical transitions, and off-equilibrium quantum criticality.* Phys. Rev. B, **88**(201110(R)) (2013).

[115] A. Silva. *Statistics of the work done on a quantum critical system by quenching a control parameter.* Phys. Rev. Lett., **101**, 120603 (2008).

[116] D. A. Smith, M. Gring, T. Langen, M. Kuhnert, B. Rauer, R. Geiger, T. Kitagawa, I. Mazets, E. Demler, and J. Schmiedmayer. *Prethermalization revealed by the relaxation dynamics of full distribution functions.* New J. Phys, **15**, 075011 (2012).

[117] S. Sotiriadis, A. Gambassi, and A. Silva. *Statistics of the work done by splitting a one-dimensional quasicondensate.* Phys. Rev. E, **87**, 052129 (2013).

[118] S. Sotiriadis, G. Takacs, and G. Mussardo. *Boundary state in an integrable quantum field theory out of equilibrium.* Phys. Lett. B, **734**, 52 (2014).

[119] M. Srednicki. *Chaos and quantum thermalization.* Phys. Rev. E, **50**, 888 (1994).

[120] R. Steinigeweg, J. Herbrych, and P. Prelovsek. *Eigenstate thermalization within isolated spin-chain systems.* Phys. Rev. E, **87**, 012118 (2013).

[121] B. Sutherland. *Beautiful Models.* Wold Scientific (2004).

[122] G. Szegő and V. Grenader. *Toeplitz forms and their applications.* University of California Press (1958).

[123] P. Talkner, E. Lutz, and P. Hänggi. *Fluctuation theorems: Work is not an observable.* Phys. Rev. E, **75**, 050102(R) (2007).

[124] P. Talkner and P. Hänggi. *The Tasaki-Crooks quantum fluctuation theorem.* J. Phys. A: Math. Theor., **40**, F569 (2007).

[125] H. Touchette. *The large deviation approach to statistical mechanics.* Phys. Rep., **478**, 1 (2009).

[126] N. Tsuji, M. Eckstein, and P. Werner. *Nonthermal antiferromagnetic order and nonequilibrium criticality in the hubbard model.* Phys. Rev. Lett., **110**, 136404 (2013).

[127] M. Vengalattore, S. R. Leslie, J. Guzman, and D. M. Stamper-Kurn. *Spontaneously modulated spin textures in a dipolar spinor bose-einstein condensate.* Phys. Rev. Lett., **100**, 170403 (2008).

[128] J. von Neumann. *Beweis des ergodensatzes und des h-theorems in der neuen mechanik.* Z. Phys., **57**, 70 (1929).

[129] P. Werner, N. Tsuji, and M. Eckstein. *Nonthermal symmetry-broken states in the strongly interacting hubbard model.* Phys. Rev. B, **86**, 205101 (2012).

[130] B. Wouters, M. Brockmann, J. D. Nardis, D. Fioretto, and J. Caux. *From néel to xxz: exact solution from the quench action.* arxiv: 1405.0172 (2014).

[131] J. B. Zuber and C. Itzynkson. *Quantum field theory and the two-dimensional ising model.* Phys. Rev. D, **15**, 2875 (1977).

[132] W. H. Zurek, U. Dorner, and P. Zoller. *Dynamics of a quantum phase transition.* Phys. Rev. Lett., **95**, 105701 (2005).